Summer 2013

The Oncogenic Role and the Prognostic Value Of Notch3 Gene In Human Malignant Glioma

Mohammad Ali Yousef Alqudah
University of Iowa

THE ONCOGENIC ROLE AND THE PROGNOSTIC VALUE OF NOTCH3 GENE IN HUMAN MALIGNANT GLIOMA

by

Mohammad Ali Yousef Alqudah

A thesis submitted in partial fulfillment
of the requirements for the Doctor of
Philosophy degree in Pharmacy
in the Graduate College of
The University of Iowa

August 2013

Thesis Supervisor: Assistant Professor Mahfoud Assem

Graduate College
The University of Iowa
Iowa City, Iowa

CERTIFICATE OF APPROVAL

_____

PH.D. THESIS

_____

This is to certify that the Ph.D. thesis of

Mohammad Ali Yousef Alqudah

has been approved by the Examining Committee
for the thesis requirement for the Doctor of Philosophy
degree in Pharmacy at the August 2013 graduation.

Thesis Committee: _____
Mahfoud Assem, Thesis Supervisor

_____
Lawrence Fleckenstein

_____
Daryl Murry

_____
Gary Milavetz

_____
Aliasger Salem

To my parents, my wife and my little son

ACKNOWLEDGMENTS

First of all, I joined the graduate program having no little drop of knowledge about how any research story can begin. Thanks to the one who took my hand as a little child with extreme patience on my faults and taught me from where to start and not to stop without making a real change, that's my advisor Dr. Mahfoud Assem. Thanks Dr. Mahfoud for your guidance not only in my project but also in different aspects of organizing my career and improving my skills. You are always there to bring my thoughts into reality and inspiring me new ideas that make the project moving forward. Next, I would like to thank my committee members Dr. Lawrence Fleckenstein, Dr. Daryl Murry, Dr. Gary Milavetz and Dr. Aliasger Salem for their directions and advice to improve and develop my research project. Thanks my committee members for many inputs and suggestions during my presentations that added new insights to my project. Then, I would like to express my deep appreciation to my parents and my wife for encouraging me to pursue my graduate studies and for their consistent prayers for me to complete my study in successful manner. Special thanks to my wife for her continuous support and patience and providing me the best environment to finish my study.

ABSTRACT

Malignant glioma have poor prognosis resulting mainly from high level of cell proliferation and invasion and resistance to conventional therapy. Identification of novel targets that are critical elements in gliomagenesis may help improve therapeutic outcome. Using genome-wide explorations of a comprehensive glioma specimen population, we identified a whole gain of chromosome 19 as one of the major chromosomal aberrations in high grade glioma that correlates to patients' outcomes. Our analysis revealed for the first time NOTCH3 as one of the most significant gene amplifications mapped to chromosome 19. This amplification is associated with the poorest outcome compared to tumors with a non-amplified locus. The NOTCH signaling pathway is essential for cell proliferation, stem cell maintenance and differentiation. Its dysregulation has been reported in several human cancers. NOTCHs are key positive regulators of cell-cell interactions, angiogenesis, cell adhesion and stem cell niche development which have been shown to play critical roles in gliomagenesis and glioma drug resistance. Our objective is to determine NOTCH3 molecular roles in glioma pathogenesis and aggressiveness. Here we show for the first time that NOTCH3 plays a role in glioma cell proliferation, cell migration, invasion and apoptosis. We also found a NOTCH3 glioma addiction phenomenon. Therefore, our study uncovers, for the first time, the prognostic value and the oncogenic function of NOTCH3 in gliomagenesis and supports NOTCH3 as a promising target of therapy in high grade glioma. Our studies allow the identification of a subset of population that may benefit from ɣ-secretase inhibitor (GSI)-based therapies. This may lead to the design of novel strategies to improve therapeutic outcome of patients with glioma by establishing the medical and scientific basis for personalized medicine.

TABLE OF CONTENTS

LIST OF TABLES

Table

LIST OF FIGURES

Figure

LIST OF ABBREVIATIONS

AA	Anaplastic astrocytoma
ABC	ATP-binding cassette
ACG	Astrocytoma
ADAM	A disintegrin and metalloproteinase
ANK	Ankyrin
AOD	Anaplastic oligodendroglioma
AOA	Anaplastic oligoastrocytoma
APP	Amyloid precursor protein
ATCC	American Type Culture Collection
bHLH	Basic-helix–loop–helix
CADASIL	Cerebral Autosomal Dominant Arteriopathy with Subcortical Infarcts and Leukoencephalopathy
CDK4	Cyclin-dependent kinase 4
CDK6	Cyclin-dependent kinase 6
cDNA	Complementary DNA
CGH	Comparative genomic hybridization
CNAs	Copy number alterations
CNS	Central nervous system
CSL	CBF1/RBP-Jk, Suppressor of Hairless, LAG-1
CSCs	Cancer stem cells
ddH2O	Double distilled water
DLL	Delta-like ligand
DMEM	Dulbecco’s modified Eagle’s medium

DMSO	Dimethyl sulfoxide
DTT	Dithiothreitol
DXR	Doxorubicin
ECD	Extracellular domain
ECL	Enhanced chemiluminescence
ECM	Extracellular matrix
EDTA	Ethylenediamine tetraacetic acid
EGF	Epidermal growth factor
EGFR	Epidermal growth factor receptor
EGFRvIII)	EGFR mutated variant 3
EMT	Epithelial to mesenchymal transition
ETP	Etoposide
FBS	Fetal bovine serum
FISH	Fluorescence in situ hybridization
GAPDH	Glyceraldehyde-3-phosphate dehydrogenase
GBM	Glioblastoma multiforme
GFAP	Glial fibrillary acidic protein
GSCs	Glioma stem cells
GSIs	γ-secretase inhibitors
HCL	Hydrochloric acid
Hes	Hairy enhancer of split
Hey or HRT	Hairy-related transcription factor
HIF-1α	Hypoxia inducible factor-1

ICD	Intracellular domain
IRB	Institutional review board
JAG	Jagged
KPS	Karnofsky Performance Status
LOH	Loss of heterozygosity
MAML-1	Mastermind-like 1
MDM2	Mouse double minute 2, human homolog of; p53-binding protein
MDM4	Mouse double minute 4, human homolog of; p53-binding protein
Mesen	Mesenchymal
MGMT	Methylguanine-DNA methyltransferase
MMPs	Matrix metalloproteinases
mTOR	Mammalian target of rapamycin
MTT	3-(4, 5-dimethylthiazol-2-yl)-2,5-diphenyltetrazolium bromide
Na2EDTA	Disodium Ethylenediamine tetraacetic acid
NaCl	Sodium chloride
NaH2PO4H2O	Sodium dihydrogen phosphate monohydrate
NF1	Neurofibromatosis-1
NICD	NOTCH intracellular domain
NLS	Nuclear localization signals
NSCs	Neural stem cells
ODG	Oligodendroglioma
OA	Oligoastrocytoma
PAGE	Poly acryl amide gel electrophoresis

PBS	Phosphate Buffered Saline
PCR	Polymerase chain reaction
PCV	Procarbazine, CCNU, vincristine
PDGFA	Platelet-derived growth factor receptor A
PDGFR	Platelet-derived growth factor receptor
PI3K	Phosphoinositide-3-kinase
PEST	Praline/glutamate/serine/threonie-rich
PFS	Progression-free survival
Prolif	Proliferative
ProN	Proneural
PTEN	Phosphatase and tensin homolog
RAM	RBP-Jκ-associated module
RB	Retinoblastoma
Rembrandt	REpository for Molecular BRAin Neoplasia DaTa
RNAi	RNA interference
rRNA	Ribosomal RNA
RT	Reverse transcription
RTK	Receptor tyrosine kinase
RTKIs	Receptor tyrosine kinase inhibitors
SDS	Sodium dodecyl sulphate
SFM	Serum free media
SHH	Sonic hedgehog
SNPs	Single-nucleotide polymorphisms

SSPE	Saline-Sodium Phosphate-EDTA
STATs	Signal transducer and activator of transcription
TACE	Tumor necrosis factor-α-converting enzyme
T-ALL	T cell lymphoblastic leukemia
TBE	Tris-Boric acid-EDTA
TBST	Tris-Buffered Saline Tween-20
TMZ	Temozolomide
TNC	Tenascin-c
TPT	Topotecan
VEGFA	vascular endothelial growth factor A
VEGFRs	Vascular endothelial growth factor receptors
WHO	World health organization

CHAPTER I

INTRODUCTION

1.1 Overview

1.1.1 Glioma classification and grading

Every year, approximately 22,000 individuals are diagnosed with central nervous system (CNS) tumors in the United States (1). In adult males younger than age of 40 years, CNS malignancies are the second leading cause of death (2). Diffuse gliomas, a glial tissue derived tumors, are the most common type of primary brain tumors in adults representing 32% of all CNS tumors and 80% of brain tumors (1). Gliomas can arise from one of two lineages: astrocytic or oligodendrocytic which are cellular structures that support the nerve cells. Therefore, they are classified histologically into astrocytoma that accounts for 70% or oligodendroglioma that accounts for 20% with the remaining 10% for mixed oligoastrocytoma (Figure 1.1) (3). In addition, gliomas are further classified according to the World Health Organization (WHO) into grade I-IV based on other histologic features present in the tumor; where, WHO grade I are mostly pediatric tumors and WHO grade II represents low grade gliomas with low mitotic index including astrocytoma (ACG), oligodendroglioma (ODG) and mixed oligoastrocytoma (OA) (3). Nuclear atypia and mitotic activity are characteristics of the anaplasitc tumors (WHO grade III) which represent anaplastic astrocytoma (AA), anaplastic oligodendroglioma (AOD) and mixed anaplastic oligoastrocytoma (AOA) (3). Necrosis and microvascular proliferation are ominous signs of aggressive glioma that is glioblastoma multiforme (GBM; WHO grade IV) (Figure 1.1) (3). Only 5-10% of GBMs result from progression of lower grade glioma in young adults and more than 90% are primary tumors (4, 5).

High grade gliomas (AA and GBM) are the most common grades; accounting for 2 and 16% of all primary brain tumors in the United States with incidences of 0.41 and 3.20 cases per 100,000 persons per year, respectively (1, 6). These tumors are characterized by high heterogeneity and infiltrating nature with high vascularity especially for GBM (3). However, differences in molecular alterations within and between glioma grades are currently paramount to distinguish such tumor groups (7). Despite maximal optimal therapy, emergence of resistance to the current therapeutic interventions often prevents complete cure that results in tumor relapse and increases the economic burden on health care system (3).

1.1.2 Management of glioma

Despite recent advances in the fields of neuroimaging, neurosurgery, radiotherapy and pharmacotherapy, the prognosis of patients with malignant glioma remains dire (8). However, the current available treatment guidelines recommend a combined approach, using surgery, radiotherapy, and chemotherapy (8). In fact, extensive tumor resection has a superior advantage by increasing patient's overall survival in both low and high grade gliomas (9). Besides, the maximal resection at recurrence can increase patient overall survival even with initial subtotal resection (10). However, the infiltrating nature of high grade gliomas and their extensive proliferation make the chance to cure these aggressive gliomas slim. Therefore, surgery is usually followed by radiotherapy in a daily fraction basis with a daily dose of 2 Gy for up to 54 to 60 Gy for better prognosis or a daily dose of 5 Gy up to 30 Gy in poor prognosis malignant gliomas (11, 12). This results in prolonging the median survival of glioma patients by 3 months which requires additional therapeutic interventions (13).

Along with radiotherapy, chemotherapy is given concurrently and adjuvantly (14). As a modality of choice, temozolomide (TMZ; Temodar®) is the most commonly used chemotherapy drug in glioma owing to its ability to cross the blood–brain barrier effectively in addition to its availability in oral dosage form (15). Upon spontaneous activation inside the body, TMZ active metabolite methylates DNA purine bases (O6-guanine; N7-guanine and N3-adenine) that leads to base mismatch and induces cell cycle arrest and apoptosis (16). Around 30% of GBMs express high levels of methylguanine-DNA methyltransferase (MGMT) which is a suicide enzyme that is mechanistically responsible for direct repair of O6-methylguanine and inducing resistance to TMZ (16). Nevertheless, TMZ (along with radiotherapy) is still used in both low and high MGMT expressing GBMs since it is more efficacious than radiation only therapy (13). Despite maximal treatment, the long-term survivors (more than two years) of high grade glioma are rare (17). However, TMZ treatment increases both the two-year overall survival rate and the median five-year overall survival rate to 26.5% and 9.8% compared to 10.4% and 1.9% with radiation only therapy, respectively (17, 18). However, other chemotherapy treatments are used in tumor relapse including nitrosoureas and topoisomerase poisons such as etoposide (ETP), doxorubicin (DXR) and topotecan (TPT) as an alternative or in addition to resurgery and/or reirradiation (13).

Generally, emergence of resistance to conventional chemotherapeutic agents is the underlying mechanism of glioma relapse and recurrence that urgently requires developing novel strategies superior to the classical approach which cannot be real without understanding the biology of glioma. Therefore, the new trend of our journey to the cancer cure is the translational research that may hold the promise of improving

therapeutic outcome (Figure 1.2). In this approach, investigators perform molecular screening for altered regulatory signals in tumor biopsies and identify candidate therapeutic targets to be further validated and translated into clinical practice. This is usually achieved with the help of newly developed research strategies that are based on genomics, transcriptomics and proteomics.

1.2 Genomic, transcriptional and proteomic profiling of malignant glioma

1.2.1 Genomic analysis

Malignant gliomas have poor prognosis because of high levels of cell proliferation, invasion and extensive angiogenesis besides resistance to various therapeutic interventions (19). The complex genetic nature of gliomas seems to be the underlying mechanism of this aggressive presentation. As a nature of any human cancer, glioma shows high levels of genetic and epigenetic alterations. Extensive genomic profiling through genome-wide explorations have identified a significant number of these alterations involved in important deregulated signaling pathways and ultimately uncovered molecular subclasses within and between glioma grades (7). Beside the WHO classification, this new understanding of glioma biology will get to the root of gliomagenesis starting from the underlying molecular pathology until development of targeted therapies and personalized medicine.

Recent integrated genomic approaches have identified profound genetic instability in malignant glioma affecting both chromosome structure and copy number (7). Combined work from both newly developed genomic and bioinformatics tools resulted in more precise and unbiased genomic analysis that accentuates the actual genomic

alteration from the background noise (20, 21). Such alterations in glioma populations include chromosomal instabilities affecting chromosomes 1, 7, 9, 10, 19, 20 and 22 (Table 1.1) (22, 23). These alterations mostly occurred as amplifications, gain or loss of function mutations, or loss of heterozygosity (LOH) (23). Consequently, activation of potential oncogenes or inactivation of tumor suppressor genes can be the driving force of these chromosomal aberrations. Genes with altered loci mapped to these altered chromosomes may be critical elements in gliomagenesis and have a central role in glioma progression. Exploring for novel genes and associated altered signaling pathways will uncover the clinical significance of these genetic alterations as they may belong to any of the altered signaling pathways involved in tumor growth, invasion, apoptosis and cell cycle regulation (24).

Several genomic profiling studies have identified three major frequently altered pathways in malignant glioma (Table 1.2) (25-28). First, impairment of p53 signaling (87%) was found through TP53 mutation or homozygous deletion (35%), CDKN2A homozygous deletion (52%), MDM2 (14%) amplification or MDM4 (7%) amplification. MDM2 and MDM4 are negative regulators of p53. In addition, p53/MDM2/p14ARF pathway could be deregulated by epigenetic alterations, namely p14ARF methylation (29, 30). Methylated p14ARF locus results in failure to inhibit MDM2-mediated p53 ubiquitination with net result of lost p53 activity (29, 30). P53 plays an important role in suppressing the oncogenic transformation by inducing growth arrest at G1 phase, given time for DNA repair or inducing apoptosis if the damage is too severe to be repaired (31).

Second, impairment of retinoblastoma (Rb) signalling (77%) was found through mutation or homozygous deletion of RB1 (11%) and amplification of CDK4 (18%),

CDK6 (1%), or CCND2 (2%) (19). CDK4, CDK6 and CCND2 are known inhibitors of Rb which in turn functions to inhibit cell cycle (19). Another such deregulation is the common allelic loss of the CDKN2A (52%) which code for p16INK4a, a known cyclin-dependent kinase inhibitor that binds to CDK4 and inhibits CDK4/cyclinD1 complex formation, thereby releasing the Rb protein. The free Rb sequesters E2F transcription factors (cell cycle activators) thus preventing G1-S transition (24, 32).

Third, alteration of RTK/RAS/PI3K pathways (88%) was found through amplification or mutation of receptor tyrosine kinases (RTKs): epidermal growth factor receptor EGFR (45%), ERBB2 (8%), platelet-derived growth factor receptor A (PDGFRA, 13%) and MET (4%). Moreover, mutations of downstream PI3K (15%), RAS (2%) and AKT (2%) were also contributing to more active (RTK/ PI3K/Ras) pathways. EGFR is amplified in 45% of GBM with half of the cases harbor additional deletion mutation known as the mutated variant 3 (EGFRvIII) that confers worse prognosis compared to intact EGFR (33). Although amplification of EGFR results in highly active (RTK/PI3K/Ras) pathway, EGFRvIII represents constitutive autophosphorylation that results in even higher activity that promotes more cell proliferation and confers higher resistance to apoptosis induced by chemotherapy (33).

Subsets of glioma cells expressing EGFRvIII are able to enhance the proliferation of the surrounding EGFR-expressing cells through paracrine signaling (34). This reflects how the heterogeneous subpopulations of cancer cells within the tumor bulk cooperate to favor the malignant phenotype. Likewise, PDGFR signaling is altered via different mechanisms including: PDGF (A-D) ligand upregulation (30%), PDGFRA amplification (15%), truncated PDGFRA expression as a result of exon deletion and in-frame gene

fusion with VEGFR2 (35-38). The last two result in constitutively active receptor signaling that activates downstream effectors.

Other contributions that lead to deregulation of (RTK/ PI3K/Ras) pathways are mutations or homozygous deletions in neurofibromatosis-1, NF1 (18%) and phosphatase and tensin homolog (PTEN, 37%) (25). In addition to its deletion, NF1 can be also inactivated via PKC-dependent proteasomal degradation (25). NF1 is a potent tumor suppressor of the proliferative Ras/mTOR signaling pathway and STAT3/cyclinD1 axis that (the later) favors cell growth (39, 40).

PTEN, a known tumor suppressor that regulates cell cycle, is frequently inactivated in anaplastic gliomas and GBMs as result of chromosome 10q loss (19). PTEN is a negative regulator of PI3K/AKT pathway which is crucial for glioma stem cell proliferation and inhibition of apoptosis (41). The stability of PTEN is regulated by post-translational phosphorylation (42) and by proteasomal degradation through NEDD4-1 which in turn found to be upregulated in GBM (43). Moreover, PTEN functions in an inhibitory network along with NHERF1 and PHLPP. NHERF1 role is to recruit PTEN and PHLPP tumor suppressors to the cell membrane to inhibit PI3K/AKT pathway. This triple inhibitory network has been found to be disabled in GBM (44). Therefore, up-regulation of NEDD4-1 or loss of NHERF1 could be the underlying mechanisms that inhibit PTEN function in the absence of PTEN genetic mutation or deletion or epigenetic silencing. Thus, genomic data may not give full estimate of PTEN inactivation, taking in consideration such collateral factors.

Finally, high expression of Tenascin-c (TNC), an extracellular matrix glycoprotein, has been found in invasive GBM (45, 46) and linked to short patient

survival (47). Interestingly, frequent amplification of the chromosome 9qter, at which TNC locus is located, has been associated with recurrent childhood ependymomas (48). Taken together, all the previous findings provide a clear picture of the genetic aberrations involved in glioma pathology and show malignant glioma as distinct histologic classes yet involves genetically heterogeneous populations within the same grade. However, some genetic aberration events may not result in a significant change in the expression level of the gene of interest. Therefore, a parallel gene expression analysis may be considered besides the genomic profiling.

1.2.2 Transcriptional analysis

Several studies have established the basis of classifying high-grade gliomas into different subtypes according to their differences in mRNA expression of certain genes important in the pathogenesis of malignant glioma (35, 36). Phillips and co-workers performed microarray mRNA expression profiling of more than 100 genes correlate positively or negatively with survival. Unsupervised clustering of these high-grade gliomas based on the most significant 35 signature genes delineated three molecular subclasses characterized by distinct gene signatures, progression profiles and patient survivals. These include proneural (ProN), proliferative (Prolif) and mesenchymal (Mesen) subtypes, such nomenclature came from the predominant gene list featured in each group.

These glioma classes have been shown as distinct subtypes with different features (Table 1.3). For instance, this classification was of prognostic value in which the ProN cases had better outcome compared to the other two subtypes which could be explained by the fact that ProN tumors not only include grade IV but also grade III gliomas and

patients' age was somehow younger compared to the other two subclasses. In addition, these groups showed unique mRNA expression of their signature markers that correlate with their phenotype with no combined expression of more than one signature gene set. However, some tumors tend to undergo ProN to Mesen transition upon recurrence, a feature that is associated with aggressive behavior and resistance to therapy (35). In fact, Prolif and Mesen tumors are characterized by aggressive features of extensive proliferation and angiogenesis, respectively that lend a poor prognosis feature on these two groups. To complete such picture of grim outcome, both Prolif and Mesen tumors were found to express markers of stem cells although Prolif tumors were also expressing markers of more downstream transit-amplifying cells which is consistent with such proliferative behavior.

By incorporating genomic data into the expression analysis, both Prolif and Mesen tumors showed deletion of chromosome 10 (and the consequent PTEN loss) and gain of chromosome 7 (and the consequent EGFR amplification) in contrast to ProN that showed intact form of both chromosomes. Further analysis of PTEN expression revealed low PTEN mRNA levels in Prolif and Mesen tumors that negatively correlated with AKT hyperphosphorylation, the dominant active signaling in these two groups. On the other hand, ProN mostly showed mRNA overexpression of two NOTCH ligands (DLL1and DLL3) and one target gene (Hey2) that put NOTCH as the dominant active signaling in ProN tumors. However, no overexpression of other NOTCH pathway constituents (NOTCH receptors, other ligands or targets) has been reported (35). Although the authors related this active NOTCH signaling in ProN tumors to better prognosis especially with high PTEN mRNA levels, it is noteworthy to take in consideration the role of NOTCH

signaling in ProN to Mesen transition and this active NOTCH signaling in ProN tumors may conspire with other pathways to favor Mesen phenotype upon recurrence.

Finally, although this and other studies provided the foundation for glioma classification based on transcriptional analysis, some drawbacks have been reported to such profiling. Most importantly, mRNA stability is highly affected during surgery or fixation procedures which may result in some degree of underestimation of gene expression and poor reproducibility. In addition, mRNA levels provide specific picture of gene expression at certain time that can be affected by regulation from other signals. Moreover, mRNA levels may not reflect the actual translated and active protein levels because of differential translational efficiencies that are usually affected by feedback mechanisms which may result in poor correlation between mRNA and protein levels (49). In addition, post-translational modification is one of the major mechanisms to achieve active signaling in many pathways such as NOTCH cleavage and β-catenin stabilization. Therefore, direct proteomic profiling of certain pathways' components is crucial to fully describe the real picture of cellular signal transduction.

1.2.3 Proteomic analysis

The implication of proteomics approach in glioma taxonomic classification has an advantage of determining whether the previous identified glioma molecular subclasses, on the basis of genomic and transcriptional analyses, explain the real biological differences among tumors within certain grade and predict the clinical outcome of such histologically similar diseases. In fact, this new approach has recently segregated GBM into different subtypes according to protein expression of certain pathways' constituents' relevant to glioma pathology (50).

In a targeted proteomic analysis of 20 GBM samples, Brennan and coworkers performed unsupervised clustering of 57 proteins (or protein products) and identified three major GBM subgroups defined by proteins associated with EGFR overexpression, PDGF overexpression or NF1 silencing in a mutual exclusive manner (50). EGFR core showed high levels of Wnt signaling (stable β-catenin) and active NOTCH signaling (ligand, cleaved receptor and target genes). PDGF core showed high levels of mTOR and its downstream targets beside sonic hedgehog (SHH) expression. NF1 silencing was associated with upregulation of mesenchymal markers such as YKL40 and vascular endothelial growth factor A (VEGFA). Interestingly, despite the small sample size, this approach identified some degree of genomic or transcriptional underestimation of certain pathways' constituents. For instance, some highly expressed signaling proteins were poorly correlated with their mRNA levels such as PDGF. Other proteins were overexpressed but had no change in their copy numbers such as NOTCH (50). Therefore, using integrated profiling schemes constitutes of copy number, mRNA and protein analyses will result in more precise and accurate estimation of certain protein-mediated biology and glean more biologically important information about such protein-based biomarkers.

1.3 General characteristics and histological features of glioma

1.3.1 Glioma stem cells (GSCs)

Cancer stem cells (CSCs) are subset of slowly proliferating cancer cells, located in rapidly growing tumor bulk, that are able to disseminate the malignancy and defy therapeutic interventions. The idea of CSCs was a brainchild of the pathologists Rudolph

Virchow and Julius Cohnheim in the early 1860s. They observed certain histological similarities between the developing embryonic tissues and cancer tissues (such as teratocarcinomas) in terms of their abilities to proliferate and differentiate (51). In the early 1990s, stem-like cells have been discovered in leukemic patient-derived-cells as they were shown to be leukemogenic when they were injected into mice (52). Thereafter, CSCs have been isolated from other types of cancer such as pancreatic cancers (53), breast cancers (54) and prostate cancers (55).

A growing body of evidence suggests that gliomas are initiated from CSCs in the brain. In 2002, CSCs have been isolated from brain tumors for the first time by Ignatova and co-workers, where surgical specimens of human GBM were shown to be clonogenic and able to form neurospheres similar in morphology to those generated by neural stem cells (NSCs) (56). Interestingly, these clones were triple positive for NSC marker (CD133), neuronal marker (β-III tubulin) and the broad astrocytic marker (glial fibrillary acidic protein, GFAP) (57). In correspondence to NSCs, these clones were named as glioma stem cells (GSCs). Glioma-derived neurospheres are tumorigenic when transplanted into SCID mice as reported by Singh et al in 2004. The injection of 100 CD133-positive GSCs derived from patients' tumor was able to form secondary tumors that are phenotypically similar to the original tumor. In contrast, CD133-negative cells were not able to form a tumor when injected in similar manner even with very high cell number such as $1*10^5$ cells (58). Interestingly, it has been found that GSCs are responsible for glioma initiation, progression, recurrence and resistance to treatment through an active DNA damage repair and expression of multidrug transporters (59). Besides, GSCs have an essential role in angiogenesis by secreting VEGFA (60).

Moreover, bevacizumab (anti-VEGF neutralizing antibody) can terminate the proangiogenic effects of GSCs on endothelial cells (60). Further, several regulatory signaling pathways have been identified to maintain a pool of GSCs including NOTCH, PI3K/AKT, c-Myc and STAT3 (61-63). Taken together, these observations explain the real signature of glioma as a hierarchy of cancer cells inferior to a small population of stem-like cells that represent GSCs which provides a powerful model to investigate the tumorigenic process in human brain and develop therapeutic strategies to target GSCs population.

1.3.2 Epithelial to mesenchymal transition (EMT)

The epithelial to mesenchymal transition (EMT) is an orchestrated process during which the well polarized epithelial cells acquire a motile mesenchymal phenotype through a series of modulatory events in cell architecture and behavior via cell-cell and cell-extracellular matrix (ECM) interactions (64). As a result, the new modulated cell is released from the surrounding tissue with a new gene expression profile that maintains the mesenchymal phenotype (64). EMT is essential for many physiological and pathological responses such as wound healing and tissue regeneration that requires gain of migratory and invasive features (65). Besides, EMT is crucial for implantation and organ formation during embryonic development (65). In neoplastic cells, EMT conspires with genetic changes that favor clonal outgrowth of localized tumors to promote a mesenchymal phenotype, a condition that confers unusual ability for the cell to invade and stimulate angiogenesis and eventually provokes the final, life-threatening picture of tumor growth (66).

Several developmental EMT signaling pathways have been identified including Wnt, TGF-β and NOTCH (67). These pathways usually act upstream to certain transcription factors regulating the real process of EMT such as Snai1, Slug, ZEB1, ZEB2, Twist1 and Twist2 (67). Known similarities between developmental and oncogenic EMT processes have led to the hypothesis that aberrant activation of these signalling pathways and downstream EMT regulators can lead to oncogenic EMT and cancer progression. For instance, in malignant glioma patient specimens, positive correlation has been found between upregulated active NOTCH signaling and the expression of the EMT markers such as Snail (68). Further *in vitro* experimental analysis revealed that NOTCH acts upstream of Snai1 to confer invasive ability and mesenchymal phenotype to glioma cells (68).

Other transcriptional profiling studies have demonstrated that mesenchymal signature genes are overexpressed at the account of proneural signature genes in subset of glioma patients with poor prognosis (69). However, such genome-wide expression studies revealed many cancer signature genes that require additional cellular-network analysis (69). Reconstruction of these regulatory networks using a special algorithm inferred that C/EBPb and STAT3 are mesenchymal phenotype driving genes of prognostic value (69). Patients with tumors that are double-positive for C/EBPb and STAT3 tended to have shorter survival when compared to patients with tumors that are single- or double-negative (69). Further experimental validation confirmed that these two genes are global regulators of mesenchymal transformation in NSCs and necessary to maintain mesenchymal phenotype in human glioma cells *in vitro* and glioma aggressiveness *in vivo* (69).

Based on such findings, this will raise the question if there is any potential crosstalk between GSC theory and the EMT process. In fact the idea of GSCs became an attractive model of tumor recurrence and resistance to therapy. Despite maximal surgical resection of tumor beside radiotherapy and adjuvant chemotherapy, tumor recurrence in the primary site or in the adjacent brain tissues is often a considerable challenge that is an intensive area of research (70). A single proposed mechanism of glioma relapse and recurrence is tumor invasion to the surrounding tissues that substantially reduces the effectiveness of therapeutic approaches (70). Sustained invasive growth of recurrent glioma requires migration of GSCs from the primary tumor followed by their incorporation in the new site to initiate a secondary glioma. A new model has been recently proposed to explain this process, the migrating stem cells (71). This model has been discussed in several studies to further correlate EMT and invasion processes the idea of GSCs.

Mani et al. has reported that EMT can generate cancer cells with stem-like properties (72). Upon acquisition of EMT phenotype at tumor-host interface, GSCs become a double-edged sword with both stemness and mesenchymal properties. Unlike other tumors that usually metastasize, this may explain to a certain extent one of the hallmarks of recurrent glioma, namely tumor invasion. In a recent report, Cheng et al. found that high expression profile of EMT markers (such as Slug) is correlated to high grade (vs. low grade) glioma and to high expression levels of the putative GSC marker, CD44, which also has been reported to promote glioma cell migration and invasion *in vivo* and *in vitro* (73-75). Moreover, high EMT marker expression is associated with low initial response to therapy and shorter time to recurrence (75). Furthermore, certain

transcription factors and signaling pathways are responsible to maintain both the stemness and the mesenchymal signatures such as STAT3 and NOTCH which contribute to tumor aggressiveness of human glioma (63, 67, 69). Therefore, it is noteworthy to explore altered signaling pathways that provide the transcriptional signature necessary for enrichment of GSCs and mesenchymal phenotype of malignant glioma.

1.3.3 Extensive angiogenesis

Angiogenesis, a process of forming new blood vessels, is a critical step for supplying oxygen and nutrients necessary for metabolic purposes, cell proliferation and expansion of the tumor mass (76). Other mechanisms involved in new blood vessel formation include differentiation of GSC into vascular endothelium in addition to the vasculogenesis, which is another mechanism that involves recruitment of endothelial progenitor cell (77, 78). Ultimately, all these processes result in an inefficient angiogenesis associated with areas of hypoxia, necrosis and edema (79). By targeting angiogenesis, cancer cells will be deprived of nutrients and thus the tumor growth is blocked.

Among all glioma grades, only GBM shows high level of microvascular proliferation and areas of necrosis since all other grades do not require neo-vascularization, rather, they acquire their blood supply of oxygen and nutrients from existing blood vessels (80). However, progression of lower grades into GBM (although not common) as a result of high cell proliferation results in initiation of angiogenesis as a response to hypoxia by the hypoxia inducible factor-1 (HIF-1α) (81). HIF-1α is overexpressed in GBM and well known to induce VEGF expression in hypoxic conditions (81). There is increasing evidence supporting that GSCs are maintained with a

vascular niche which in turn is maintained with VEGF secreted by GSCs and acting through VEGFR-2/KDR (60). This bi-directional relationship puts VEGF pathway as the rate-limiting step of angiogenesis.

In fact, what comprising the angiogenesis transition is the balance between pro- and anti-angiogenesis factors (82). Other mediators that have been shown to play a central role in angiogenesis in GBM include NOTCH, angiopoietins, PDGF, FGF, integrins, ephrins and IL-8 (83-85). On the other hand, endogenous inhibitors of angiogenesis oppose the action of these mediators which include angiostatin, thrombospondins, endostatin, tumstatin, and interferons (82). Recently, several anti-angiogenic inhibitors have been developed to be used in GBM, most commonly targeting VEGF ligand or VEGFR-2/KDR, the key players in the angiogenesis process (86, 87).

In 2009, bevacizumab was approved by the FDA for recurrent GBM and is now currently used in the clinic (88). In fact, this approval came after several clinical trials that have been conducted to evaluate bevacizumab efficacy (86, 89). Two phase II trials evaluated bevacizumab and irinotecan combination, one in high-grade gliomas and the other only in GBM (86, 89). In both trials, the combination showed superior efficacy compared with controls which was represented by 50% increase in both 6-month progression-free survival (PFS) and median survival (86, 89). However, the potential occurrence of short or long-term side effects is common and unpredictable which includes gut perforations, bleeding, thrombosis and impaired wound healing (85). Besides, long-term use of anti-angiogenic drugs has led to emergence of resistance since various mediators involved in angiogenesis are up-regulated as a compensatory mechanism (85). In addition, when patients on long term anti-angiogenic therapy

developed recurrence, they showed rapid disease progression and failed to respond well to additional chemotherapy (90, 91) which highlights the need for new therapeutic approach based on more understanding of the vascular biology and the collateral pathways involved in such vital process for tumor growth. Anti-angiogenesis combination therapy targeting multiple pathways is now a new trend of the current clinical trials to overcome redundant vascular pathways and thus drug resistance. One of the ongoing clinical trials of such combination targeted drug therapies is combination of NOTCH inhibitors and bevacizumab (clinicaltrials.gov).

1.3.4 Oncogene addiction

The term “oncogene addiction” has been initially coined by the physician Bernard Weinstein in the late 1990s when he observed that in esophageal cancer cells overexpressing cyclinD1, a single inhibition of this protein was enough to arrest cell cycle and malignant growth (92). He proposed that cancer process is a multistage scenario driven by the accumulation of chromosomal, genetic and epigenetic abnormalities during which the cancer cell malignant phenotype and survival can be addicted to a single gene (or pathway) aberration (92). Surprisingly, reversal of this abnormality is able to abolish the growth of tumor cells, suggesting that the cancer cell growth program is highly dependent on such an oncogene (92). In fact, inactivation of the normal negative regulator of this addicted oncogene product is well-tolerated in non-cancer cells which suggests that the cancer cell genetic network has been re-programmed to gain such addiction (93).

Evidence of this concept has been obtained from *in vitro* and *in vivo* experimental studies and from clinical trials conducted in cancer subjects (Table 1.4) (94). First, simple

RNA interference (RNAi) directed against single oncogenes can profoundly inhibit the growth of human cancer cell lines, increase sensitivity to chemotherapy and inhibit *in vivo* tumorigenicity. Such oncogenes include HER2/neu, K-ras, β-catenin, cyclin D1 and cyclin E1 in human cancer cells of breast, pancreas, colon and liver cancers (94). Second, transgenic mice overexpressing c-myc, Bcr-Abl, H-ras, K-ras, Her-2/neu, or Wnt developed T-cell leukemias, myelocytic leukemia, melanoma, lung tumors, pancreatic β-cell tumors and breast tumors, respectively (94). Conversely, switch off of certain oncogenes such as c-myc results in tumor regression (94). However, some tumors showed partial regression and recurrence which was explained by a switch in addiction to another oncogene such as c-myc/K-ras switch and Her-2/Snai1 switch in breast cancer (94). Finally, the concept of oncogene addiction was also obtained from prospective randomized trials. Targeting specific oncogenes using monoclonal antibodies or small molecules have been evaluated in several human cancers (94). For instance, trastuzumab, which targets the receptor tyrosine kinase HER-2/neu, has been shown to improve survival rates in patients with metastatic breast cancer when given in combination with paclitaxel (95).

Several genetic aberrations have been identified to have significant clinical relevance to glioma pathogenesis. However, these well-identified regulatory signal alterations fall in a large number of aberrations at both single molecular and pathway levels. Therefore, identifying oncogene addiction for these novel targets followed by inhibition of this addicted oncogene(s) will add another criterion for glioma molecular subtyping beside the known histological classification. One such example is the use of small molecules receptor tyrosine kinase inhibitors (RTKIs) that target EGFR which is

known to be amplified or overexpressed in 45% of gliomas. Targeting EGFR using RTKIs is one of the current modalities of choice in lung cancer which results in 60% response rate exceeding that for conventional chemotherapy (96). Interestingly, RTKIs have shown cytotoxic effects in glioma tumors harboring oncogenic EGFR. However, this response was only observed in certain contexts represented by co-existence of oncogenic EGFR with intact PTEN (97). In phase II trial evaluating RTKIs as monotherapy, the 12-month survival was achieved by 57% of patients with non-progressive GBM receiving erlotinib in post-radiation settings (98). However, it did not show any benefit to patients with recurrent GBM which suggests activation of other oncogenic RTKs that could result in addiction switch and thus tumor resistance (99). In such contexts, deep identification of the addicted oncogene or targeting multiple oncogenes is required to achieve therapeutic outcome.

Another potential oncogene addiction in glioma is E2F1 addiction which acts downstream to Rb and regulates the G1 checkpoint (100). E2F1 is a transcription factor that has been shown to be overexpressed and/or overactive in most of human gliomas which suggests that to certain extent glioma cells are addicted to this protein (100). In fact, a positive auto-regulatory loop for E2F1 has been identified to be highly active in case of Rb axis disruption (100). Interestingly, restoration of Rb activity has effectively inhibited E2F1 activity *in vitro* (101). In addition, the use of an oncolytic virus has been recently introduced in glioma studies (100). This virus represents a mutant form of adenovirus that exploits the free E2F1 activity in disrupted Rb-axis cells to activate viral replication and eventually kill the tumor cells (100). What is attractive in this approach is the absence of viral replication in normal astrocyte cells that are normally having an

active Rb-axis which inhibits E2F1 activity and thus viral replication (100). Although several oncolytic viruses have shown promising efficacy and safety results in preclinical studies, the clinical efficacy has not been achieved in glioma clinical trials which could be related to the fact that in contrast to small molecule, the biological activities of viruses are highly variable when tested in one species compared to others (102).

Overall, identification of network addiction instead of individual oncogene addiction using high throughput screening and establishing combinations of target therapies directed to these networks may be one of the potential approaches toward personalized medicine in glioma.

1.4 The NOTCH pathway: Role in glioma development

1.4.1 NOTCH biology and signaling

The NOTCH gene was discovered, for the first time, by Thomas Morgan in 1917 in the fruit fly Drosophila melanogaster with phenotype consisting of “notches” at the margin of adult wing (3). Analysis of NOTCH loss-of-function mutations showed an expanded neuroblast population at the expense of epidermal cells in fly embryos (103). This mutation was described as a neurogenic mutation in which the wild type NOTCH promotes the differentiation of ectoderm cells into epidermis rather than neuroblasts which provided the first evidence that NOTCH determines the cell fate decision between neuroblast and epidermal cells during Drosophila development. In 1983, NOTCH gene was cloned for the first time by Artavanis-Tsakonas and co-workers (104). NOTCH gene encodes a transmembrane receptor which is a hetero-oligomer that is mainly composed of two subunits that are bound together by non-covalent interactions. The outer subunit

consists of a large portion of the extracellular domain (ECD), and the inner subunit is composed of a small portion of the ECD, the transmembrane domain and the intracellular domain (ICD). The ECD is comprised of 36 tandem epidermal growth factor (EGF)-like repeats, responsible for ligand binding, and 3 LIN12/NOTCH repeats that prevent ligand independent receptor activation. The ICD is mainly composed of four conserved domains: the RBP-Jκ-associated module (RAM) domain, ankyrin (ANK) repeats, two nuclear localization signals (NLSs) and the praline/glutamate/serine/threonie-rich (PEST) domain that is involved in protein degradation (105).

In mammals, there are four NOTCH receptors (NOTCH1-4) and five NOTCH ligands, namely: jagged 1 (JAG1) and JAG2 in addition to delta-like ligand 1 (DLL1), DLL3 and DLL4 which are also transmembrane proteins (106). NOTCH signaling is mediated by cell-to-cell contact and initiated via binding a NOTCH ligand to a NOTCH receptor. This binding induces conformational change in the ECD and triggers two successive cleavages by the metalloproteinase tumor necrosis factor-α-converting enzyme (TACE or ADAM) and the presenilin–γ-secretase complex that releases the active ICD (Figure 1.2). The translocation of the ICD into the nucleus leads to its binding to the CSL (CBF1/RBP-Jk, Suppressor of Hairless, LAG-1) repressor complex and recruitment of the co-activator protein mastermind-like 1 (MAML1). This transcriptional complex is required for activation of NOTCH target genes such as the basic-helix–loop–helix (bHLH) transcriptional repressors hairy enhancer of split (HES) family, the hairy-related transcription factor (HRT or HEY) family, cyclin D1 and c-MYC (105, 107). HES (Hes1, 5, 7) and HEY (Hey1, 2, L) families are transcriptional repressors which inhibit the expression of proneuronal bHLH proteins (Mash-1 and Hash-1) to promote glial

(astrocytic) fate (108). Other NOTCH targets include GFAP, p21 and p53 (106). Targeting this pathway at any point results in its inactivation and prevents expression of NOTCH effector genes. The only available therapy is the γ-secretase inhibitors (GSIs) which block the terminal cleavage and hinder the release of the active ICD (106).

1.4.2 NOTCH role in glioma

In 1991, NOTCH has been shown, for the first time, to be involved in human cancer when Ellisen and coworkers reported that the acute T cell lymphoblastic leukemia (T-ALL) translocation t(7;9)(q34;q34.3) gives rise to a constitutively active NOTCH1 ICD domain which in turn responsible for the neoplastic transformation of T cells (109). However, intensive research on wide range of human cancers revealed that NOTCH can act as oncogene or tumor suppressor gene depending on the cellular context (110). For instance, NOTCH has a tumor suppressor function in skin, in which it induces cell differentiation by inhibiting proliferation pathways and upregulating cell cycle inhibitors (111). On the other hand, NOTCH is oncogenic in variety of solid tumors, with gene amplification in ovarian, breast and lung cancers, in which amplification of NOTCH3 locus is the driving force of aggressive tumor behavior and poor patient survival through crosstalk with EGFR/RAS/MAPK signaling and activation of other proto-oncogenes (112-114). In addition, Hes1 which is a known effector of NOTCH negatively regulates the expression of PTEN (a known PI3K/AKT pathway inhibitor) (115), reflecting the significance of NOTCH pathway activation in human cancer.

In human brain, NOTCH is important in stem cell maintenance, binary cell division and terminal differentiation (116-118). NOTCH has a pivotal role in maintaining a pool of NSCs at the account of the more differentiated progenitors. In addition,

NOTCH promotes differentiation of neural precursors into glial cells versus neurons and particularly into astrocytes versus oligodendrocytes (116-118). In line with this, the major oncogenic function of NOTCH in gliomas is based on maintaining a pool of GSCs by preventing their differentiation into intermediate neural progenitors (119). Besides, constitutive overexpression of NOTCH in NSCs results in formation of human glioma like tumors in mouse brain (120). Targeting NOTCH by GSIs exhausts GSCs by suppressing proliferation and promoting differentiation (119), suggesting the central role of NOTCH pathway in gliomagenesis.

Other oncogenic functions of NOTCH include promoting glioma cell proliferation and invasion and inhibition of apoptosis in cooperation with major aberrant signaling pathways (121, 122). In fact, proteomic analysis of GBM revealed the presence of expression patterns of glioma-relevant signaling pathways components (50). In particular, overexpressions of NOTCH ligands (DLL1 and JAG1), NOTCH1 ICD and downstream effector Hes1 are eminently correlated with EGFR amplification in GBM (50) which in turn associated with the allelic loss of the CDKN2A locus (123). Moreover, NOTCH1 has been found to regulate EGFR transcription through p53 (124). Furthermore, inhibition of NOTCH1 via siRNA results in proliferation inhibition and apoptosis induction in glioma cell lines (122). These findings implicate NOTCH pathway as an activator of EGFR pathway, the major altered regulatory signal in GBM; and open new insight toward combining NOTCH and EGFR inhibitors in such glioma subgroups which will be directed to GSCs population and survival pathways.

Loss of chromosomes 1p/ 19q signature has been linked to the better outcome of oligodendroglioma patients (22). Further analysis to explore for the underlying tumor

suppression etiology of this signature revealed distinct deletions converge to the NOTCH2 gene (which is mapped to chromosome 1p) that correlates positively with patient survival (125). In addition, loss of function mutation in the NOTCH2 RAM domain (at which ICD binds to CSL) has been shown to abolish NOTCH2-mediated activation of downstream genes (121). As stated earlier, TNC is a glycoprotein that has been found in invasive GBM. In fact, NOTCH2 loss of function mutation has been correlated to the absence of TNC expression in glioma cell line Hs683 as a result of impaired NOTCH2-mediated activation of TNC promoter and thus prevention of TNC-mediated invasion in GBM (121). Recent studies have related NOTCH-induced glioma invasion to β-catenin and matrix metalloproteinases (MMPs) stimulation via activation of AKT pathway (68, 126). Interestingly, inhibition of both NOTCH and AKT pathways via GSI and AKT inhibitor respectively, has superior effects on glioma cell migration and invasion than either drug alone (127). Together, these findings implicates NOTCH pathway in promoting glioma cell migration and invasion and illustrate the importance of targeting NOTCH in glioma as one of the routes to minimize tumor recurrence.

Sustained tumor growth requires consistent blood supply that is mediated by soluble factors secreted by tumor cells (128). VEGF-induced angiogenesis is the principal mediator that offers the necessary route for oxygen and nutrients supply (129). As stated earlier, emergence of resistance to angiogenesis inhibitors (most commonly VEGF inhibitors) is a major clinical problem. NOTCH has been implicated as one of the mediators of tumor angiogenesis. Therefore, studying the contribution of NOTCH in mediating resistance to angiogenesis inhibitors in glioma is an attractive area of research. A study from Jargon group showed that DLL4- NOTCH signaling can confer resistance

to anti-VEGF therapy. In this study, when glioma cell lines were infected with retroviruses encoding DLL4 and grown as tumor xenografts, formation of large blood vessels and resistance to bevacizumab were observed. Conversely, inhibition of NOTCH signaling via GSI inhibited the large vessel formation and abolished the tumor resistance to bevacizumab (130), suggesting that NOTCH could be one of the important pathways involved in resistance to VEGF inhibitors.

Figure 1.3 illustrates a summary of the NOTCH role in glioma with GSIs as potential therapeutic strategies. These contributions to glioma pathogenesis have not been solely referred to a single NOTCH receptor, rather for active signaling of one or more NOTCH receptor. However, it is worth noting that NOTCH receptors have a context dependent function in human cancer that highlights possible divergent roles of NOTCH in glioma (122). In addition, the function of NOTCH in human glioma has not been well-established for all NOTCH receptors and gliomas are genetically complex. Therefore, to optimize the utility of GSI therapy in malignant glioma, understanding the functional role of all NOTCH receptors in glioma is necessary as GSIs are non-specific inhibitors. Given that, this may uncover the prognostic or predictive values of one or more NOTCH receptors and establish GSIs as a new targeted therapy in malignant glioma.

1.5 Objectives

As discussed above, NOTCH receptors have been implicated in many human cancers and particularly in glioma. Despite the well-known oncogenic role of NOTCH1 and NOTCH2 in glioma, additional investigations for a potential oncogenic function of other NOTCH members are needed to fully utilize GSI therapy in malignant glioma. In a

preliminary study, we identified a number of CNAs in a comprehensive tumor specimen population. Specifically, we demonstrated that patients with chromosome 19 amplification have the poorest prognosis. Further genetic analysis revealed NOTCH3 as a candidate oncogene mapped to chromosome 19. However, the *in vitro* and *in vivo* relevance of this genetic signature is currently unknown. So, the overall objective of this research is to conduct an investigational study on glioma cell lines to evaluate the putative oncogenic role of NOTCH3 amplification and to delineate mechanisms of its aggressiveness, as explained in the following objectives and specific aims:

Objective 1: Validation of NOTCH3 as an active oncogene of prognostic value.

Specific Aim 1.1: Determine whether NOTCH3 amplification is associated with active NOTCH3 signaling (Chapter 2, section 2.3.4).

Specific Aim 1.2: Evaluate the prognostic significance of NOTCH3 gene amplification (Chapter 2, section 2.3.4).

Objective 2: Evaluation of NOTCH3 as a critical element in gliomagenesis.

Specific Aim 2.1: Determine the functional role of NOTCH3 in glioma (Chapter 3, sections 3.3.1-3.3.3)

Specific Aim 2.2: Determine the molecular mechanisms of NOTCH3 oncogenic function (Chapter 3, section 3.3.3).

Objective 3: Evaluation of NOTCH3 as a potential target of therapy in glioma.

Specific Aim 3.1: Determine the consequences of NOTCH3 modulation on response to conventional chemotherapy (Chapter 3, section 3.3.4).

Specific Aim 3.2: Analyze the effects of a NOTCH inhibitor on glioma cell lines (Chapter 3, section 3.3.4).

Table 1.1: Common chromosomal alterations in glioma according to glioma grade.

Chromosomal region	Gain vs. loss	Grade
1p arm	Loss	Grade II and III
Whole chr.7	Gain	Grade III and IV
9q arm	Gain	Grade III and IV
9p arm	Loss	Grade III and IV
Whole chr.10	Loss	Grade III and IV
19q arm	Loss	Grade II and III
Whole chr.19	Gain	Grade III and IV
22q arm	Loss	Grade III and IV

Table 1.2: Summary of the three major altered pathways in malignant glioma.

	Alteration of P53 signaling	**Alteration of Rb signaling**	**Alteration of RTK/RAS/PI3K signaling**
Reported alterations	- TP53 mutation or deletion - CDKN2A deletion - MDM2 or MDM4 amplification - p14ARF methylation	RB1 mutation or deletion - CDK4, CDK6, or CCND2 amplification	- EGFR, ERBB2 PDGFRA or MET mutation or amplification - PI3K, RAS or AKT mutation - NF1 deletion - PTEN deletion
Functional consequences	- Loss of p53 expression or activity - Absence of G1/S transition block	- Loss of Rb expression or activity - Absence of G1/S transition block	- Activation of RTK/RAS/PI3K signaling - Activation of cell proliferation, invasion and inhibition of apoptosis

Table 1.3: Summary of glioma subtypes based on transcriptomic analysis.

	ProN	**Prolif**	**Mesen**
WHO grade	Grade III or IV	Grade IV	Grade IV
Age	Younger (<40)	Older (>50)	Older (>50)
Prognosis	Better	Poor	Poor
Active process	Neurogenesis	Proliferation	Angiogenesis
Cell marker	Neuroblast	Stem cell marker	Stem cell marker
Chr. CNA	Normal chr.7 Intact chr.10	Gain of chr.7 Loss of Chr.10	Gain of chr.7 Loss of Chr.10
EGFR/PTEN loci	Normal EGFR Intact PTEN	Amplif. of EGFR Loss of PTEN	Amplif. of EGFR Loss of PTEN
Signaling	NOTCH	AKT	AKT
Origin	Primary	Primary	Primary or ProN-Mesen transition

Table 1.4: Evidence of oncogene addiction from studies conducted on mice, human cancer cell lines and clinical trials.

In vitro evidence		
Oncogene addiction	**Cancer cell line**	
HER2/neu	Breast	
K-ras	Pancreatic	
B-catenin	Colon	
CyclinD1	Colon, pancreatic	
CyclinE1	Liver	
In vivo evidence		
Oncogene addiction	**Cancer type**	
C-myc	T-cell and acute myeloid Leukemia, Pancreatic β-cell, osteogenic sarcoma, breast	
Bcr-Abl	Leukemia	
H-ras	Melanoma	
K-ras	Lung	
Her-2/neu	Breast	
Wnt-1	Breast	
Clinical evidence		
Oncogene addiction	**Cancer type**	**Targeted therapy**
HER-2	Breast	Trastuzumab (combination)

Table 1.4: Continued.

BCR/ABL	Chronic myeloid leukemia	Imatinib (monotherapy)
EGFR	NSCLC	Gefitinib, erlotinib (monotherapy)
EGFR	Head and neck, colorectal	Cetuximab (combination)
EGFR	Pancreas	Erlotinib (combination)
VEGF	Breast, colorectal, kidney	Bevacizumab (combination)
VEGFR, RAF	Kidney	Sorafenib (monotherapy)

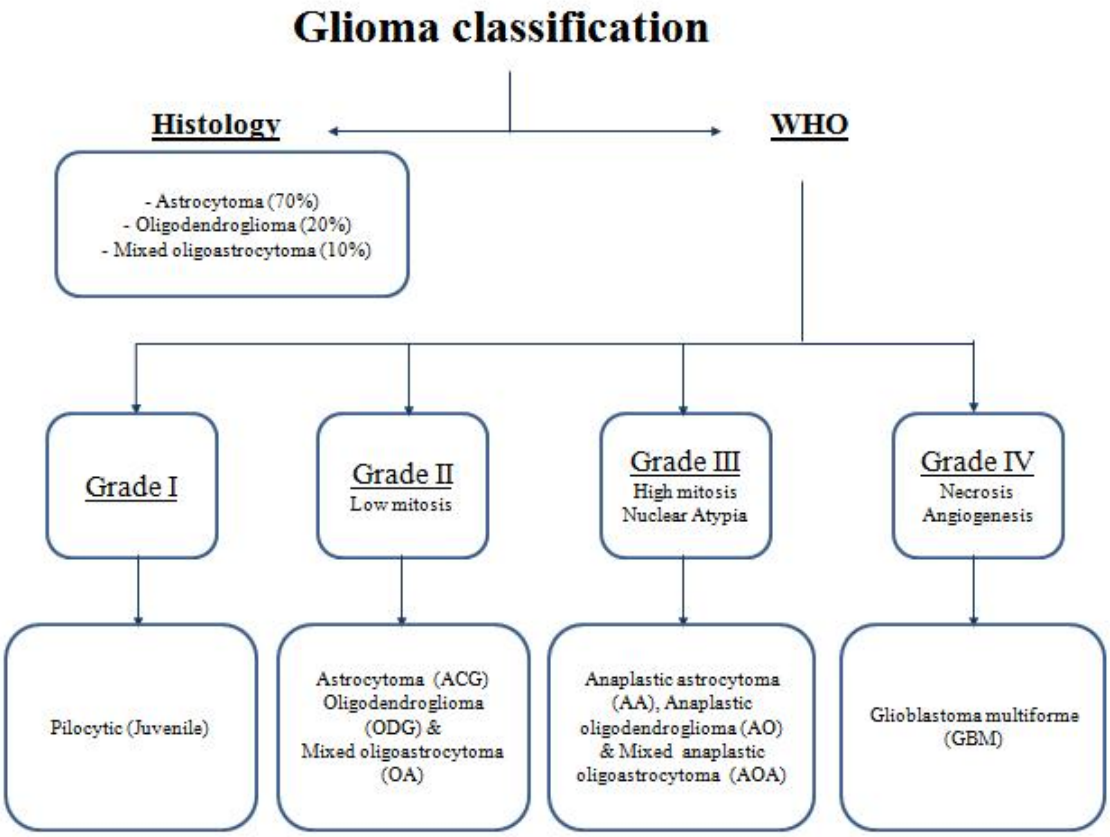

Figure1.1: Classification of glioma according to histology and to the World Health Organization (WHO) grading system. The WHO classification is based on other histological features of each grade in addition to the lineage of origin.

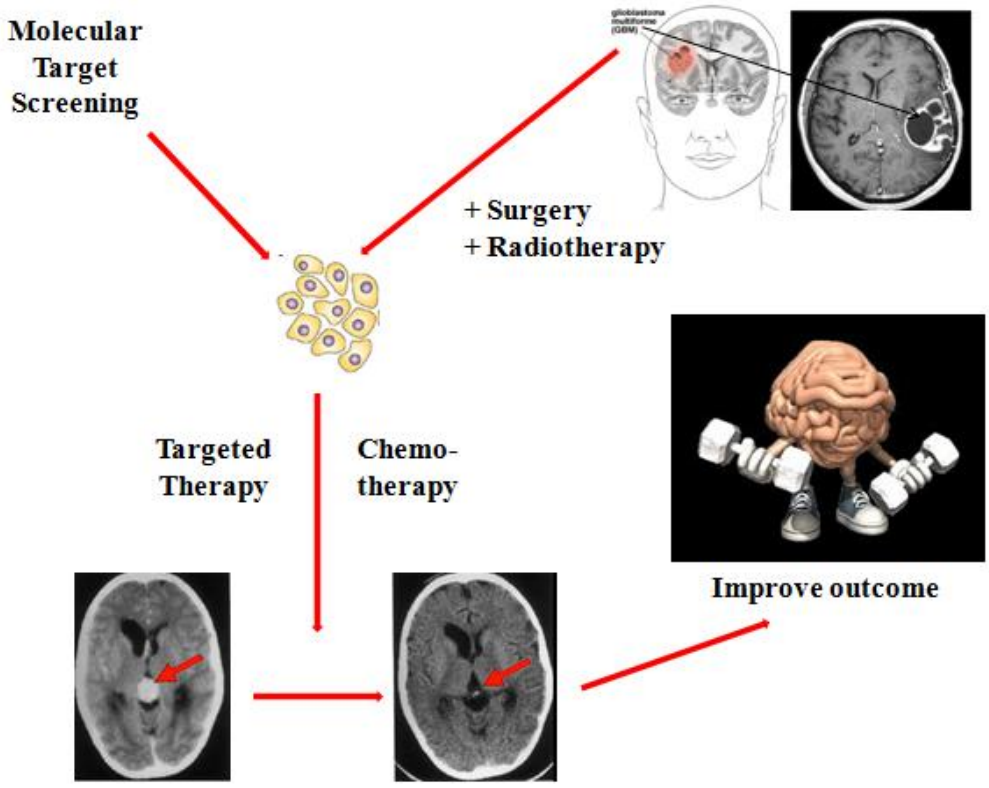

Figure1.2: The role of translational research in glioma therapy. Analysis of deregulated pathways in tumor biopsies obtained after surgery will help in identifying new molecular targets and developing new targeted therapies that can be given along with chemotherapy to prevent tumor resistance and recurrence and improve outcome.

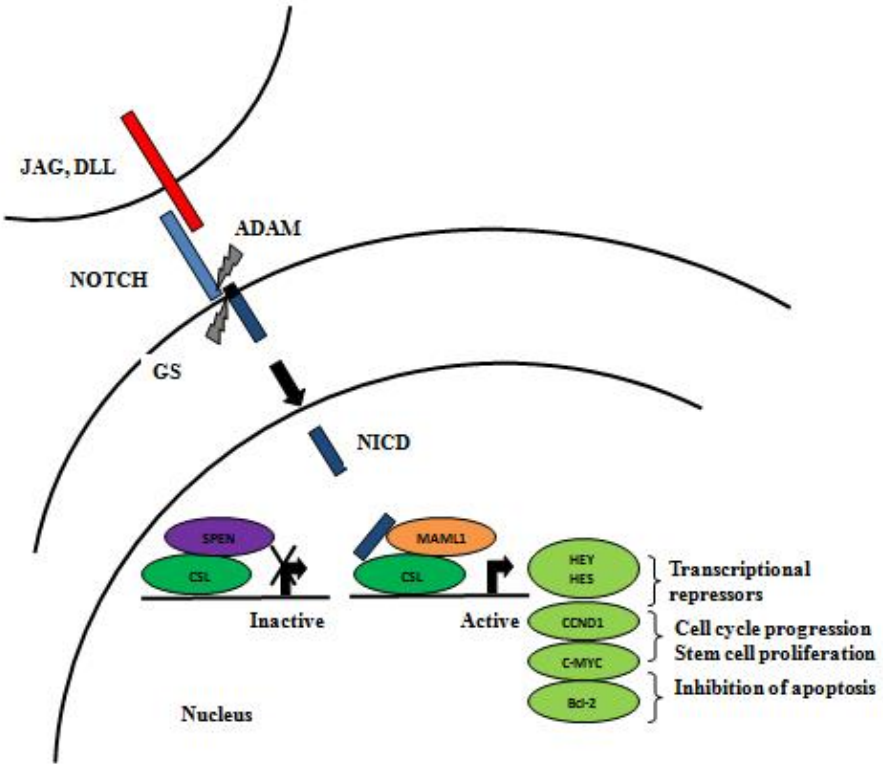

Figure1.3: The NOTCH signaling pathway. Proteolytic processing of NOTCH receptors via metalloprotease (ADAM) and secretase (GS) cleavages leading to NICD generation that act as a transcriptional activator of target genes.

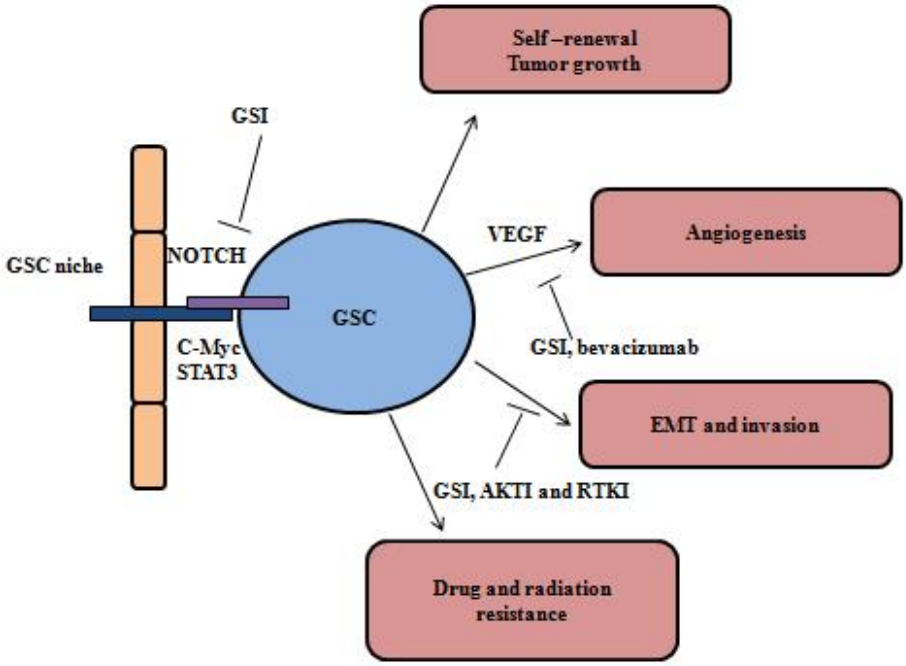

Figure1.4 : Contribution of NOTCH signaling to glioma pathogenesis. NOTCH maintains GSC pool which in turn mediates various cellular processes responsible for tumor progression. Potential therapeutic strategies are shown.

CHAPTER II

GENOMIC ANALYSIS OF MALIGNANT GLIOMA REVEALED NOTCH3 AS A POTENTIAL ONCOGENE THAT IS ASSOCIATED WITH POOR PROGNOSIS

2.1 Introduction

High grade gliomas are one of the major subtypes of glioma that include either grade III or IV by the WHO system (6). In contrast to low grade gliomas, many high grade gliomas have poor prognosis resulting mainly from high levels of cell proliferation, invasion and extensive angiogenesis (19). These hallmarks of glioma make the surgery difficult and increase the incidence of tumor recurrence and resistance to therapies, in particular to combined chemo- and radiotherapy (19). Some tumors may have some initial response; nonetheless, these tumors show rapid recurrence with short term survival which highlights the need for better therapeutic approaches (131). Many studies aim at overcoming these sources of resistance through identifying potential prognostic and predictive biomarkers. The only valid prognostic factors in malignant gliomas include age, Karnofsky Performance Status (KPS) and histology (132, 133). Other criteria that may be used to predict a response to therapy and patient outcome include tumor location, extent of surgical resection and proliferation indices (6). However, these additional factors are not globally of prognostic and predictive values. Although it has not been discovered yet, a current search for robust molecular factors is an intensive area of research that may aid in predicting patient prognosis and response to therapy and improve outcome. The most recent and promising trend is to explore genetic alterations in cohorts of tumor specimens.

There is increasing evidence about the relevance of certain genetic alterations in malignant gliomas to chemosensitivity and patient survival. For instance, more than 50% of oligodendrocytic lineages have chromosomes 1p/19q codeletions (23, 134). In fact, regardless of histological classification in gliomas, this chromosomal aberration has been recently shown to correlate with higher sensitivity to chemotherapy and better prognosis (23, 135, 136). However, whether these patients are treated with PCV (procarbazine, CCNU, vincristine) or radiotherapy, they still have superior prognosis which reflects the prognostic rather than the predictive value of chromosomes 1p/19q codeletions (136).

In human cancers, chromosomal gains have been shown as a whole chromosome gain, partial gains (or so-called large-scale gains that include >25% of chromosome arm) or as focal events (137-139). Such amplification events can cause subsequent overexpression of potential oncogenes such as EGFR. As a result, consequent high levels of signaling activity from such oncogenes promote tumor growth (23). In GBM, chromosome 19 is the second most frequently gained chromosome after chromosome 7 (23, 140, 141). In fact, chromosome 19 gains in glioma have been shown as one of three gain forms mentioned above (137-139). Whole chromosome 19 gains have been reported in 28% of primary and 19% of recurrent GBM cases and associated with short term survival (137, 138, 141). Simultaneous gains of chromosomes 7 and 19 are one of the common genetic alterations in GBM that has been found in 30% of the radiation resistant (but absent in radiation sensitive) GBM cases (138). Practically, this reflects the importance of chromosomes 19 genetic status as a useful prognostic marker since chromosome 19q allelic loss (as part of 1p/19q codeletion) was solely associated with

longer survival while whole chromosome 19 gain was associated with shorter survival (23).

In several human malignant tumors, chromosome 19 gains are considered one of the frequent genetic alterations that are associated with aggressive tumor behavior (139, 142-145). The role of this chromosomal aberration in the pathogenesis of human cancer has been thoroughly studied via pinpointing several presumptive oncogenes on certain amplicons as targets of this genetic signature (139, 142-145). However, no detailed genomic analysis has to date implicated candidate oncogenes as targets of chromosome 19 gain in human glioma. Besides, previous studies about chromosome 19 gain in malignant glioma have been performed using chromosomal comparative genomic hybridization (CGH) technology that is capable of detecting copy number changes at the levels of chromosomes (137, 138). Thus, it is difficult to know whether these tumor specimens of certain genetic alterations harbor a single or multiple common amplicons on that particular chromosomal aberration. The use of more advanced genomic tools such as DNA microarrays will allow a genome-wide exploration and enable more precise and unprecedented detection of common altered regions and narrow the search for candidate oncogenes which, at the gene level, may be responsible for the chromosomal aberration-associated outcome.

In the current study, we used SNP (single-nucleotide polymorphisms) array analyses to identify potential chromosomal aberrations in cohort of sixty glioma patient specimens. We found gain of chromosome 19 (in 10 out of 60 glioma patients) as one of these frequent chromosomal aberrations that correlates to patients' outcomes. We

performed further genetic and statistical analyses to elucidate the significance of chromosome 19 gain and identify potential candidate oncogenes that may act as the driving force of this genetic signature and participate in the pathogenesis of human gliomas. In addition, further gene expression analyses at both RNA and protein levels and comparison to independent dataset have been performed.

2.2 Materials and methods

2.2.1 Tumor specimens

For SNP arrays, tissue samples, including 29 GBM, 13 AAC, 7 AOD, 6 ODG and 5 ACG, were obtained from the Department of Neurosurgery at the University of Iowa Hospital and Clinics. Acquisition of patient specimens and clinical information was approved by an institutional review board (IRB approval #200707727). After surgical resection in the operating room, tissue specimens were quickly snap frozen in liquid nitrogen until the day of tissue analysis. No chemo- or radiotherapy was given to the patients before surgery. Clinical data were recorded, including histology, diagnosis, age and KPS. Non-tumor (epilepsy patients) specimens were used as control samples for gene expression. Beside tumor tissue biopsies, a paired peripheral blood was also collected from 24 recent patients as control for CNA.

2.2.2 DNA extraction

Genomic DNA was extracted from the biopsies and blood samples using DNeasy Blood & Tissue kit (Qiagen, Germany). Briefly, tissue samples were disrupted using rotor–stator homogenizer to enable more efficient lysis and then placed in 1.5 ml microcentrifuge tube. 50 µl proteinase K and 200 µl tissue lysis buffer were mixed with

the homogenized tissues and incubated at 56°C until complete lysis of the tissues. Then the mixture was pipetted into the DNeasy Mini spin column placed in a 2 ml collection tube and centrifuged at 6000 x g for 1 minute in a table top microcentrifuge (Spectrafuge 16M, Elisalink, USE). For washing step, 500 µl washing buffer 1 was added to the DNeasy Mini spin column placed in a new 2 ml collection tube and centrifuged at 6000 x g for 1 minute. Then, 500 µl washing buffer 2 was added to the DNeasy Mini spin column placed in a new 2 ml collection tube and centrifuged at 20,000 x g for 3 minutes to dry the DNeasy membrane. These buffering and centrifugation steps maintain optimal and selective DNA adsorption to the DNeasy silica-based membrane while the contaminants are removed and pass through.

Finally, 200 µl elution buffer was added immediately to the DNeasy membrane of the spin column placed in 1.5 ml microcentrifuge tube. Then, the spin column incubated for 1 minute at room temperature and centrifuged at 6000 x g for 1 minute to elute DNA as ready for use. DNA integrity was assessed on 1% agarose gel in 1× Tris-Boric acid-EDTA (TBE) buffer and visualized using ethidium bromide under UV fluorescence (Alpha imager TM 2700, Protein Simple, USA). Good quality DNA appears as a distinct band while the poor quality DNA is represented by more diffuse band as a result of the presence of shorter DNA fragments (Figure 2.1A). DNA was quantified using HP 8453 UV-visible spectrophotometer (Hewlett Packard, Wilmington, Germany) at 260 nm/280 nm. Relatively pure DNA has A260/A280 ratios of (1.7–1.9). DNA amount was calculated using this formula (DNA amount (µg/ µl) = Absorbance at 260 nm * 10 (µg/ µl)).

2.2.3 SNP array

SNPs and CNAs were genotyped using Affymetrix GeneChip^{R} Human SNP Mapping 6.0 array (Affymetrix, Santa Clara, CA) in the DNA Facility at the University of Iowa. The Genome-Wide Human SNP Array 6.0 contains probes for 906,600 SNPs and 945,826 non-polymorphic probes featuring a total of 1.8 million probes. An amount of 250 ng of genomic DNA was cleaved with the restriction enzyme *Sty*I or *Nsp*I (New England Biolabs, Ipswich, MA), ligated with *Sty*I or *Nsp*I specific adaptors using T4 DNA ligase (New England Biolabs, Ipswich, MA), followed by PCR amplification using Titanium *Taq* (Clontech, Mountain view, CA) and a single primer complementary to the adaptor sequence. The PCR products were purified from excess primer and salts by column filtration and then digested with DNaseI to a size less than 200 bp. An aliquot of the fragmented DNA was separated and visualized on a 4% agarose gel in 1× TBE buffer and visualized using ethidium bromide under UV fluorescence (Alpha imager TM 2700, Protein Simple, USA); to confirm that most of the DNA products had been properly fragmented to the appropriate size.

To identify the SNPs and CNAs, fragmented PCR products were then end-labeled with biotin using terminal deoxynucleotidyl transferase and hybridized to the Genome-Wide Human SNP Array 6.0. The labeled DNA was hybridized onto Human Genome-Wide 6.0 SNP arrays for 16 h at 50°C. Arrays were then washed with 0.6X SSPE, 0.01% Tween-20 at 45°C and stained with R-phycoerythrin (Life technologies, Carlsbad, CA) on the Affymetrix Fluidics Station 450. Imaging of the microarrays was performed using a GCS3000 high-resolution scanner (Affymetrix, Santa Clara, CA). The probe intensity data were collected using Affymetrix GCOS v1.4 software. PartekGS software (Partek,

St. Louis, MO) and Nexus (BD Biosystems, El Segundo, CA) were used to evaluate copy number abnormalities and loss of heterozygosity (LOH) status. Data files (.Cel files) were compared to a baseline generated using 270 normal HapMap samples (www.HapMap.org) (for Partek) or using NCBI built 36.1 (for Nexus) and normalized using a Hidden Markov Model. Genomic segmentation was used to determine regions of deletions or duplications in copy number. Statistically significant copy number changes by cancer type were determined by chi-square test. Other comparisons were generated using matched blood samples from 24 recent patients as a baseline and pair-wise comparisons between paired blood and tumor samples.

2.2.4 RNA extraction

Total RNA was extracted from the glioma biopsies and non-tumor tissue samples using TRIzol reagent (a mono-phasic solution of phenol and guanidine isothiocyanate that dissolves cell components but maintains RNA integrity) according to the manufacturer's protocol (Life technologies, Carlsbad, CA). Briefly, tissue samples were homogenized using 1ml TRIzol reagent per 50-100 mg of tissues. The homogenized samples were incubated for 5 minutes at room temperature to completely permit the dissociation of nucleoprotein complexes. 0.2 ml chloroform per 1 ml TRIzol reagent was added to the homogenized samples followed by vigorous shaking for 15 seconds. After 2-3 minutes incubation at room temperature, samples were centrifuged at 12,000 x g for 15 minutes at 4°C (Centrifuge 5810r, Eppendorf, USA). The mixture was separated into three phases: a lower red protein-containing organic phase, a white DNA-containing interphase, and an upper colorless RNA-containing aqueous phase. The aqueous phase was transferred to a fresh tube. For RNA precipitation from the aqueous phase, 0.5 ml

isopropyl alcohol was added to the aqueous phase then the samples were incubated for 10 minutes at room temperature and centrifuged at 12,000 x g for 10 minutes at 4°C. Supernatant was discarded and the RNA gel-like pellet was washed once with 200 µl 70% ethanol, vortexed and centrifuged at 7,500 x g for 5 minutes at 4°C. Ethanol was aspirated and the RNA pellet was air-dried and dissolved in RNase-free water.

RNA quality was assessed on 1% agarose gel in 1× TBE buffer and visualized using ethidium bromide under UV fluorescence (Alpha imager TM 2700, Protein Simple, USA). Good quality RNA appears as two distinct fragments representing the 28S and 18S subunits of the ribosomal RNA (rRNA) with the upper fragment appears thicker as the 28S subunit contains higher number of RNA base pairs than the 18S subunit (Figure 2.1B). RNA was quantified using HP 8453 UV-visible spectrophotometer (Hewlett Packard, Wilmington, Germany) at wavelength ratio of 260 nm/280 nm. A260/A280 ratios of (1.6-1.8) represent relatively pure RNA with minimal protein and DNA contamination. RNA amount was calculated using the same formula used for genomic DNA. RNA solution was divided into aliquots of 5 ug and stored at -80°C to avoid repeated freeze-thaw cycles and prevent RNA degradation.

2.2.5 Reverse transcription

Reverse transcription (RT) from single-stranded RNA was used for complementary DNA (cDNA) synthesis using MyCycler Thermal Cycler system (Bio-Rad, USA) and MuMLV retrotranscriptase/OligodT according to the standard protocol (Life technologies, Carlsbad, CA). Briefly, 5 µg RNA, 0.5 µg OligodT and Diethyl pyrocarbonate (DEPC)-treated H_2O (q.s 11 µl) were mixed per one reaction tube, heated to 65°C for 5 minutes to allow OligodT alignment to the RNA single strand and then

quickly chilled on ice for 2 minutes. Then, 7 µl master-mix (1 ul 10 mM dNTPs, 4 µl 5X First-Strand Buffer, 2 µl 0.1 M Dithiothreitol (DTT) as antioxidant and 1 µl RNase inhibitor) was added to the content and incubated at 37°C for 2 minutes. Finally, 1 µl (200 units) of MuMLV retrotranscriptase was added and then the mixture incubated for 50 minutes at 37°C before the reaction was inactivated by heating at 70°C for 15 minutes. The cDNA quality was assessed on 1% agarose gel in 1× TBE buffer and visualized using ethidium bromide under UV fluorescence (Alpha imager TM 2700, Protein Simple, USA). cDNA was quantified using HP 8453 UV-visible spectrophotometer (Hewlett Packard, Wilmington, Germany) at wavelength ratio of 260 nm/280 nm. cDNA amount was calculated using the same formula used for genomic DNA. 50 ng of cDNA was used for further analyses.

2.2.6 RT-PCR and Real time PCR

RT-PCR was performed using MyCycler Thermal Cycler system (Bio-Rad, USA) and Taq polymerase (NEBiolabs). Primer concentrations were normalized via mixing gene-specific forward and reverse primer pair. The concentration of both primers (forward and reverse) in the mixture was 10 µM. For RT-PCR reaction, cDNA from glioma biopsies was used as a template to detect expression level of gene transcripts using specific primers for VEGFA and GAPDH as internal control (Primers are listed in Table 2.1). Briefly, 50 ng cDNA was mixed with 18 µl mastermix (2µl 10X buffer, 0.4 µl 10 mM dNTPs, 1 µl primers, 1U Taq polymerase and 14.4 µl DEPC-treated H_2O) and incubated at 58°C annealing temperature for 35 cycles for VEGFA or at 55°C annealing temperature for 19 cycles for GAPDH. The amplified fragments were analyzed by electrophoresis on 2% agarose gel in 1X TBE buffer and visualized using ethidium

bromide under UV fluorescence (Alpha imager TM 2700, Protein Simple, USA).

Quantitative real time PCR analysis was performed using the ABI StepOne machine (Applied Biosystems, Foster City, CA) using cDNA from primary glioma biopsies and specific primers for NOTCH3 and GAPDH as internal control (Table 2.1). Briefly, reaction mixture was prepared by adding: 2 µl primers, 7.5 µl SYBR green master mix (a fluorescent dye that reflects the amount of PCR product, Clontech), 0.3 µl the passive reference (ROX, an internal reference to normalize well-to-well fluorescent fluctuations, Clontech) and DEPC-treated H_2O (q.s 15 µl). The following conditions used for the real-time PCR reaction: 95°C for 30 sec, 58°C annealing for 30 sec and 72°C for 30 sec, for 40 cycles. Data were collected and analyzed using the Delta CT method and NOTCH3 transcript levels was calculated relative to GAPDH.

2.2.7 Western blotting

For tissue homogenization, 5 mg tissues were placed in a per-cooled microcentrifuge tube contains 0.4 ml lysis buffer (150 mM sodium chloride, 1.0% Triton X-100, 0.5% sodium deoxycholate, 0.1% sodium dodecyl sulphate (SDS), 50 mM Tris, pH 8.0, 1x protease inhibitor cocktail, 1 mM EGTA, 5 mM EDTA, 5 mM sodium fluoride and 1 mM PMSF). To release and solubilize the cellular proteins of interest, tissues were homogenized with an electric homogenizer and maintained in vortexing every 5 minute for 1 hour at 4°C. Tissue homogenates were then centrifuged at 11,000 rpm for 15 min at 4°C and the supernatant was aspirated and placed in a fresh pre-cold tube kept on ice, while the pellet was discarded. Protein concentration was determined using bicinchoninic acid assay (Pierce BCA assay, Rockford, IL, USA). To further denature the proteins, equal volume of 2x anionic denaturing detergent SDS laemmli

sample buffer (Bio-Rad, Hercules, CA), mixed with 0.05% β-mercaptoethanol that reduces the disulfide linkages, was added to the lysates and then the mixture was heated at 95^{o}C for 5 minutes. Total protein extracts (50 µg/lane) were separated electrophoretically in 7.5% SDS-polyacrylamide gel. Proteins were transferred to nitrocellulose membrane (Invitrogen Ltd, Paisley, UK) using wet transfer method in which the gel and membrane are sandwiched between two absorbent papers and two sponges clamped between solid supports and the whole sandwich is merged in transfer buffer. Ponceau red dye was used to assess the efficiency of transfer by quickly visualizing protein bands.

For membrane blocking, 10% nonfat dry milk in Tris-Buffered Saline Tween-20 (TBST) buffer was used to cover the membrane for 2 hours at room temperature, to prevent non-specific binding of the antibodies, and then rinsed with TBST for 5 seconds. NOTCH3 protein expression was analyzed using NOTCH3 primary antibody recognizing an epitope on the intracellular domain (ab23426, Abcam, Cambridge, MA) at dilution of (1:1000) in TBST. GAPDH primary antibody (ab8245, Abcam, Cambridge, MA, USA) was used as a loading control at dilution of (1: 50,000) in TBST. The membrane was incubated with primary antibodies for 3 hours at room temperature. Subsequently the membrane was washed with TBST for three times and incubated with horseradish peroxidase -conjugated secondary antibodies to rabbit or mouse immunoglobulin G (GE Healthcare, Piscataway, NJ) at dilution of (1:5000) in 10% nonfat dry milk in TBST for 2 hours at room temperature followed by another washing with TBST for three times. The blocking and antibody incubation steps were performed under shaking to ensure homogenous membrane covering and equalize the binding. Finally, immunoreactive

proteins were detected with enhanced chemiluminescence (ECL) (GE Healthcare, Piscataway, NJ) using manual x-ray film development.

2.2.8 Survival and statistical analyses

Chi-square test was used to determine statistically significant copy number changes by cancer type. Kaplan-Meier analysis was used to generate the overall survival curve and the log rank test was used to compare median survival. For NOTCH3 RNA gene expression in different glioma grades, statistical significance was detected using one-way analysis of variance (ANOVA) and multiple group comparisons were analyzed with Tukey's multiple comparison tests. Statistical analyses were performed using SAS 9.3 software. $P < 0.05$ was considered to be statistically significant.

2.3 Results

2.3.1 Clinical data

A total of 60 glioma patients, who were admitted to the University of Iowa Hospitals and Clinics, were included in this study: 36 males and 24 females with a median age at diagnosis of 51 years (range: 18 to 79 years). The median KPS was 90 and the median survival was 31 months, with 22 patients alive at the time of the last follow-up. All the patients underwent surgery without any prior chemo- or radiotherapy. Only 20% of the samples were from low grade gliomas (grade II: ACG or ODG) while more than 80% were high grade gliomas (grade III: AAC or AOD, grade IV: GBM) with 50 % of the samples were GBMs. This is consistent with the real incidences of various glioma grades in the United States. Detailed patient data for each grade are illustrated in Table 2.2.

Since age and histology are among the most widely accepted prognostic factors in malignant glioma, we assessed whether these patient data of our glioma population correlate to patient outcome. We found that age was significantly associated with outcome when patients were clustered into two age groups; above the median age and below or equal to the median age (cut-off value = 51 years, p = 0.0025, Log-Rank test). The data indicate that glioma patients with age older than 51 years have poorer outcomes compared to younger patients. Moreover, histology and diagnosis were also associated with outcome. Patients who were diagnosed with GBM have the worst outcome while patients diagnosed with ODG have the best outcome (18 vs. 56 months). Besides, glioma patients with oligodendrocytic origin have better outcome compared to those with astrocytic origin (41 vs. 22 months). These data are strongly consistent with previous studies that reported the significant relevance of age, histology and diagnosis to glioma patient survival (132, 133).

2.3.2 Genome-wide explorations revealed multiple chromosomal alterations in glioma

Using SNP array tool, we identified a large number of CNAs in our glioma population spanning the whole genome. Although some of these CNAs were previously reported, most of them were discovered for the first time by our study. These genetic alterations occurred as whole or partial chromosomal aberrations or more commonly as focal events. Grade III and IV patients had more genetic aberrations compared to lower grades. Our genetic analysis of glioma patient specimens revealed several chromosomal instabilities in terms of frequent changes in DNA copy numbers involving chromosomes 1, 7, 9, 10, 13, 14, 19, 20 and 22 (Table 2.3). In fact, gains were mainly involving

chromosomes 7, 9q, 19 and 20, while deletions were involving one or both copies of chromosomes 1p, 9p, 10, 13, 14, 19q and 22. Frequency of these chromosomal aberrations in our glioma population, segregated according to clinical diagnosis, is illustrated in Figure 2.2A and B.

Chromosome 1p deletions, chromosome 19q deletions and chromosomes 1p/19q codeletions were mainly observed in oligodendrocytic lineages that are well-known to have better prognosis compared to astrocytic ones (Figure 2.2B). In line with previous studies, chromosomes 1p/19q codeletions were observed in 61% of oligodendrocytic tumors but less frequent in astrocytic tumors (17%) (134). These observations reflect a potential prognostic role of such deletions as they mainly occurred in oligodendrocytic lineages. Patients with chromosome 1p deletions had better survival than patients with intact chromosome 1 ($p = 0.0027$, 33 vs. 18 months, Log-Rank test). Similarly, patients with chromosomes 1p/19q codeletions had better survival than patients with intact chromosomes 1 and 19 ($p = 0.0025$, 20 vs. 83 months, Log-Rank test). Accordingly these findings suggest that chromosomes 1p/19q codeletions can be used to cluster glioma patients into better or worse outcome. Surprisingly, we reported for the first time that chromosome 7 gains occurred in most of the glioma grades in both lineages (47% astrocytic, 30% oligodendrocytic) and most of the tumors gained up to 11 copies (Figure 2.2A). These gains were associated with losses in chromosomes 9p and 10. Although statistically not significant, patients with chromosome 7 gains (and subsequent EGFR amplifications) tended to have lower survival than patients with intact chromosome 7 ($p = 0.0825$, 29 vs. 37 months, Log-Rank test). Finally, whole chromosome 19 gains were mainly observed in high grade tumors (grade III or IV) and in most of the cases

associated with chromosomes 7 and 20 gains as well as losses of chromosome 10 (Figure 2.2A). These observations reflect certain patterns of distribution in these chromosomal aberrations. Such patterns may reflect neoplastic variants that can survive under the conditions of selective pressure through a series of chromosomal and genetic mutations that favor tumor growth.

2.3.3 Chromosome 19 alterations in malignant glioma.

Among the gain group, one of the most common alterations was involving chromosomes 7 and 19. In fact, chromosome 7 gains and the subsequent EGFR amplification have been analyzed in previous studies (23, 146, 147). Therefore, we aimed at analyzing the significance of chromosome 19 alterations. A composite of SNP array results related to chromosome 19 alterations for all patients is shown in Figure 2.3. Unsupervised clustering of 60 glioma tumors by chromosome 19 CNAs reveals three tumor clusters (Figure 2.4). Whole gains of chromosome 19 were found in significant number of patients and most of the tumors gained up to 4 copies. In addition, chromosome 19q deletions (correspond to complete loss of q-arm, 19q12-19qter) were also reported. The rest of patients had normal chromosome 19 status although in some cases there were some focal events of loss or gain. Segregation of these data according to the clinical diagnoses showed distinct distributions of such CNAs (Figure 2.2A). As expected, chromosome 19q losses were seen more frequently in the oligodendrocytic lineage (with better prognosis) than in the astrocytic lineage while chromosome 19 gains were observed mainly in grade III and IV. Further, GBMs have the lowest frequency in chromosome 19q losses but the highest in chromosome 19 gains. This is consistent with

the aggressive clinical behavior of GBM and suggesting that chromosome 19 gains signature may be a characteristic feature of aggressive high grade gliomas.

To confirm the relevance of chromosome 19 CNAs to patient diagnosis, the prognostic significance of these clustered signatures were evaluated using Kaplan-Meier survival analysis (Figure 2.5). Interestingly, whole chromosome 19 gain signature was correlated with a poorer outcome compared to chromosome 19q loss ($p = 0.0002$, 16 vs. 31 months, Log-Rank test). On the other hand, deletions of chromosome 19q correlate better with outcome compared to intact chromosome 19 in both oligodendrocytic and astrocytic lineages ($p = 0.0214$, 31 vs. 23 months, Log-Rank test). Taken together, these findings indicate the clinical significance of chromosome 19 genetic signature. Besides, genes that are mapped to chromosome 19 and playing critical roles in important oncogenic pathways may be prone to genetic alterations. In fact, chromosome 19 contains several genes important in angiogenesis, NOTCH, MAPK, cell cycle, ubiquitination, cell–cell adhesion, cell invasion and pro-survival pathways. Analyzing the alterations in gene copy numbers belonging to such pathways will help in identifying the most significant amplification in one or more of these genes that cause this dismal outcome. Thus, this will help in individualizing therapies based on these alterations which eventually may improve patients' outcomes.

2.3.4 NOTCH3 as a candidate oncogene in malignant glioma

We identified a novel chromosome 19 gain genetic signature in high grade gliomas that associates with dismal outcome (23). We found several distinct

amplifications for many genes on chromosome 19 specific to high-grade glioma. To narrow down the candidate gene lists that may be responsible for this grim outcome, we selected 41 genes mapped to chromosome 19. The products of these genes contribute to many important pathways, such as MAPK, JAK-STAT, ubiquitination, cell adhesion, NOTCH and VEGF pathways (Table 2.4). To identify the candidate oncogene, we performed statistical analysis of the gene copy number for the selected genes in tumor specimens with chromosome 19 gain in comparison to normal brain tissues. The analysis revealed NOTCH3 (19p13.12) as the most significant gene amplification ($p = 1.4x10^{-8}$) along with several mutations. This novel amplification may be a critical step in glioma progression as NOTCH3 is normally expressed in embryonic brain neural progenitors. It functions to maintain the neural precursors in an undifferentiated state (148). Therefore, we selected NOTCH3 for further RNA and protein expression analyses.

Using quantitative real time PCR, we assessed NOTCH3 transcript levels in glioma biopsies and found that NOTCH3 RNA levels were significantly higher in tumor vs. non tumor specimens which suggests that NOTCH3 overexpression is one of the genetic alterations that may conspire with other altered regulatory signals to favor glioma phenotype (Figure 2.6A). Moreover, NOTCH3 RNA expression was significantly higher in astrocytic lineages that are known to have poor prognosis compared to the oligodendrocytic lineage (Figure 2.6B) (23). Notably, higher NOTCH3 transcripts were found in ACG, AAC and GBM compared to ODG and AOD (Figure 2.6C). To show that NOTCH3 is the major element in this pathogenesis, other NOTCH members were also analyzed at the transcript levels. Our results showed no significant difference in NOTCH1, 2 and 4 mRNA content between tumor and non tumor specimen (Figure

2.6D). Moreover, these genes are expressed at much lower levels compared to NOTCH3. In addition, we used immunoblot to compare NOTCH3 protein expression in glioma patient biopsies clustered according to chromosome 19 status. As expected, NOTCH3 protein levels were significantly higher in NOTCH3 locus amplified biopsies than their non-amplified locus glioma counterparts. This protein overexpression was observed at both NOTCH3 full length (FL, 244 kda) and its cleaved intracellular domain (NICD3, 100 kda) (Figure 2.7). This confirms upregulation of NOTCH3 receptors and suggests high levels of signal transduction through NOTCH3 receptors which is reflected by detection of high content of the active NICD3 (that acts as a mediator of NOTCH3 signaling).

Since chromosome 19 gain was found to have prognostic value, we evaluated the prognostic significance of NOTCH3 gene amplification using Kaplan-Meier survival analysis (Figure 2.8). NOTCH3 genomic status was associated with patient outcome (P=0.00098, median survival 10 vs. 28 months, Log-Rank test). Theses data indicate that patients with amplified NOTCH3 (17%) have poorer outcomes compared to patients with non-amplified locus. To validate our results, we used Rembrandt (REpository for Molecular BRAin Neoplasia DaTa) as an independent dataset. Rembrandt contains datasets related to gene expression, copy number data and clinical data of glioma patients from different grades (https://rembrandt.nci.nih.gov). NOTCH3 status at transcriptomic levels was shown to predict outcome as shown in Figure 2.9. The data indicate that upregulated NOTCH3 RNA expression is associated with lower patient survival compared to normal or intermediate NOTCH3 RNA expressions ($p = 1.7*10^{-9}$, Log-Rank test). Interestingly, none of the other NOTCH receptors (1, 2 or 4) was significantly

associated to glioma patient outcome in these datasets (Figure 2.10), suggesting that NOTCH3 alterations could be the central player in gliomagenesis.

Finally, tumor biopsies with chromosome 19 gains were found to have extensive angiogenesis compared to tumors with chromosome 19 loss or intact statuses, therefore, we analyzed VEGFA expression levels in both groups as a surrogate marker for angiogenesis. Interestingly, higher levels of VEGFA transcripts were found in tumors with chromosome 19 gain and subsequent amplified NOTCH3 locus compared to tumors with chromosome 19 loss or intact statuses (Figure 2.11). Association of NOTCH3 amplification with a high level of VEGFA transcripts may be related to the cross talk between NOTCH and VEGF pathways and a possible direct or indirect molecular interaction between NOTCH3 and VEGFA, in particular; which require further investigations. Together, these data strongly provide evidence that NOTCH3 could be a critical element in gliomagenesis of prognostic value.

2.4 Discussion

Chromosomal aberrations have been recently reported as a common feature of tumor progression, recurrence and resistance to therapy in many human cancers (23, 138, 149). As a major mechanism to promote cancer cell survival and tumor progression, a new genetic material that harbors pro-survival genes is generated during uncontrolled cell growth and unchecked cell cycle (150). In parallel, part of the genetic material that harbors tumor suppressor genes is deleted at certain point when the cells move from one division to another (151). The ultimate net result of this process is continuum in tumor progression and intrinsic resistance to therapy, presenting a major challenge in the

clinical management of human cancer. In several studies, investigators aimed at exploiting the current available research tools for more understanding of the tumor biology and developing new targeted therapies. Variety of cytogenetic techniques has been recently employed to detect chromosomal aberrations in several types of human cancers including malignant glioma (23, 147, 152). These include but are not limited to karyotyping, fluorescence in situ hybridization (FISH), CGH and microarrays (23, 147, 152). In fact, microarray screening is considered one of the gold standards in identifying small regions of CNAs in superior to the classical cancer diagnostic tools (26). In the present study, we employed SNP array as a diagnostic tool to explore genome-wide alterations in our glioma populations. We identified several chromosomal aberrations that correlate with diagnosis and patient outcome. Here, we confirm the presence of chromosome 19 aberration as one of the most frequent alterations in high grade gliomas and the importance of altered chromosome 19 status as an essential determinant of patient outcome in glioma subgroup. In addition, we show that NOTCH3 is the driving force of chromosome 19 gain-associated poor outcome in high grade gliomas.

Previous studies have reported several chromosomal gains in malignant glioma, most constantly those which affect chromosomes 1, 7, 10, 19 and 20 (23). In line with previous studies, we confirm the prognostic significance of chromosomes 1p/19q codeletions (134). In fact, translocation between 1p and 19q followed by loss of the fusion arms is the underlying mechanism that eventually gives rise to chromosomes 1p/19q codeletions (153). Using mutational analyses of human gliomas, several studies have aimed at pinpointing putative tumor suppressor genes mapped to these deleted arms that could be linked to patient outcome or chemosensitivity (154-157). Few interesting

minimal regions have been identified to harbor potential tumor suppressor genes such as CAMTA1 and STATHMIN (155, 157). However, validation of such findings on larger cohort of glioma is still in need. For chromosome 10 deletions, further genetic analysis has been performed in several studies and revealed PTEN as a novel tumor suppressor associated with poor prognosis (158).

Among the chromosomal gains, chromosomes 7 and 19 are the most common reported aberrations in glioma (23, 146, 147). In fact, several studies have performed subsequent genetic analysis that revealed EGFR as a novel amplified gene mapped to chromosome 7 (23, 146, 147). Exploiting this signature in glioma subgroups with chromosome 7 gains may help individualize therapies by using EGFR inhibitors (RTKIs) which have been shown to be effective in lung cancer (96). However, none of these glioma studies have reported any genetic analysis that may reveal candidate oncogenes mapped to chromosome 19, the second most commonly gained chromosome in glioma. In fact, amplification of chromosome 19 has been also reported in other types of cancers such as ovarian (139), breast (142), cervical (143), gastric (144), and lung cancers (145). In these studies, a number of presumptive oncogenes have been pinpointed as targets of this signature such as LYL1 (angiogenesis), BRD4 (cell division), ICAM1 (cell adhesion), JAK3 and TYK2 (inflammatory response), cyclin E1 (cell cycle), and NOTCH3.

In our study, we identified many amplified genes on chromosome 19 that may drive the poor prognosis associated with this genetic signature. We focused our search on 41 relevant genes that are known to have a role in tumor development particularly, in cell proliferation, cell cycle, apoptosis, cell invasion and angiogenesis. We found NOTCH3

as the most significant candidate-amplified tumor-associated gene mapped to chromosome 19p13.12 cytoband. Our findings are in line with previous glioma studies about this minimal amplicon (137). As stated earlier, chromosome 19 gains have been reported as a whole chromosome gain, one-arm amplification or as focal events. In more detailed reports, 19p arm gain was reported in 50% of primary and 8% of recurrent GBM while 19q arm gain was reported in 38% of primary GBM (137, 141). Interestingly, 19p arm gains with or without 19q arm gains have been reported as a common feature of aggressive clinical behavior of GBM in terms of short term survival and resistance to radiotherapy (137, 138). Moreover, 19p arm gain was previously reported as an isolated alteration in contrast to 19q arm gain that always occurs in association of 19p arm gain (137). These observations suggest that 19p arm may contain the minimal region that harbors primary candidate oncogenes such as NOTCH3.

However, some amplification events detected by SNP array may not necessarily have overexpression of the gene of interest (139). Therefore, to confirm that the amplified tumor-driving gene is overexpressed to activate its tumorigenic pathway, we subjected NOTCH3 for further RNA and protein expression analyses. Interestingly, NOTCH3 RNA levels were significantly higher in glioma biopsies than non-tumor brain tissues. Moreover, its RNA expression was specifically higher in astrocytic compared to oligodendrocytic lineages that are known to have relatively better prognosis (23). In addition, the highest NOTCH3 expression was mainly observed in GBM which indicates that NOTCH3 overexpression is one of the major alterations that conspires to promote tumor aggressiveness as it mainly occurs in such advanced state. The frequency of NOTCH3 overexpression is somehow comparable to that in other human cancers such as

high-grade ovarian serous carcinomas, hepatocellular carcinoma, lung and pancreatic cancer (159-162), which makes NOTCH3 a rational target for therapeutic intervention. In fact, overestimation of gene expression may result from translational deficiencies caused by other feedback mechanisms, high protein degradation via ubiquitination or ineffective post translational modification which may result in poor correlation between mRNA and protein levels (49). Therefore, we analyzed the protein content of both FL NOTCH3 receptors and its cleaved product to fully describe the actual state of NOTCH3 signaling. Interestingly, NOTCH3 protein contents at both full length and NICD3 levels were significantly higher in NOTCH3 locus amplified biopsies than their non-amplified locus glioma counterparts. NICD3 is not only considered as a surrogate marker for NOTCH3 pathway activation, but also an important factor that activates transcription of NOTCH target genes which are known to have a putative role in tumorigenesis (107). In fact, NOTCH acts upstream of wide variety of genes important in stem cell maintenance, cell proliferation, differentiation, cell cycle, apoptosis and cell invasion (107). High levels of NICD3 in glioma specimens suggest a potential role of NOTCH3 signaling in these tumors in some if not all of these tumor progression mechanisms.

In our study, we did not find any changes in gene copy number for other NOTCH receptors (NOTCH1, 2 and 4). Further expression analysis of other NOTCH pathway constituents revealed no major changes in NOTCH1, NOTCH2 or NOTCH4 transcript levels in our glioma biopsies, thus confirming that NOTCH3 might be the central player in gliomagenesis. Differential expression of NOTCHs has however been previously reported in other brain tumors. For instance, NOTCH1 expression is almost undetectable while NOTCH2 is highly expressed in medulloblastoma when compared to normal fetal

cerebellum (163). The exact molecular significance of this different expression is still unknown and may relate to the cancer stem cell of origin. Taken together, our findings confirms that NOTCH3 is amplified at gene level with subsequent overexpression at both RNA and protein levels that are necessary to activate NOTCH3 signaling pathway, reflecting the robustness of our approach in identifying such cancer driving gene. Our finding of high frequency NOTCH3 gain in glioma is novel and suggests that these alterations may be early and major events in gliomagenesis

Cellular necrosis and extensive angiogenesis are common clinical features of high grade gliomas as result of EMT that conspire with GSCs to predominate mesenchymal gene expression and therefore promote angiogenesis (69). NOTCH is one of the most important pathways that contribute to EMT and tumor angiogenesis (130). In addition, NOTCH3 mutations have been found to cause vascular smooth muscle degeneration of small and middle-sized arteries and result in a dementia syndrome called Cerebral Autosomal Dominant Arteriopathy with Subcortical Infarcts and Leukoencephalopathy (CADASIL) (164). Recurrent subcortical infarcts as a result of vascular defects followed by migraines, cognitive impairment, depression and dementia are the main clinical presentation of this syndrome (164). This is highlighted in our study in the co-expressions of NOTCH3 and VEGFA (a mesenchymal gene) in high grade glioma biopsies accompanied by high level of angiogenesis. Many studies have reported the cross-talk between NOTCH and VEGF pathways (130). Thus, it is noteworthy to consider anti-NOTCH and anti-VEGF combination therapy in subset of glioma patients with chromosome 19 genetic signature, namely GSI and bevacizumab as one of the genetic characterizations that may help in individualizing therapies.

In conclusion, DNA stability over RNA or protein during surgery or fixation procedures makes the SNP array a suitable genomic tool to identify CNA and underpins the utility of genomic analysis in diagnostic, prognostic and predictive purposes of malignant glioma. Although our findings are based on a pilot study of relatively small population, our study demonstrates that for the first time that DNA copy number at the chromosome 19p13.12 cytoband that harbor NOTCH3 is increased in approximately one sixth of high grade gliomas which correlates to patient outcome at both genomic and transcriptomic statuses. Given this evidence of the prognostic value and the high expression of NOTCH3 at both RNA and protein level, this suggests a putative contribution of NOTCH3 in glioma development and progression which requires a detailed study for the functional role of NOTCH3 in malignant glioma.

Table 2.1: List of primers used in this study.

Gene	Forward primer (5…3)	Reverse primer (5…3)
NOTCH3	AGGTGATCGGCTCGGTAGTAA	TTACTACCGAGCCGATCACCT
VEGFA	ACCACAGTCCATGCCATCAC	TCCACCACCCTGTTGCTGTA
GAPDH	ACCACAGTCCATGCCATCAC	TCCACCACCCTGTTGCTGTA

Table 2.2: Clinical data for glioma patients enrolled in this study.

Glioma	Grade	# of patients	% of females	Median age at diagnosis (years)	Median survival (months)	Recurrence (number of patients)	KPS score
ACG	II	5	38	32	26	0	94
ODG	II	6	29	40	56	4	85
AOD	III	7	33	39	29	6	84
AAC	III	13	20	48	25	5	92
GBM	IV	29	55	59	16	17	85

Table 2.3: Summary of chromosomal alterations identified in this study.

Chromosome number	Gain vs. loss	Whole vs. arm	Correlation to patient outcome	Lineage	Pattern
Chr.1	loss	1p arm	Significant better survival	Mainly oligo	Co-deletion with 19q
Chr.7	Gain	Whole	Trend of lower survival	Both	Loss of chr10 & 9p
Chr.9	Gain	9q arm	No correlation	Both	None
Chr.9	Loss	9p arm	No correlation	Both	None
Chr.10	Loss	Whole	No correlation	Both	None
Chr.19	loss	19q arm	Significant better survival	Mainly oligo	Co-deletion with 1p
Chr.19	Gain	Whole	Significant lower survival	Both	Gain of chr.7 & 20, Loss of chr.10

Table 2.4: Chromosomal regions with highly statistically significant amplification in glioma biopsies with chromosome 19 gain genetic signature.

Start	End	RefSeq ID	Gene Symbol	P-value (Tumor vs. control)
15131444	**15172793**	**NM_000435**	**NOTCH3**	**1.40077E-08**
44681397	44690962	NM_203486	DLL3	5.11272E-06
1456017	1464189	NM_213604	ADAMTSL5	0.000017598
8551126	8581589	NM_030957	ADAMTS10	5.16278E-06
17691303	17706325	NM_018174	MAP1S	5.13534E-06
4041320	4075127	NM_030662	MAP2K2	2.15738E-05
7874765	7885364	NM_145185	MAP2K7	1.7964E-06
45389491	45413322	NM_002446	MAP3K10	1.27375E-05
43770121	43800484	NM_001042600	MAP4K1	5.14583E-06
1988470	2002244	NM_199054	MKNK2	2.54267E-05
55064109	55072457	NM_001098632	AKT1S1	1.15657E-05
45428064	45483106	NM_001626	AKT2	9.32822E-06
18125016	18142344	NM_005027	PIK3R2	1.14877E-05
5156519	5291815	NM_130855	PTPRS	0.000022929
18543614	18549271	NM_003333	UBA52	1.57161E-05
4396004	4408792	NM_025241	UBXN6	2.61535E-05
9799568	9801798	NM_001048241	UBL5	3.78E-07
39611108	39652639	NM_005499	UBA2	7.03849E-06
54149929	54156332	NM_004324	BAX	1.0853E-06

Table 2.4: Continued.

49943818	49955142	NM_005178	BCL3	1.91927E-06
54860211	54868986	NM_138639	BCL2L12	1.21572E-05
15218847	15252263	NM_014299	BRD4	2.21528E-05
34995401	35007060	NM_057182	CCNE1	1.97604E-06
10538138	10540656	NM_079421	CDKN2D	1.6699E-06
17796593	17819842	NM_000215	JAK3	1.54129E-05
51498716	51538531	NM_152794	HIF3A	9.33468E-07
4311367	4351472	NM_003025	SH3GL1	6.79683E-06
367583	411997	NM_012435	SHC2	7.52708E-06
46528653	46551672	NM_000660	TGFB1	1.23035E-05
10305452	10311346	NM_002162	ICAM3	9.99E-07
10261655	10268455	NM_003259	ICAM5	1.15258E-06
50004178	50015451	NM_001013257	BCAM	1.91062E-06
47703298	47724480	NM_001024912	CEACAM1	3.58992E-06
46992374	47007432	NM_001815	CEACAM3	2.55207E-06
46904370	46926278	NM_004363	CEACAM5	3.71295E-06
46951238	46967954	NM_002483	CEACAM6	8.93471E-06
46869075	46883937	NM_006890	CEACAM7	2.51886E-06
47776235	47790923	NM_001816	CEACAM8	7.85081E-06
56671650	56678424	NM_001080405	CEACAM18	1.14817E-06

Table 2.4: Continued.

49702051	49725389	NM_001102597	CEACAM20	3.9553E-06
46774371	46785038	NM_033543	CEACAM21	5.70171E-06

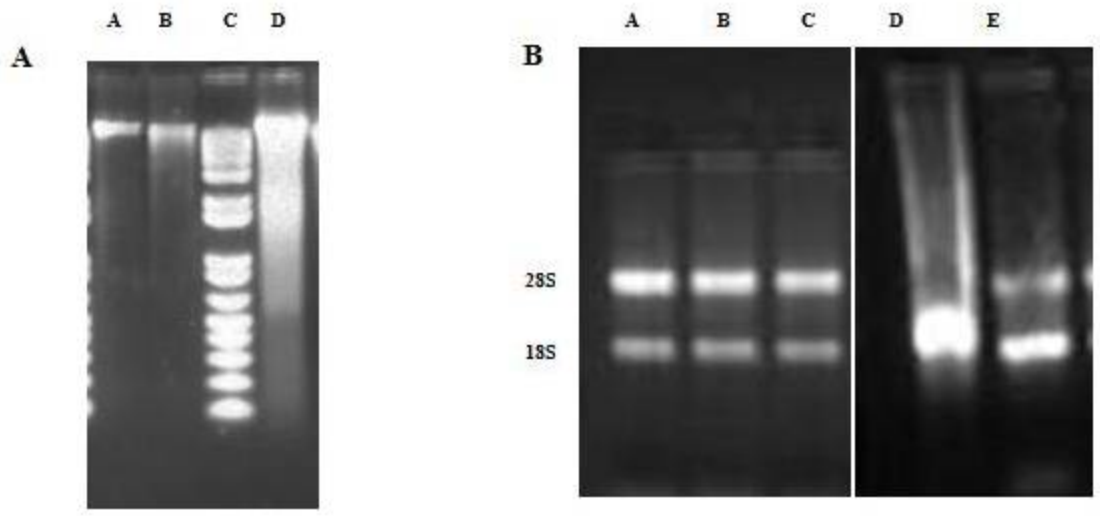

Figure 2.1: DNA and RNA quality assessment on agarose gel. (A) Total DNA was isolated from glioma biopsies. Lanes A and B represent good quality DNA that appears as a distinct band while lane D represents DNA with some diffuse appearance indicating some degradation. Lane C represents a molecular weight marker. (B) Total RNA extracted from glioma biopsies. Lanes A-C represent good quality RNA with two distinct fragments corresponding to the 28S (upper band, more intense) and 18S (lower band) subunits of the rRNA. Lanes D and E represent completely degraded RNA and low quality RNA, respectively.

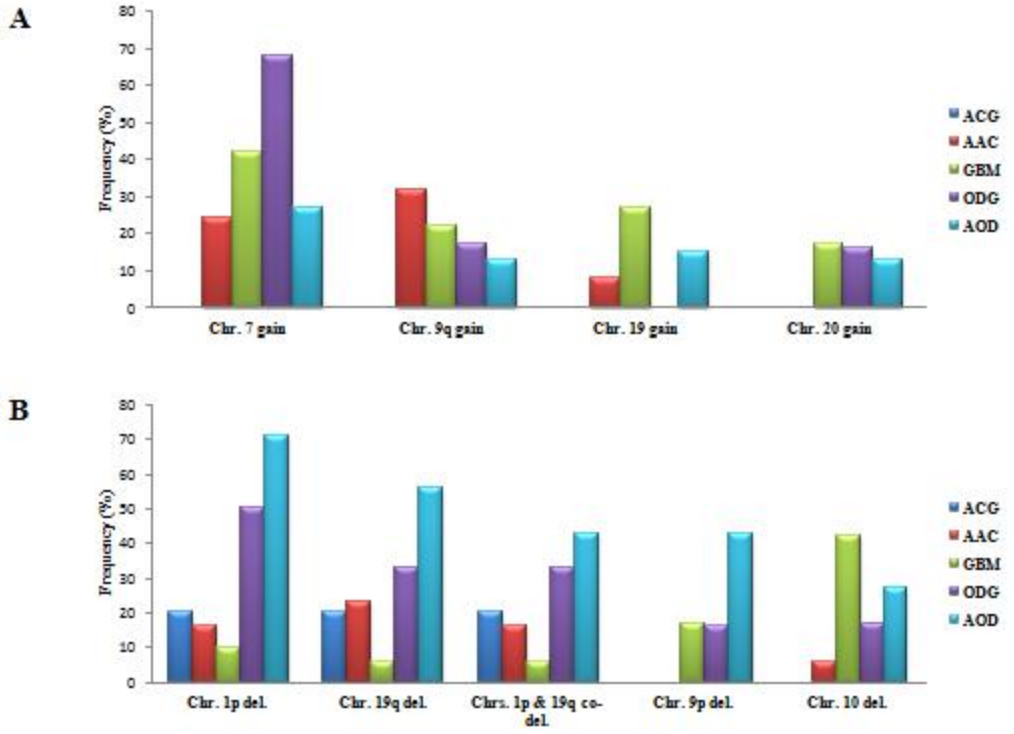

Figure 2.2: Frequency of chromosomal CNA detected in glioma samples. The CNA are stratified according to histological subtypes for chromosomal gains (A) and chromosomal deletions (B). ACG, astrocytoma grade II (n=5); AAC, anaplastic astrocytoma grade III (n=13); GBM, glioblastoma grade IV (n=29); ODG, oligodendroglioma grade II (n=6); AOD, anaplastic oligodendroglioma grade III (n=7).

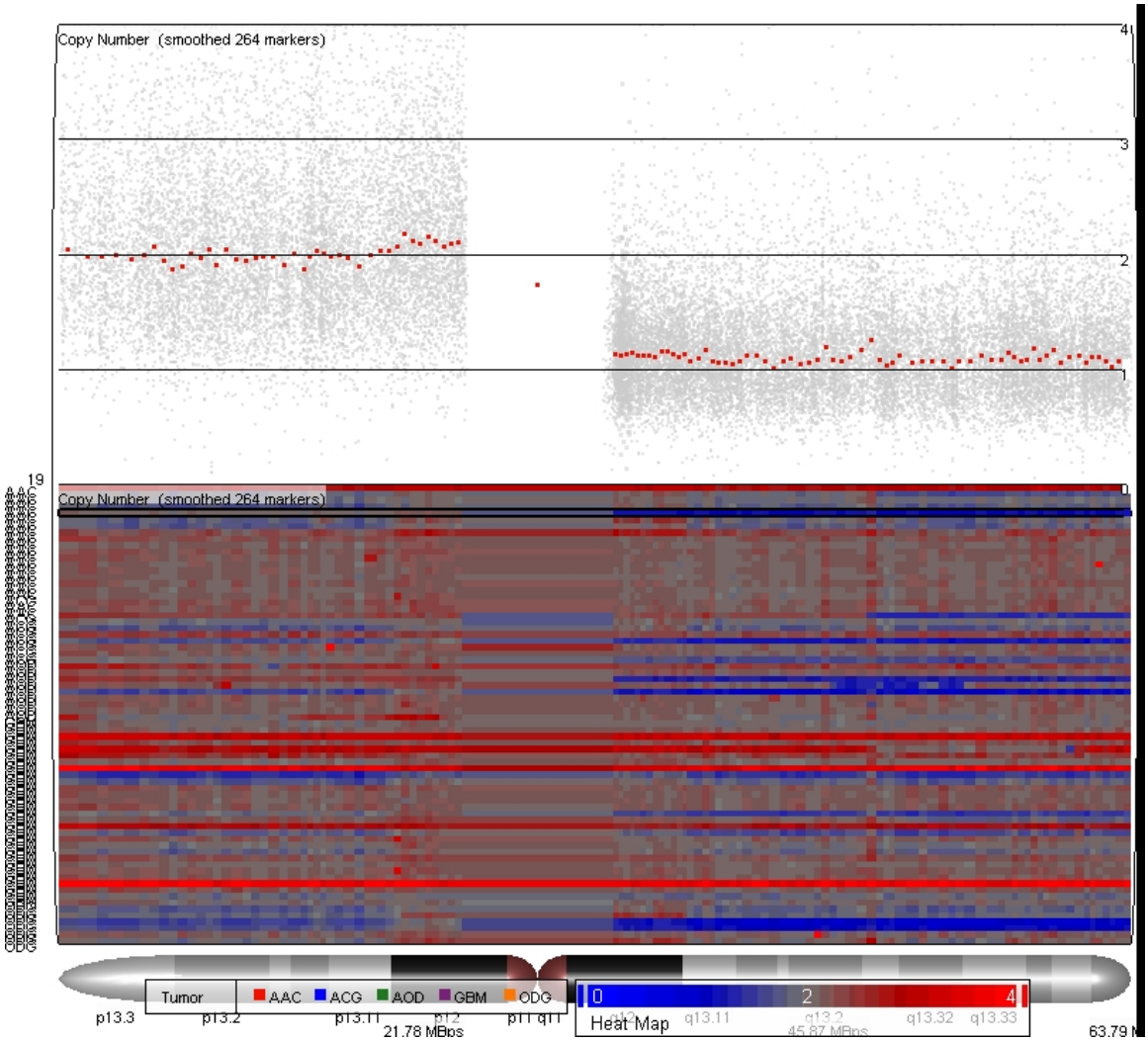

Figure 2.3: Summary of SNP array raw data based on chromosome 19 CNA of 60 glioma patient samples. Shown are heat maps illustrating gains (in red) and losses (in blue) for chromosome 19 in each patient. The intensity of the colors is proportional to CNA. Each row represents an individual patient sample.

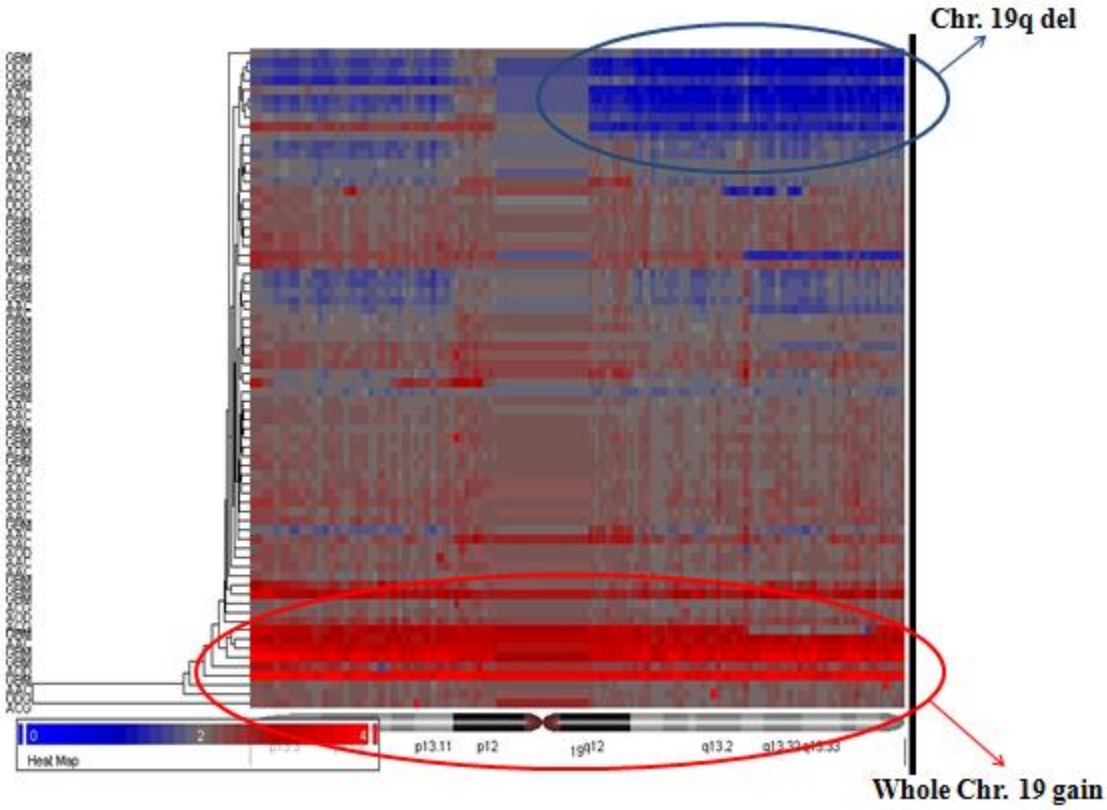

Figure 2.4: Clustering of chromosome 19 CNA-raw data into three groups. Unsupervised clustering of glioma tumors by chromosome 19 CNAs revealed three tumor clusters: Whole gain of chromosome 19, loss of 19q arm and third group of focal events or unchanged CNAs.

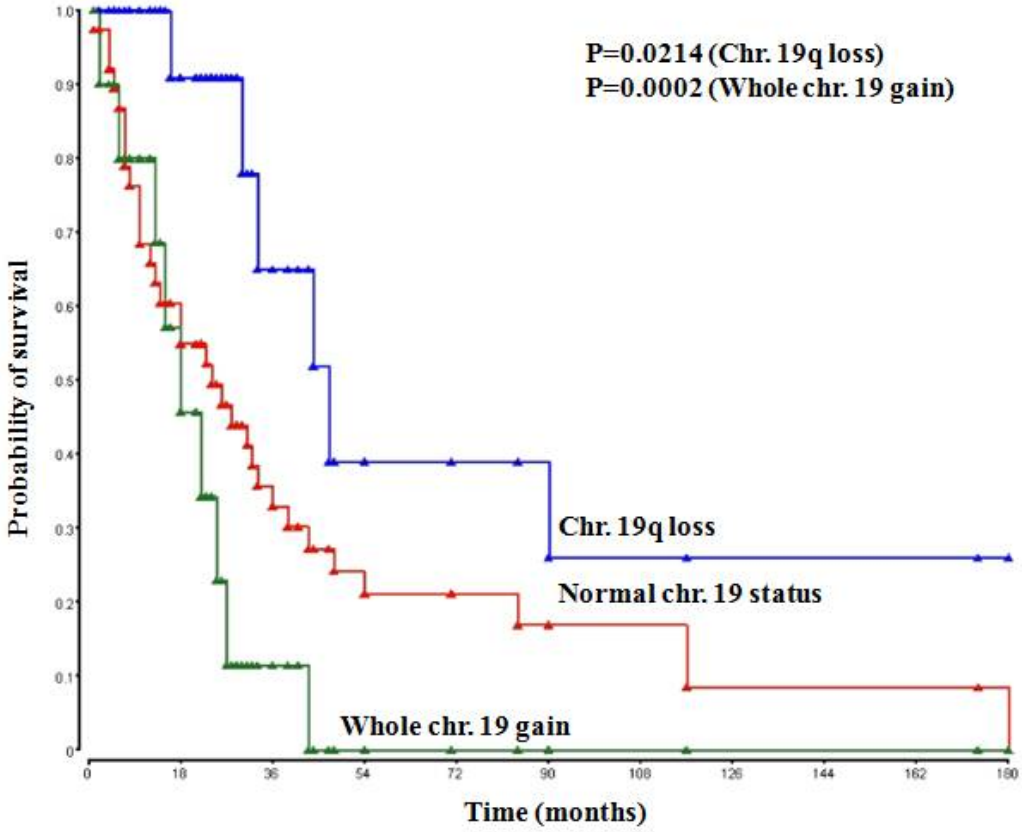

Figure 2.5: Kaplan-Meier estimate of probability of survival stratified according to chromosome 19 signature. Chromosome 19q deletions are associated with better outcome compared to intact chromosome 19 (p = 0.0214, 31 vs. 23 months, Log-Rank test). Whole chromosome 19 gains are associated with dismal outcome compared to chromosome 19q deletions (p = 0.0002; 16 vs. 31 months, Log Rank test).

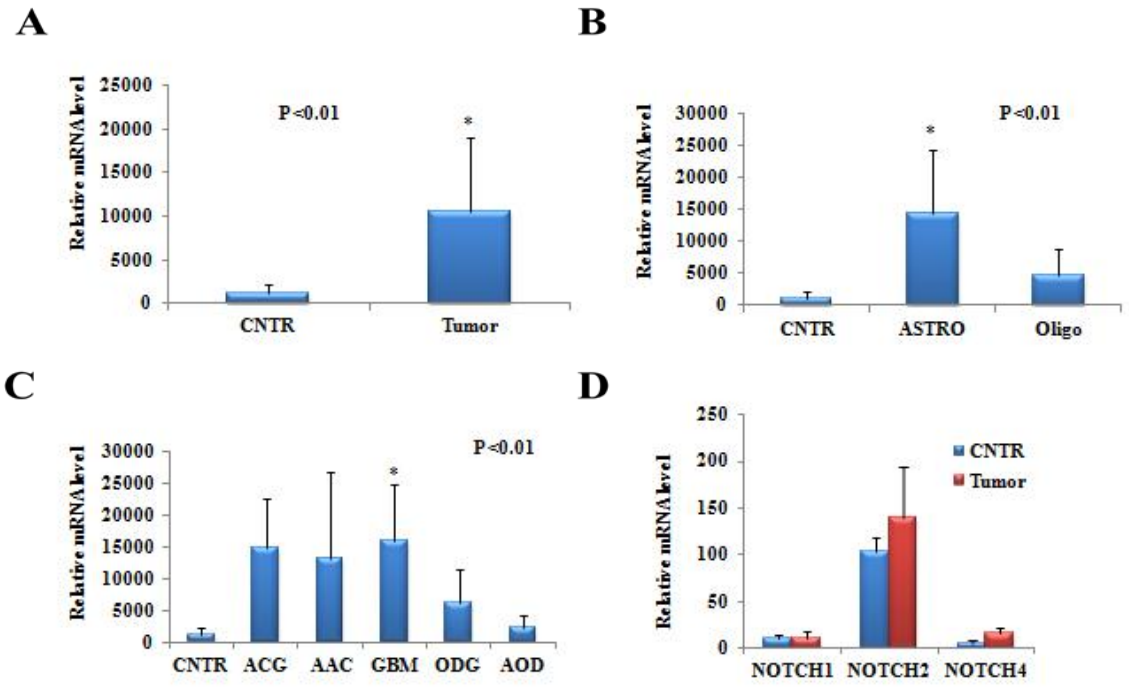

Figure 2.6: NOTCH gene expression in representative glioma specimens. Quantitative-real time PCR, showing high levels of NOTCH3 transcripts in tumor vs. non-tumor samples (epilepsy biopsies; CNTR) in (A) and mainly in astrocytic lineages in (B and C), thus confirming genomic data. Other NOTCH members were not overexpressed in tumor vs. CNTR.

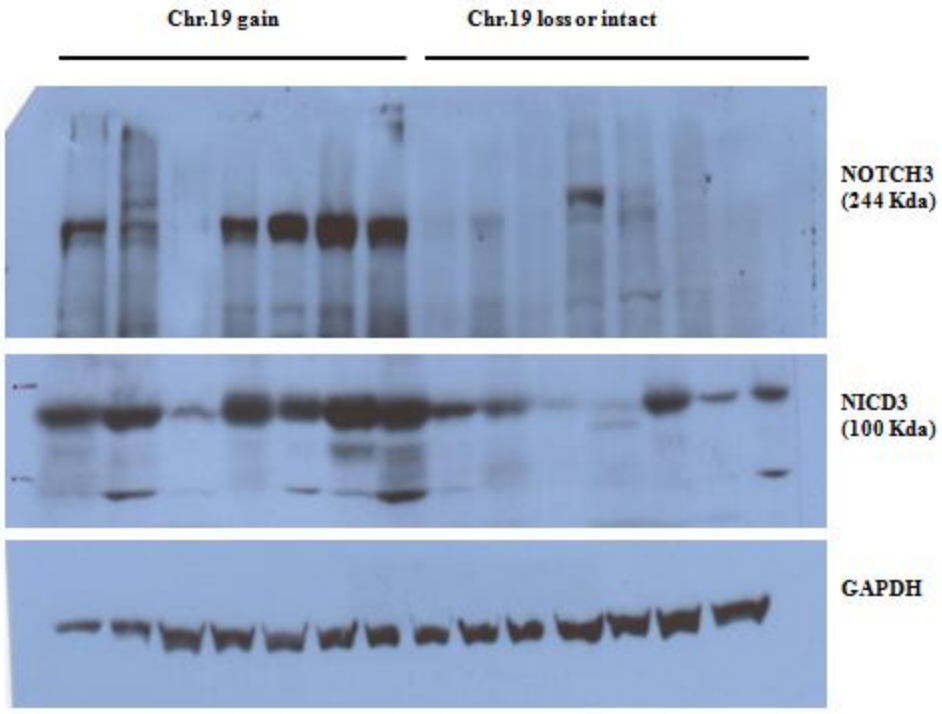

Figure 2.7: NOTCH3 protein expression comparisons in representative tumor specimens using western blot clustered according to chromosome 19 status. Tumors with chromosome 19 gain and subsequent amplified NOTCH3 locus showing high levels of full length NOTCH3 protein (FL, 244 Kda) and its cleaved intracellular domain (NICD3, 100Kda) compared to chromosome 19 loss or intact statuses. Immunoblot was performed using an antibody against the NICD3 thus recognizing both FL and NICD3 that (the latter) represents highly active NOTCH3 signaling pathway. GAPDH was used as a loading control.

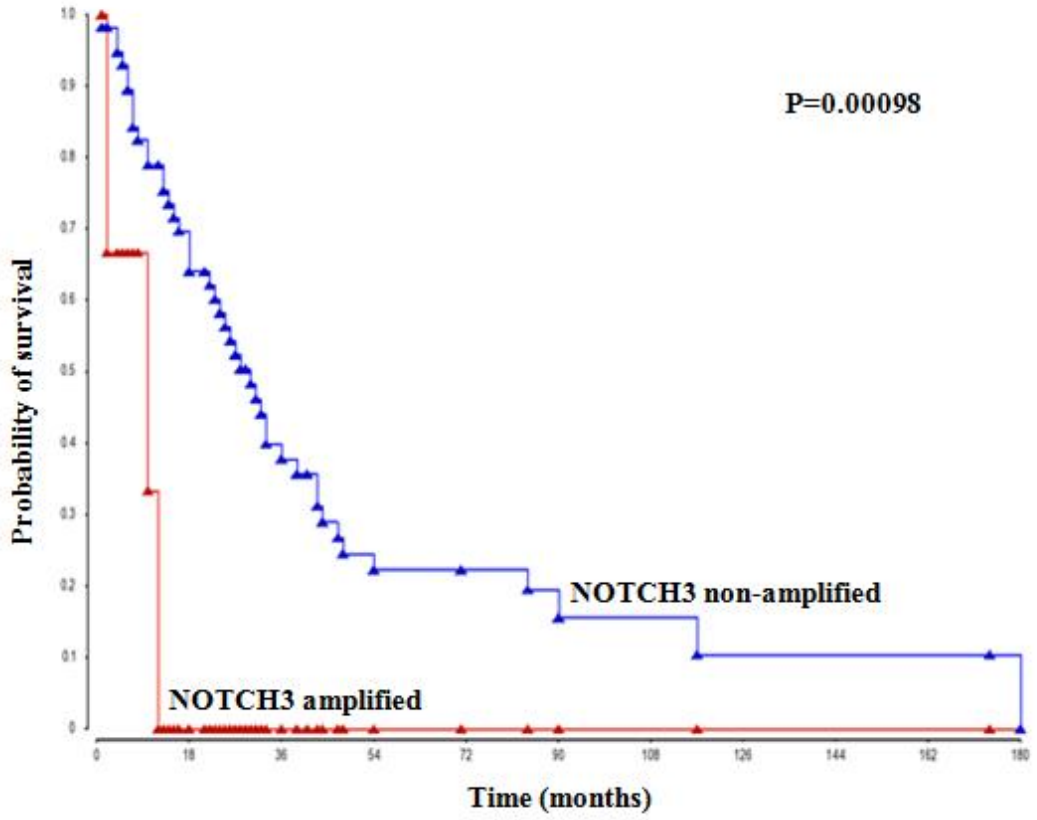

Figure 2.8: Kaplan-Meier estimate of probability of survival stratified according to NOTCH3 genomic status. NOTCH3 locus amplification is associated with dismal outcome (Log Rank test, P=0.00098; median survival 10 vs. 28 months) compared to non amplified locus.

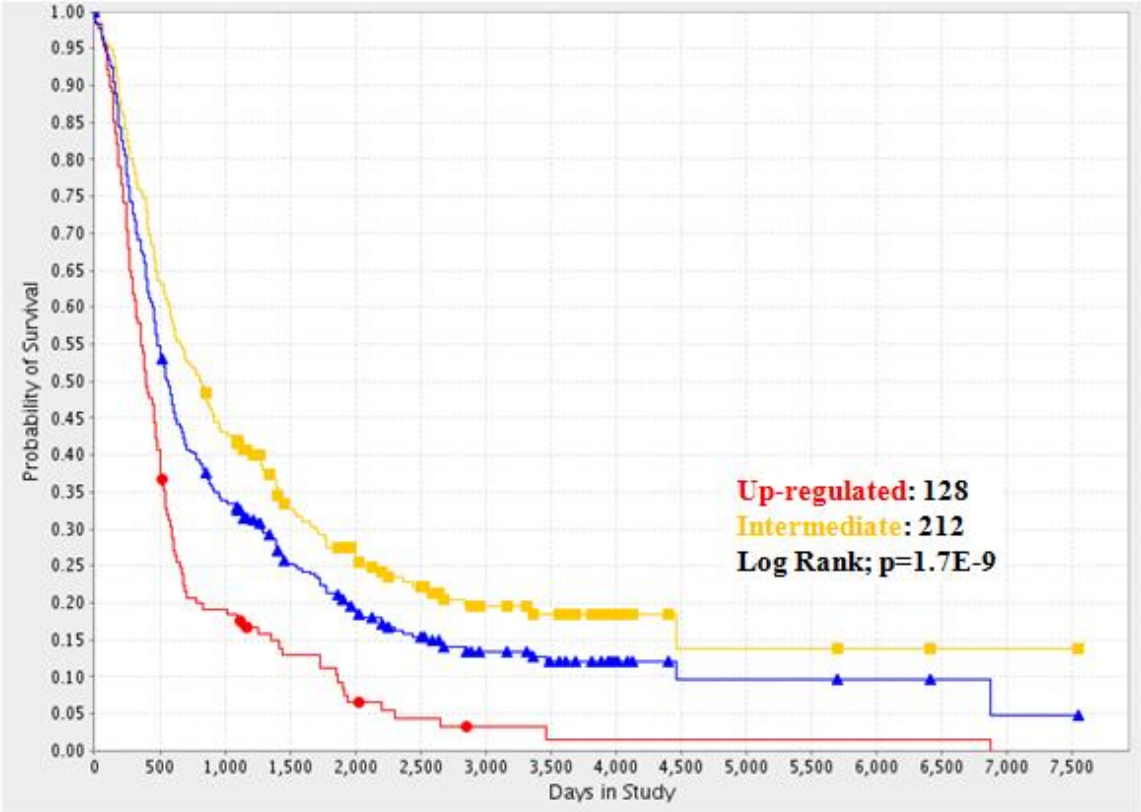

Figure 2.9: NOTCH3 transcriptomic status in independent dataset of glioma patients predicts survival: Kaplan-Meier curve for overall survival of glioma patients in independent dataset according to NOTCH3 transcriptomic levels were plotted. REMBRANDT National database of adult gliomas was used for independent analysis of NOTCH3 prognostic significance. P=1.7E-9 for up-regulated NOTCH3 curve compared to all other samples.

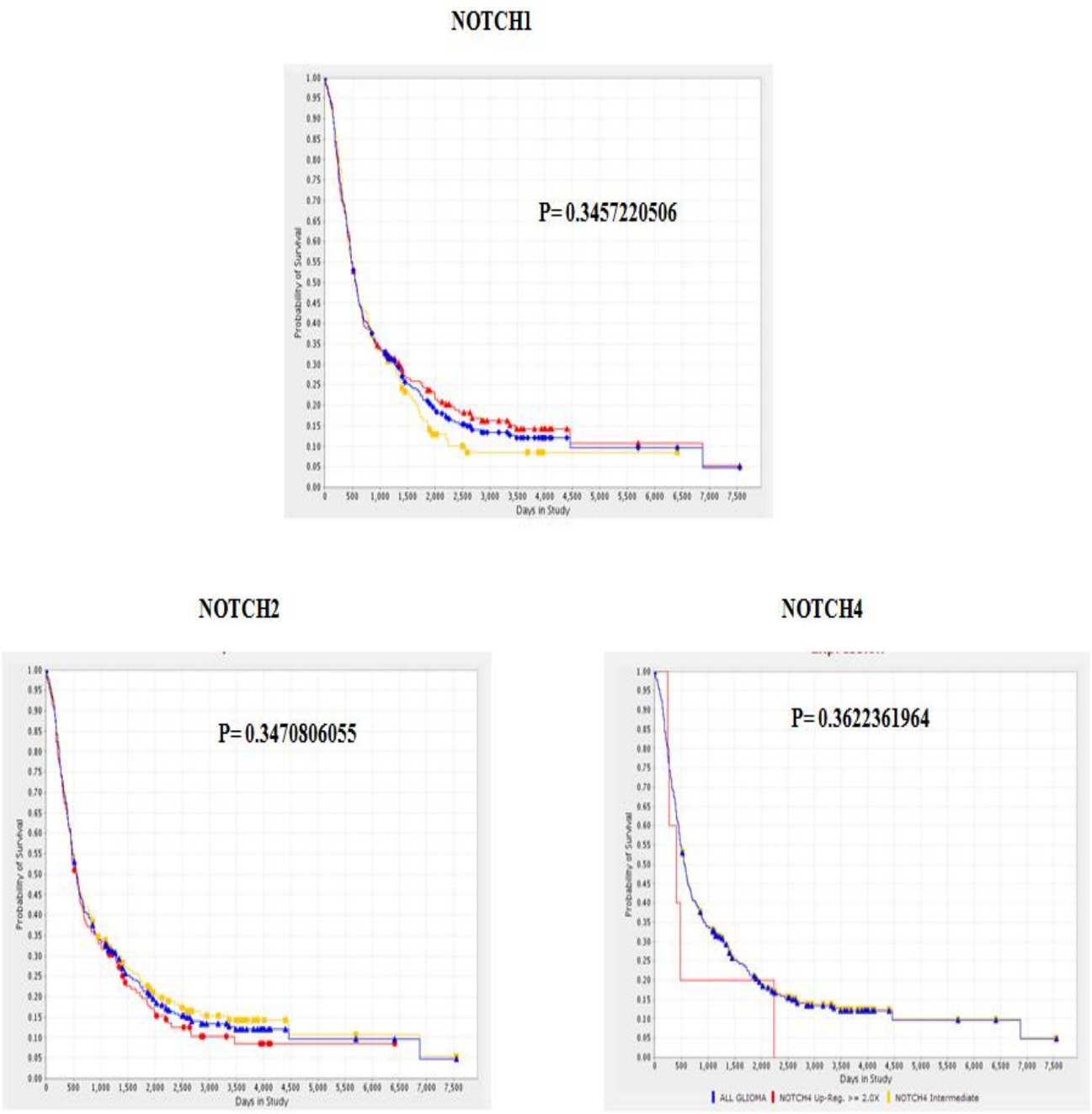

Figure 2. 10: NOTCH 1, 2 and 4 transcriptomic statuses in REMBRANDT National database of adult gliomas do not predict survival. Kaplan-Meier curve for overall survival of glioma patients in independent dataset according to NOTCH 1, 2 or 4 transcriptomic levels were plotted. None of these NOTCH transcript levels was significantly associated to outcome. Red: upregulated, yellow: intermediate.

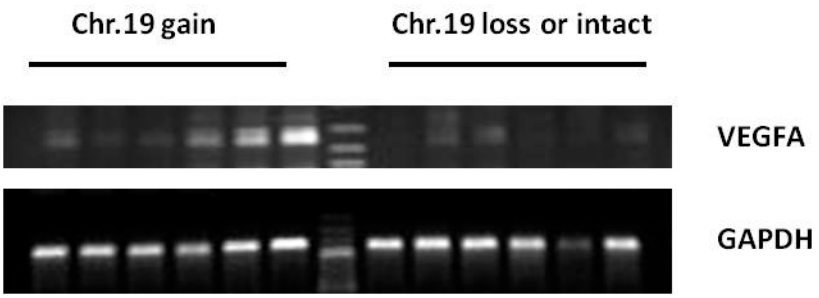

Figure 2.11: VEGFA gene expression comparison in representative tumor specimens using semi-quantitative RT-PCR clustered according to chromosome 19 status. Tumors with chromosome 19 gains and subsequent amplified NOTCH3 locus showing high levels of VEGFA transcripts compared to tumors with chromosome 19 loss or intact statuses.

CHAPTER III

NOTCH3 PROMOTES GLIOMA CELL PROLIFERATION, MIGRATION AND INVASION VIA ACTIVATION OF CYCLIND1 AND EGFR

3.1 Introduction

Malignant gliomas are the most common type of primary adult brain tumors (23). Despite some advances in the management of glioma, an increase in the incidence of tumor recurrence and resistance to chemotherapies is still a considerable challenge to improve patient outcome (165). The clinical benefits of the current modalities of choice remained poor because of high level of cell proliferation and invasion (70). Recent advances in molecular genetic techniques enable better understanding of tumor biology and open new directions toward establishing targeted therapies in glioma that could improve the overall benefits of conventional treatments.

Recent genomic studies in glioma have shown high levels of chromosomal instability in terms of frequent changes in DNA copy number (25, 26). Using SNP array analyses, we previously found gain of chromosome 19 as one of these frequent chromosomal aberrations (23). This genetic signature was observed mainly in high grade astrocytic lineages. Following copy number analysis of highly statistically significantly deregulated genes mapped to chromosome 19, we found NOTCH3 locus (19p13.12) as one of the most significant amplification in 17% of glioma biopsies. NOTCH3 is frequently deregulated in many malignancies and its role in cancer is now firmly confirmed (139, 166). However, it is currently not known whether NOTCH3 receptors are involved in gliomagenesis.

NOTCH, a highly conserved signaling pathway among species, plays an important role in cell fate decisions during human development, maintenance of stem cell proliferation and vascular formation (106). NOTCH proteins are type I transmembrane receptors all of which have a central role in the pathogenesis of human cancer (167). Upon initiation of NOTCH signaling that is mediated via cell-to-cell contact, a set of NOTCH target genes are activated such as HES and HEY family, cyclin D1 and c-Myc, all of which are important regulators of cell cycle, apoptosis and cell survival (105, 107). NOTCH receptors regulate differentiation, proliferation, self-renewal and participate in cell-cell communication (106). Interestingly, NOTCH pathway also regulates development of stem cells and activates the epithelial-to-mesenchymal transition and renders the GBM more invasive and aggressive (3, 69). Moreover, NOTCH modulators, such as γ-secretase inhibitors, have been shown to influence the proliferation and differentiation of the stem cells niche (61, 168). Stem cell niche and brain cancer stem cells roles in glioma are increasingly investigated and constitute a potential target in anticancer research.

There are increasing evidences supporting the association of one or more NOTCH pathways in a wide range of neoplasms including malignant glioma development. For instance, siRNA targeting NOTCH1 could inhibit proliferation and invasion of glioma cells and induce apoptosis *in vitro* and *in vivo* (126). Moreover, constitutive expression of NOTCH2 into NSCs resulted in their transformation into malignant tumor stem cells in transgenic mice (120). However, NOTCH3 which is expressed at much higher levels in brain compared to other NOTCHs has not yet been implicated in gliomagenesis. In the current study, we investigated the functional role of NOTCH3 in glioma cell lines to

further elucidate the significance of NOTCH3 gene amplification. In addition, the cellular and molecular effects of NOTCH3 knockdown and overexpression on malignant glioma cells were assessed, therefore providing us major insights into the role of NOTCH3 in gliomagenesis.

3.2 Materials and Methods

3.2.1 Cell culture and transfection

U87-MG human glioma cell line was obtained from ATCC (Manassas, VA) and U251-MG human glioma cell line was a kind gift from Dr. Maltese (169). U87-MG and U251-MG glioma cells were maintained in Dulbecco's modified Eagle's medium (DMEM) (Invitrogen, Carlsbad, CA) supplemented with 10% fetal bovine serum (FBS) (Hyclone, Logan, UT), 1% penicillin/streptomycin and 1% glutamine under a humidified atmosphere containing 5% CO2 at 37°C. Cells were transfected at approximately 50% confluency with a control PCLE plasmid or plasmid expressing NICD3 (Addgene plasmid 26894) using Xfect transfection reagent according to manufacturer's standard protocol (Clontech, Palo Alto, CA). After 48 hours, cells were harvested and used for further experiments.

3.2.2 Virus preparation and transduction

TSA201 cell line, used as packaging cells, was maintained in DMEM (Invitrogen, Carlsbad, CA) supplemented with 10% fetal bovine serum (Hyclone, Logan, UT), 1% penicillin/streptomycin and 1% glutamine under a humidified atmosphere containing 5% CO2 at 37°C. Lentiviral vectors encoding short hairpin RNA (shRNA) targeted to human NOTCH3 or empty vector (PLKO.1) as a control, were purchased

from Sigma-Aldrich (ThermoScientific-OpenBiosystems, Huntsville, AL). Five different shRNA sequences were initially used to select the best shRNA with maximum gene knockdown to be used for further experiments (Table 3.1).

For virus production, TSA201 cells were cultured in six-well plate (1 x 10^6 cells /well). Cells were transfected with NOTCH3 shRNAs or PLKO.1 plasmid along with envelope and packaging plasmids using Polyfect transfection reagent (QIAGEN) according to the manufacturer's protocol to generate NOTCH3 specific shRNA or control lentivirus. Vesicular stomatitis virus G (VSV-G) expressing plasmid and PAX2 expressing plasmid were used as lentivirus envelope and packaging plasmids, respectively. Media were changed 16 hours following transfection. Subsequently, lentivirus supernatants were harvested at 24 and 48 hours, pooled and frozen at -80°C until the day of usage. Control empty vector expressing lentivirus was derived similarly.

For transduction, U87-MG or U251-MG cells were plated in six well plate then the lentivirus supernatants were added next day with 8ug/ml polybrene (Sigma-Aldrich, St. Louis, MO). 1µg/ml puromycin was used to select the positive clones 48 hours post transduction (Sigma-Aldrich, St. Louis, MO). 72 hours after puromycin selection, cells were harvested and used for assays. Efficiency of NOTCH3 knockdown was assessed at both mRNA and protein levels.

3.2.3 RNA extraction

Total RNA was extracted glioma cells using TRIzol reagent according to the manufacturer's protocol (Life technologies, Carlsbad, CA). Briefly, cells were homogenized using 1ml TRIzol reagent one well of six well plate. The homogenized

samples were incubated for 5 minutes at room temperature to completely permit the dissociation of nucleoprotein complexes. 0.2 ml chloroform per 1 ml TRIZOL reagent was added to the homogenized samples followed by vigorous shaking for 15 seconds. After 2-3 minutes incubation at room temperature, samples were centrifuged at 12,000 x g for 15 minutes at 4°C (Centrifuge 5810r, Eppendorf, USA). After separation the mixture into three phases, the aqueous phase was transferred to a fresh tube. For RNA precipitation, 0.5 ml isopropyl alcohol was added to the aqueous phase then the samples were incubated for 10 minutes at room temperature and centrifuged at 12,000 x g for 10 minutes at 4°C. Supernatant was discarded and the RNA gel-like pellet was washed once with 200 ul 70% ethanol, vortexed and centrifuged at 7,500 x g for 5 minutes at 4°C. Ethanol was aspirated and the RNA pellet was air-dried and dissolved in RNase-free water.

RNA quality was assessed on 1% agarose gel and visualized using ethidium bromide under UV fluorescence (Alpha imager TM 2700, Protein Simple, USA). RNA was quantified using HP 8453 UV-visible spectrophotometer (Hewlett Packard, Wilmington, Germany) at wavelength ratio of 260nm/280nm. RNA amount was calculated using this formula (RNA amount (µg/µl) = Absorbance at 260 nm * 10 (µg/µl)). RNA solution was divided into aliquots of 5 ug and stored at -80°C to avoid repeated freeze-thaw cycles and prevent RNA degradation.

3.2.4 Reverse transcription

Reverse transcription (RT) from single-stranded RNA was used for cDNA synthesis using MyCycler Thermal Cycler system (Bio-Rad, USA) and Superscript

III/OligodT according to the standard protocol (Life technologies, Carlsbad, CA). Briefly, 5µg RNA, 0.5 µg OligodT and DEPC-treated H_2O (q.s 10 µl) were mixed per one reaction tube, heated to 65°C for 7 minutes to allow OligodT alignment to the RNA single strand and then quickly chilled on ice for 2 minutes. Then, 10 µl mastermix (4 µl 5X First-Strand Buffer, 2 µl 0.1 M DTT, 1 µl 10 mM dNTP, 50U Superscript III and DEPC-treated H_2O, q.s 10 µl) was added to the tube content and incubated at 50°C for 90 minutes before the reaction was inactivated by heating at 70°C for 15 minutes. The cDNA quality was assessed on 1% agarose gel in 1X TBE buffer and visualized using ethidium bromide under UV fluorescence (Alpha imager TM 2700, Protein Simple, USA). cDNA was quantified using HP 8453 UV-visible spectrophotometer (Hewlett Packard, Wilmington, Germany) at wavelength ratio of 260 nm/280 nm. cDNA amount was calculated using the same formula used for RNA. 50 ng of cDNA was used for further analyses.

3.2.5 Reverse Transcription PCR and Real time PCR

RT-PCR was performed using MyCycler Thermal Cycler system (Bio-Rad, USA) and Taq polymerase (NEBiolabs). Primer concentrations were normalized via mixing gene-specific forward and reverse primer pair. The concentration of both primers (forward and reverse) in the mixture was 10 µM. For RT-PCR reaction, cDNA from glioma cells was used as a template to detect expression level of gene transcripts using specific primers for NOTCH3 for 27 cycles at 58°C annealing temperature and GAPDH as internal control for 19 cycles at 55°C annealing temperature. The amplified fragments were analyzed by electrophoresis on 2% agarose gel in 1X TBE buffer and visualized

using ethidium bromide under UV fluorescence (Alpha imager TM 2700, Protein Simple, USA).

Quantitative real time PCR analysis was performed using the ABI StepOne machine (Applied Biosystems, Foster City, CA) using specific primers for NOTCH3, Hey2, c-Myc, CyclinD1 and GAPDH as internal control. All genes were amplified for 40 cycles at 58 °C annealing temperature. List of primers used in this study are illustrated in Table 3.2.

3.2.6 Western blotting

For cell lysate preparation, cell culture six-well plate was placed on ice, culture media were aspirated and the cells were washed twice with ice-cold HBSS to remove traces of culture media. To release and solubilized the cellular proteins of interest, cells were lysed at 4°C in 1 ml lysis buffer per well (150 mM sodium chloride, 1.0% Triton X-100, 0.5% sodium deoxycholate, 0.1% sodium dodecyl sulphate (SDS), 50 mM Tris, pH 8.0, 1x protease inhibitor cocktail, 1 mM EGTA, 5 mM EDTA, 5 mM sodium fluoride and 1 mM PMSF). Cells were scraped off the plate using a cold plastic rubber policeman cell scraper, and then the cell suspension was transferred into a pre-cooled microcentrifuge tube with vortexing every 5 minute for 1 hour at 4°C. Cells were then centrifuged at 11,000 rpm for 15 min at 4°C and the supernatant was aspirated and placed in a fresh pre-cold tube kept on ice, while the pellet was discarded. Protein concentration was determined using bicinchoninic acid assay (Pierce BCA assay, Rockford, IL, USA). Equal volume of 2x SDS laemmli sample buffer (Bio-Rad, Hercules, CA), mixed with 0.05% β-mercaptoethanol, was added to the lysates and then the mixture was heated at 95^{o}C for 5 minutes. Total protein extracts (50 µg/lane) were separated on (7.5-10) %

polyacrylamide gel and transferred into nitrocellulose membrane (Invitrogen Ltd, Paisley, UK) using wet transfer method. The membrane was blocked with 10% nonfat dry milk in TBST buffer (20 mmol/L Tris-HCl, 0.5 M NaCl, and 0.1% Tween 20) for 2 hours at room temperature.

Protein expressions were analyzed using primary antibodies against NOTCH3 (ab23426, Abcam, Cambridge, MA) at dilution of (1:1000), EGFR (A1308, Selleckchem, Houston, TX) at dilution of (1:1000), cyclinD1 (2978P, Cell signaling Beverly, MA) at dilution of (1:1000), β-catenin (A1013, Selleckchem, Houston, TX) at dilution of (1:1000) or Mdm2 (OP46, Calbiochem, Billerica, MA) at dilution of (1:500). GAPDH primary antibody (ab8245, Abcam, Cambridge, MA) was used as a loading control at dilution of (1: 50,000) in TBST. The membrane was incubated with primary antibodies for 3 hours at room temperature, followed by washing with TBST for three times. Subsequently the membrane was incubated with horseradish peroxidase -conjugated secondary antibodies to rabbit, mouse or sheep immunoglobulin G (GE Healthcare, Piscataway, NJ) at dilution of (1:5000) at dilution in 10% nonfat dry milk in TBST for 2 hours at room temperature followed by another washing with TBST for three times. Finally, immunoreactive proteins were detected with ECL (GE Healthcare, Piscataway, NJ) using manual x-ray film development.

3.2.7 Proliferation assays

Evaluation of cell proliferation was accomplished using MTT colorimetric assay (Sigma-Aldrich, St. Louis, MO) and in vitro growth curve assay. U87-MG and U251-MG glioma cell lines were transduced with NOTCH3 specific shRNA lentivirus (sh235 or

sh237) or control empty vector expressing lentivirus for 5 days and used for cell proliferation assays.

For MTT colorimetric assay, 5000 cells/well were plated in a 96 well plate in triplicate for each condition and allowed to grow for 96 hours by incubation at 37°C. Cell viability was assessed by adding 10 µl of filter sterilized 3-(4, 5-dimethylthiazol-2-yl)-2,5-diphenyltetrazolium bromide (MTT) solution (final concentration 0.5 mg/ml in Phosphate Buffered Saline (PBS)) to each well. Following a 4 hours incubation period with MTT, media were removed and the blue formazan crystals trapped in cells were dissolved in (100 µl/well) sterile dimethyl sulfoxide (DMSO) (Fisher Scientific, Pittsburgh, PA) by incubating at 37 ºC for 20 minutes. The absorbance was measured at 570 nm using a microplate spectrophotometer (Spectra Max Plus, Molecular Devices, CA). Background absorbance was measured at 690 nm. The results represent the mean ± SE values of three independent experiments, expressed as a percentage of viable cells relative to mock cells.

For growth curve assay, 15,000 cells/well were seeded into a 12 well plate in triplicates per sample and allowed to grow for time points 1, 3, 5 or 10 days. At each time point, the wells were rinsed twice in PBS, fixed for 5 minutes in 100% ethanol and stained with 0.1% crystal violet for 10 minutes. Stained cells were washed twice with ddH_2O and allowed to dry by inverting the plates. 750 µl of 100% methanol was then added to each well to dissolve the stain. Absorbance of the dissolved stain was measured at 540 nm using a microplate spectrophotometer (Spectra Max Plus, Molecular Devices, CA). Results were expressed as the average growth (A540 nm of methanol-solubilized

cell stain at defined time points) ± SE. The assay was repeated in 3 independent experiments.

3.2.8 Colony forming assay

Anchorage-independent growth was analyzed with soft agar colony formation assay. After gene knockdown, U87-MG or U251-MG cells (15000 cells/well) were plated, in a six-well plates, in 0.35% agar over a solid layer of 0.55% agar in DMEM medium with 20% FBS. Plates were then incubated for 3-4 weeks at 37°C in humidified conditions. The resulting colonies were stained with 0.1 % crystal violet and visualized by light microscopy (Jenco, Portland, OR) using an attached digital camera. Colonies were counted in 10 random fields at 4x magnification. Results were expressed as average colony count ± SE from three independent experiments relative to the mock cells, which was considered as 100% of colony formation.

3.2.9 Flow cytometry analysis

U87-MG cells were synchronized using serum starvation for 24 h then transiently transduced with NOTCH3 sh235, sh237 or control lentivirus. After gene knockdown, cell cycle analysis was performed using flow cytometry with propidium iodide (PI) to evaluate the effect of NOTCH3 knockdown on the cell cycle. Briefly, cells were harvested with 0.05% trypsin (Invitrogen) and the pellets (5×10^5 cells) were suspended in 500 µl cold, hypotonic PI staining solution (50 ug/ml propidium iodide, Sigma Aldrich, St. Louis, MO) containing 0.1% Triton X-100 in 0.1% sodium citrate solution and 10 µg /ml final concentration of RNase A). The stained cells were incubated for 15 minutes on ice. The cell cycle analysis of nuclei suspension was analyzed on the flow

cytometer (Becton Dickinson LSR II). ModFit^{TM} software was used to analyze the resulted DNA content curves and generate the DNA histograms.

3.2.10 DNA extraction and analysis

Cellular apoptosis was analyzed with DNA laddering. Briefly, U87-MG cells were transiently transduced with NOTCH3 sh235, sh237 or control lentivirus. After gene knockdown, media was changed into fresh DMEM with 10% FBS. After 48 hours, DNA was extracted from the cells using standard techniques (DNAeasy, Qiagen, Germany). DNA was quantified using HP 8453 UV-visible spectrophotometer (Hewlett Packard, Wilmington, Germany) at 260nm/280nm. DNA laddering was analyzed on 1% agarose gel electrophoresis using 2 µg of total DNA. Intact genomic DNA was shown as a unique band at the top of the lane, while fragmented DNA populations were represented by a ladder pattern corresponding to the internucleosomal processing.

3.2.11 Wound healing assay

Cell migration was measured using the scratch wound healing assay as described previously (170). Briefly, after transduction of NOTCH3 shRNA lentivirus or transfection of NICD3 plasmid, U87-MG or U251-MG glioma cells were cultured in 6 well plate at 37°C in DMEM supplemented with 10% FBS until confluence and then serum starved for 6 hours. A wound was introduced in the confluent monolayer of glioma cells using a pipette tip, washed twice with serum free media (SFM) and then the cells maintained in SFM until closure of wounds. The wound images were captured using a digital camera attached to the microscope (Jenco, Portland, OR) at baseline, 12 hours and 24 hours. The wounds were analyzed using NIH-Image J software. Cell migrations at 24

hours were expressed as percentages of the baseline wound area. The results represent the average of cell migration rate ± SE. The assay was repeated in 3 independent experiments.

3.2.12 Transwell assay

For invasion assay, BD BioCoat Matrigel invasion chambers (BD Biosciences, Bedford, MA) were used according to the manufacturers' instructions. Briefly, the transwell membrane filter inserts with 8-μm pore size were rehydrated and placed in a 24-well tissue culture plates. U87-MG cells were transiently transduced with NOTCH3 sh235, sh237 or control lentivirus. After trypsinization, cells were counted, centrifuged and resuspended into SFM. (5×10^4) cells/well from serum-free cell suspension were added to the top chambers, and 10% serum-containing DMEM media was added to bottom chambers then the plates were incubated at 37°C. After 48 hours, the invading cells were fixed with 100% cold ethanol for 5 minutes and stained with 0.1% crystal violet solution in 20% ethanol for 30 minutes. The non-invading cells were removed from the upper surface of the membrane using a cotton swab. Stained cells were washed twice with PBS and left to air-dry. Membrane pictures were captured using a digital camera attached to a light microscope. Stained cells were counted in four random fields per sample using NIH-image J software. Results were expressed as average values ± SE relatively to the mock invading cells.

3.2.13 Treatments

Stock of DXR (Novaplus, Bridgewater, NJ) was supplied as ready-to-use. TMZ, ETP (Sigma-Aldrich; St. Louis) and the NOTCH inhibitor "GSI-RO49" (Hoffmann-La

Roche, Nutley, NJ) were reconstituted with DMSO for the highest concentrations and serial dilutions were made in the culture media. All the drugs were added to the media on day2 and day3.

3.2.14 Cytotoxicity assay

U87-MG cells were transiently transduced with NOTCH3 sh235, sh237 or control lentivirus. U251-MG cells were transiently transfected with control or NICD3 expressing plasmid. Cell viability was determined using the colorimetric MTT assay (Sigma-Aldrich, St. Louis, MO). Briefly, cells were then trypsinized, plated in a 96 well plate (5,000 cells/well) and allowed to adhere after overnight culture at 37°C. The cells were then treated with various concentrations of DXR, ETP or TMZ on day 2 and day 3 in quadruplicates. On day 5, cell viability was assessed by adding 10 µl of filter sterilized MTT solution (final concentration 0.5 mg/ml in PBS) to each well. Following a 4 hours incubation period with MTT, media was removed and the blue formazan crystals trapped in cells were dissolved in sterile DMSO (100 µl/well) by incubating at 37 ºC for 20 min. The absorbance was measured at 570 nm using a microplate spectrophotometer (Spectra Max Plus, Molecular Devices, CA). Background absorbance was measured at 690 nm. Results were expressed as the percentage of MTT reduction in which MTT values of treatment groups were normalized to the mean MTT values of untreated cells ± SE. The assay was repeated in 3 independent experiments.

3.2.15 Statistical analysis

Statistical significance was detected using one-way ANOVA to compare differences between means of cell viabilities, cell growth curves, number of colonies, cell

migration and cell invasion rates of shRNA and control groups. Multiple group comparisons were analyzed with Tukey's multiple comparison tests. Statistical analyses were performed using SAS 9.3 software. $P < 0.05$ was considered to be statistically significant. All data are represented as mean value ± SE of at least triplicate experiments.

3.3 Results

3.3.1 NOTCH3 modulates glioma cell proliferation

To determine the functional role of NOTCH3 in malignant glioma, we first produced NOTCH3 specific shRNA lentivirus to establish an *in vitro* model for further experiments. Initially, five different shRNAs were screened to select the best shRNA with maximum gene knockdown to be used for further experiments in U87-MG cells. Using RT-PCR and real-time PCR, the efficiency of lentiviral transduction in U87-MG cells was assessed for the five used shRNAs. All the shRNAs (except sh234) were effectively able to silence NOTCH3 gene expression at mRNA level compared to the control-transduced (mock) cells (Figure 3.1A and B). Sh235 and sh236 decreased NOTCH3 mRNA levels by more than 80%. Sh237 and sh238 decreased NOTCH3 mRNA levels by 60%. In order to confirm that the NOTCH3 shRNAs effectively blocked NOTCH3 signaling in U87-MG cells, we tested the expression of Hey2, c-Myc and cyclinD1 using real-time PCR, all of which are downstream targets of NOTCH3 signaling pathway. Sh235 was the best shRNA for downregulation the expression of Hey2 and c-Myc compared to all other shRNAs. Sh237 was the best shRNA for downregulation of the expression of c-Myc and cyclinD1 compared to all other shRNAs

(Figure 3.1C). Therefore, we selected sh235 and sh237 as the best two NOTCH3 shRNAs, to exclude any off-target effect, to be used for further experiments.

Efficiency of gene knockdown using sh235 or sh237 was verified in triplicates on U87-MG cells using RT-PCR, real time PCR and Immunoblot (Figure 3.2A, B and C). Both selected shRNAs were able to reduce NOTCH3 expression at mRNA and protein levels. Downregulation of NOTCH3 protein levels at both full length (FL) and cleaved form (NICD3) with both shRNAs was consistent with the corresponding downregulated NOTCH3 mRNA levels. In addition, the expression of downstream NOTCH3 target genes was remarkably downregulated with both shRNAs (Figure 3.2B). The results were consistent with the initial testing for NOTCH3 and target genes mRNA levels. Transduction was performed also on U251-MG cells that however have relatively lower endogenous level of NOTCH3. Sh235 efficiently silenced NOTCH3 protein expression at both FL and NICD3 levels compared to the mock. Consistent with U87-MG cells, sh237 was somehow less efficient than sh235 in silencing NOTCH3 in U251-MG cells (Figure 3.2C).

We previously identified high levels of NOTCH3 transcripts and protein in high-grade glioma biopsies compared to low-grade glioma biopsies and non-tumor brain tissues. We hypothesized that high NOTCH3 expression in glioma is critical for glioma cell growth. Therefore, we were interested in studying the biological effects of NOTCH3 knockdown on U87-MG and U251-MG cell proliferation. Following silencing of NOTCH3 expression, the morphology of U87-MG cells turned into round slowly growing cells (Figure 3.3). In addition, U251-MG cells lost their adhesion capabilities after loss of NOTCH3. Further, in our lab, we found that U87-MG cells are tumorigenic

when injected into mice (data not shown), which indicates the presence of stem cell niches. To assess the effect of NOTCH3 knockdown on neurosphere formation, U87-MG cells were allowed to grow until confluence with or without NOTCH3 silencing. We found that loss of NOTCH3 resulted in smaller size neurospheres compared to the mock cells which suggest a pivotal role for NOTCH3 in regulation of stem cell proliferation by mediating cell-cell interaction (Figure 3.4).

The biological effect of NOTCH3 knockdown on glioma cell viability was measured by MTT cell proliferation assay. Interestingly, the viabilities of U87-MG and U251-MG cells were reduced after NOTCH3 knockdown. U87-MG cell viability was significantly decreased by 30-40% with both shRNAs compared to the mock (Figure 3.5A, $P < 0.0001$). U251-MG cell viability was significantly decreased by more than 80% with sh235 and 40% with sh237 compared to the mock (Figure 3.5B, $P < 0.0001$). We further confirmed these finding by studying the growth curves of transduced U87-MG and U251-MG cells at different time points. NOTCH3 knockdown significantly reduced the growth of U87-MG cells by (60 and 80%) with sh235 and (40 and 60%) with sh237 on day5 and day10 compared to the mock, respectively (Figure 3.6A, $P<0.0001$). U251-MG cell growth was reduced by more than 70% with sh235 and 40% with sh237 on day3 and day5 compared to the mock (Figure 3.6B, $P < 0.0001$). The growth inhibitory effect of NOTCH3 knockdown was maintained for 5-10 days of observation, whereas mock cells were not affected.

Moreover, we examined whether NOTCH3 knockdown will alter anchorage-independent cell proliferation using soft agar colony formation assay. Loss of NOTCH3 significantly suppressed colony formation of glioma cells on soft agar (Figure 3.7A and

B, $P<0.0001$). The colonies were clearly smaller in size and less in number when compared to the mock. There was an approximately 2-3 fold reduction in the number of colonies when of U87-MG and U251-MG cell lines were transduced with the NOTCH3 shRNA lentivirus. However, the extent of colony formation was not significant with sh237 in U251-MG cells which is related to its lower efficiency of gene knockdown. Taken together, these data suggest a major role for NOTCH3 in malignant glioma cell proliferation.

In parallel, we overexpressed NICD3 in U251-MG cells that relatively express low endogenous level of NOTCH3. The efficiency of transfection was demonstrated using quantitative real-time PCR and western blot (Figure 3.8A and B). Ectopic NICD3 transfection resulted in high RNA and protein levels of the cleaved product. In addition, NICD3 overexpression had positive effect on NOTCH3-FL expression at both RNA and protein level that suggests an autoregulatory loop (Figure 3.8A and C). Moreover, NICD3 transfection was associated with upregulation of NOTCH target genes which suggests activation of NOTCH3 signaling (Figure 3.8D). To assess the effect of NOTCH3 overexpression on U251-MG cell proliferation, MTT assay was used to measure cell proliferation in control and NICD3 transfected groups. Ectopic NOTCH3 overexpression was not associated with significant increase in U251-MG cell proliferation (Figure 3.9). This may be explained by the fact that these glioma cells are highly proliferating cells and introducing additional factors may not potentiate their original high level of cell proliferation.

3.3.2 NOTCH3 promotes glioma cell migration and invasion

Malignant gliomas are characterized by invasion to the brain parenchyma despite maximal surgical resection. Therefore, identifying molecular targets that have critical roles in glioma cell invasiveness may help minimize such aggressive presentation. Based on previous studies about the important roles of NOTCH1 and NOTCH2 in glioma cell invasiveness, we hypothesized that NOTCH3 may promote glioma cell migration and invasion.

Using an *in vitro* wound healing assay, confluent monolayers of U87-MG cells transduced with control or shRNA lentivirus were scratched and then the healing of the created wounds were followed up for 24 hours. Specific NOTCH3 knockdown resulted in marked suppression of U87-MG cell migration at 12 and 24 hours for both shRNAs compared to the mock (Figure 3.10A) as shown by less number of migrated cells into the created wounds. In contrast, complete wound closure was observed in case of mock cells when compared by slowly migrating shRNA-transduced cells. Quantitative analysis showed significant reduction of cell migration by 50% and 75% for sh235 and sh237, respectively compared to the mock (Figure 3.10B $P<0.0001$).

In parallel, we analyzed the effect of NOTCH3 overexpression on U251-MG cell proliferation. As expected, using wound healing assay, NICD3 transfection resulted in marked increase of U251-MG cell migration at 24 and 48 hours compared to the control transfected cells (Figure 3.11A) as shown by higher number of migrated cells into the created wound. NICD3-transfected cells were migrating in faster fashion and almost complete wound closure was observed when compared to control transfected cells.

Quantitative analysis showed that NICD3 overexpression had positive effect on U251-MG cell migration that was represented by 50% and 25% increase in cell migration at 24 and 48 hours, respectively; compared to the control transfected cells (Figure 3.11B).

Similarly, we confirmed these findings by studying the effects of NOTCH3 knockdown on cell invasion using matrigel invasion chambers that simulate the major components of extracellular matrix (ECM) and mimic the in vivo process of cell invasion. The results of the invasion assay indicate that NOTCH3 knockdown had a prominent inhibitory effect on U87-MG cell invasion (Figure 3.12A). Both sh235 and sh237 significantly suppressed cell invasion by more than 75% compared to the mock (Figure 3.12B, $P<0.0001$). Thus, for the first time our studies show that NOTCH3 signaling promoted both migratory and invasive abilities of glioma cells.

3.3.3 Loss of NOTCH3 alters cell cycle and induces apoptosis in U87-MG cells

Since NOTCH3 knockdown caused growth suppression of glioma cells, we further investigated the underlying molecular mechanism related to this growth inhibition by analyzing cell cycle and apoptosis response. We performed flow cytometry analysis in mock and NOTCH3 shRNA- transduced U87-MG cells. Cell cycle kinetics showed that NOTCH3 knockdown significantly increased the percentage of U87-MG cells at G0/G1 phase by 16% for sh235 and 25% for sh237 with lower cell fraction at S phase compared to the mock cells (Figure 3.13). This result is expected as both shRNAs downregulated cyclinD1 (Figure 3.2B) that has a crucial role in cell cycle progression in G1 phase (171). Then, we explored whether NOTCH3 knockdown-mediated-cell cycle arrest could have an effect on U87-MG cells apoptotic response. Cellular apoptosis was suggested by DNA

integrity analysis. NOTCH3 knockdown clearly induced cellular DNA fragmentation using both shRNAs with no DNA fragmentation for the mock cells (Figure 3.14) in correlation with the cell cycle analysis data. The findings therefore indicated that NOTCH3 knockdown caused cell growth suppression at least by down-regulating cyclinD1 expression and inducing cell cycle arrest with subsequent apoptosis. Based on cell cycle data and on the intensity of DNA apoptotic fragmentation bands, we estimated that approximately 10% of cells were in apoptosis.

To shed a light on the molecular mechanism of these alterations that resulted from NOTCH3 specific knockdown, RNA and protein levels of potential targets were assessed using real time PCR and immunoblot. As shown in Figure 3.15, knockdown of NOTCH3 is associated with significant reduction in EGFR and Cyclin D1 protein content especially with sh235, the more efficient shRNA. β-Catenin and Mdm2 levels were however not altered. Phosphorylation status of β-Catenin was not measured as NOTCH pathway doesn't directly alter phosphorylation status of several known targets. Alteration of cyclinD1 and c-Myc mRNA levels was also observed (Figure 3.2B).

3.3.4 NOTCH3 modulation and response to conventional anticancer therapy

The gold standard treatment for glioma involves TMZ as the first line in combination with radiotherapy. Other conventional anticancer drugs are added as a second line such as DXR and ETP. However, emergence of drug resistance is one of the main factors that contribute to tumor recurrence. As shown earlier, NOTCH3 silencing inhibits cell proliferation and invasion and induces apoptosis. We therefore investigated whether NOTCH3 inhibition could increase glioma cell sensitivity to these conventional

anticancer therapies. We hypothesized that glioma cells without NOTCH3 will respond better to conventional chemotherapies than glioma cells expressing NOTCH3. U87-MG cells were chosen since they express high endogenous level of NOTCH3. As expected, U87-MG cells infected with NOTCH3 shRNA lentivirus were found to be more sensitive to DXR and ETP compared to control virus-infected cells (Figure 3.16). Our results showed that NOTCH3 knockdown was sufficient to sensitize glioma cells to conventional anticancer therapy. In parallel, we used U251-MG cells that are transfected with NICD3 to confirm these results. Although it was not statistically significant, there was a trend for U251-MG cells in the NICD3 transfected group to be slightly more resistant to DXR and ETP than cells in the control plasmid transfected group (Figure 3.16). However, no increase in U87-MG cells sensitivity or U251-MG resistance to TMZ was observed following NOTCH3 modulation which might be related to the innate resistance of these glioma cells to TMZ owing to high level of MGMT expression (Figure 3.17).

In order to translate our findings into clinical practice, we used GSI-RO49 to inhibit NOTCH pathway in U87-MG and U251-MG cells. However, both cell lines were resistant to this NOTCH inhibitor and the treatment was not associated with down regulation of NICD3 or NOTCH3-FL protein content (Figure 3.18A and B). In contrast, the drug was effective in inhibiting NOTCH signaling in normal human brain cells (Figure 3.18C). This differential sensitivity suggests the presence of certain molecular players specific to the cancer cells while absent in normal brain cells. Investigations for such response marker will predict response to GSI-RO49 and eliminate any unnecessary use of this drug in glioma patients.

3.4 Discussion

Gene amplification is a well-known ubiquitous mechanism to activate oncogenes in human cancers (172). In our previous genomic study, we identified several chromosomal aberrations that associate with patients' outcomes. Specifically, gain of multiple copies of chromosome 19 is one among the major chromosomal instabilities frequently associated with poor outcome (23). We previously showed that gains of chromosome 19 are associated with the aggressive clinical behavior of gliomas which is mainly related to resistance to therapy and short term survival (23, 137, 138). In our glioma population, detailed genomic analysis of chromosome 19 amplification revealed NOTCH3 as one of the most significant amplifications that was highly expressed at both RNA and protein levels. Moreover, no alterations in gene copy number or mRNA levels have been reported for other NOTCH receptors. Therefore, we aimed at analyzing the functional role of NOTCH3 in gliomagenesis.

Gaiano and Eberhart's groups have implicated NOTCH3, for the first time, in brain development and brain tumors (173, 174). They demonstrated that retroviral injection of the active NICD3 into forebrain ventricles of mouse embryos resulted in formation of postnatal choroid plexus tumors (CPT) (173). In the present study, we explored the oncogenic role of NOTCH3 in malignant glioma in an *in vitro* study of NOTCH3 modulation using NOTCH3 specific shRNA lentivirus and NICD3 expressing plasmid. Here, we show the importance of NOTCH3 amplification as the driving force of chromosome 19 grim genetic signature. Moreover, our results elucidate for the first time the pivotal role of NOTCH3 in glioma cell proliferation and invasion, cell cycle and

apoptosis. Our data are consistent with previous studies about the oncogenic role of NOTCH3 in other malignancies (166, 175, 176).

Previous studies have shown the expression of NOTCH3 in U87-MG and U251-MG cell lines at both RNA and protein levels (177). However, no study has specifically reported the role of NOTCH3 in glioma cell proliferation. Our data not only confirm the expression of NOTCH3 in glioma cell lines and gliomas patient specimens, but also show the essential role NOTCH3 in glioma cell proliferation and survival. Inhibition of NOTCH3 through shRNA-expressing lentivirus resulted in significant decrease of glioma cell survival. The effect of growth suppression was maintained to the extent that we were not able to create stable cell lines that express NOTCH3 shRNA since the cells died by 2-3 weeks after gene knockdown. This suggests that glioma cells are dependent on NOTCH3 expression and their survival is abolished after NOTCH3 inactivation demonstrating an oncogene addiction phenomenon (94). This concept has been previously reported for several oncogenes such as HER2/neu, K-ras and cyclin D1 in human cancer cell lines of breast, pancreas and colon cancers, respectively (94).

The role of NOTCH3 in glioma invasion, adhesion and diffusion was not previously known. Interestingly, loss of NOTCH3 marked the morphology of glioma cells with new phenotype characterized by round slowly growing cells with deficient adhesion capabilities. This new morphology was more prominent with U251-MG cells. Few U251-MG cells were able to attach to the plate after overnight incubation. Previous studies have implicated NOTCH pathway in mediating cell adhesion to fibronectin (glycoprotein of the ECM) via activation of β1-integrin axis, a well-known transmembrane glycoproteins that mediate cell-cell and cell-ECM interactions in

response to intracellular signals. It has been shown that NOTCH1 signaling could promote cellular adhesion capabilities to the ECM via activation of natively expressed fibronectin receptor, α5β1-integrin, in response to NICD1 signal (178). Although NOTCH receptors may have different roles in certain contexts, the redundant effect of NOTCH receptors is well established (178, 179), particularly we reported anti-glioma effect of NOTCH3 knockdown similar to that previously reported about silencing of NOTCH1 in glioma (126). These data strongly support the role of NOTCH pathway in cell-ECM adhesion besides the well-established cell-cell interaction. The anti-proliferative effects of NOTCH3 knockdown in glioma cells extended to the *in vitro* assays of tumorigenicity, in which glioma cells, without NOTCH3, were not capable of proliferation independent of external signals as confirmed in soft agar colony formation. Collectively, our findings suggest that NOTCH3 signaling is crucial for the proliferation of glioma cells which is consistent with previous studies on other human cancers such as lung and breast cancer (114, 180).

NOTCH3 signaling starts with proteolytic cleavage that release NICD3 with subsequent translocation into the nucleus. NICD3- activated CSL binds to target genes' promoters to activate transcription. NOTCH target genes are important for cell survival and maintenance a pool of glioma stem cells. CyclinD1 and c-Myc are known targets for NOTCH and key regulators of cell cycle and proliferation. In our study, we revealed that NOTCH3 knockdown reduce their expression levels. This cyclinD1 downregulation is known to decrease activation of cyclin-dependent kinases Cdk4 and Cdk6, not only key steps for a cell to move from G1 phase to S phase during cell cycle progression but also major players in interaction with stromal cells that sustain tumor growth (181). As a

result of NOTCH3 silencing, we confirmed downregulation of cyclinD1 at both RNA and protein levels accompanied by accumulation of glioma cells at G0/G1 which might be the underlying mechanism of low proliferative capabilities of glioma cells upon silencing of NOTCH3. C-Myc is essential for glioma stem cell cycle progression and proliferation and loss of c-Myc abrogates their tumorgenic potential (182). This is highlighted in our study by the deficient neurosphere formation upon loss of NOTCH3 which was accompanied by c-Myc downregulation. These data suggest that NOTCH3 has a pivotal role in regulation of the glioma cell proliferation at least by c-Myc and cyclinD1 downregulation.

Proliferation and invasion are two of three hallmarks of glioma pathogenesis beside tumor angiogenesis (183). Surgery and anti-proliferative chemo- and radiotherapy may target the proliferative cells; however, glioma invasiveness substantially reduces the effectiveness of these approaches (70). NOTCH pathway has been recently implicated in glioma cell invasion. For instance, overexpression of NOTCH1 promotes the invasive capabilities of glioma cells (68, 126). Therefore, we hypothesized that NOTCH3 may induce cell invasion in glioma based on the similar oncogenic roles between NOTCH1 and NOTCH3. We found that loss of NOTCH3 could inhibit glioma cell migration and invasion and demonstrated that NOTCH3 regulates glioma cell invasion via interaction with the EGFR/PI3K/AKT signaling pathway, however β-catenin levels were not changed. All these proteins are key players in glioma cell invasion (126). Xu et al has reported the effect of NOTCH1 on glioma cell invasion via interaction with the major altered EGFR/PI3K/AKT signaling pathway and MMP family, well known enzymes that degrade the ECM to mediate cell invasion (126). In this study, NOTCH1 knockdown

downregulated the expression of EGFR and downstream proteins as well as MMPs, all of which are key factors for glioma cell invasion (126). In another study, global NOTCH pathway inhibition using a GSI in hepatocellular carcinoma suppresses cell invasion via downregulation of MMPs (184). Furthermore, Zhang et al has reported that NOTCH1 mediate glioma cell invasion via stimulation of β-catenin and NF-κB signaling through AKT activation (68). In our study, we identified co-amplification of both NOTCH3 and EGFR in the same glioma biopsies (23) and our findings uncovered the major role of NOTCH3 in promoting glioma cell invasion via EGFR. Therefore, considering NOTCH and EGFR inhibition in subset of glioma patients with NOTCH3 amplification could be a promising strategy toward personalized medicine that may improve therapeutic outcome.

Cellular apoptosis is a well programmed-process of cell death as part of normal development, protective mechanism against oncogenic transformation or as a result of external stress such as chemicals or drug treatment (185). As a response to apoptotic stimuli, several morphological changes occur that ultimately lead to cell death (185). These include but are not limited to: cell membrane shrinkage, mitochondrial swelling and chromosomal DNA fragmentation as a result of nuclease activation (185). Detection of apoptosis can be reported via exploring such changes. In our study, we reported that NOTCH3 knockdown resulted in cellular apoptosis shown by marked DNA fragmentation. In fact, we aimed at identifying possible mechanisms for induction of such apoptosis following loss of NOTCH3. We found that NOTCH3 knockdown resulted in downregulation of EGFR. In fact, previous studies have reported direct regulation of EGFR by NOTCH pathway (124, 186). For instance, NICD1/CSL transcription complex has been reported to induce EGFR promoter activity and this activation is abolished by

NOTCH1 knockdown (124). Thus, NOTCH regulates EGFR expression directly via NICD/CSL.

EGFR has been reported to mediate NOTCH–dependent regulation of the anti-apoptotic Mcl-1 protein at both transcriptional and post-translational level (186, 187). EGFR-induced phosphorylation of STAT3 is one possible mechanism for upregulation of Mcl-1 transcription (186). At post-translational level, EGFR can affect the E3-ligases expression or activity, well-known set of enzymes involved in Mcl-1 ubiquitination (187). These findings are highlighted in our study by downregulation of EGFR protein expression and downstream consequences following NOTCH3 knockdown. Besides, we reported co-amplification of EGFR and NOTCH3 in the same glioma biopsies (23). This may indicate that these tumors are addicted to both NOTCH and EGFR or may reflect the selective pressure to favor cell survival. Further, NOTCH3 expression has been correlated to EGFR expression in lung cancer and inhibition of NOTCH3 increased sensitivity to RTKIs (180). Together, these results strongly indicate the anti-apoptotic effect of NOTCH3 in glioma.

Since NOTCH3 silencing was associated with suppression in glioma cell proliferation and invasion, we speculated that NOTCH3 could be a therapeutic target for high grade gliomas that predict response to therapy. This view of NOTCH3 role in aggressive behavior of high grade gliomas is supported by our in vitro study showing that NOTCH3 knockdown is sufficient to sensitize U87-MG cells to DXR and ETP whereas NICD3 overexpression in U251-MG cells confers some resistance to these drugs. NOTCH3 is known to upregulate ABCB1 which is a member of the superfamily of ATP-binding cassette (ABC) transporters (149). ABCB1 up-regulation by NOTCH signaling is

responsible for decreased drug accumulation (DXR and ETP) in cancer cells and mediates drug resistance (59). Furthermore, ABCG2 is another target of NOTCH signaling that maintain neural stem cell phenotype (188) and more importantly a known transporter that efflux DXR (59) and therefore mediates resistance to this drug. Taken together, it is highly likely that NOTCH3 knockdown downregulates ABCB1 and ABCG2 which increases drug accumulation in cancer cells that increase U87-MG sensitivity to conventional chemotherapeutic agents. On the other hand NICD3 overexpression upregulates ABCB1 and ABCG2 and confers resistance to these drugs.

When we aimed at translating these finding into clinical practice through the use of GSI-RO49, we found unexpected resistance from two different glioma cell lines (U87-MG and U251-MG). In fact, Boylan's group has shown the preclinical profile of GSI-RO49 as a potent NOTCH inhibitor *in vitro* and *in vivo,* which induced tumor cell differentiation and inhibited angiogenesis (189). However, the same group has reported that high tumor levels of IL-6 and IL-8 are associated with resistance to GSI-RO49 that was shown in thirteen cell lines from different tumor types, U87-MG cells were among the top resistant ones (190). U87-MG cells were shown to express 35-fold higher IL6 mRNA and 85-fold higher IL8 mRNA compared to a control cell line. In addition, xenograft from these glioma cells did not show any response when treated with GSI-RO49 in contrast with xenograft from cell lines with low expression levels of IL-6 and IL-8 (190). Further, in phase I dose escalation study, almost one fifth of patients who did not respond to GSI-RO49 treatment had high baseline levels of IL-6 and IL-8 (190). On the other hand, we found normal brain cells to be sensitive to GSI-RO49 possibly because these normal cells have low cytokines expression and secretion levels opposite to

tumor cells that upregulate IL-6 to promote EMT and GSC growth and survival (191, 192). In addition, these tumor-derived factors were shown to be overexpressed and in certain cancers and in patient sera with poor outcome (191). Overall, these findings suggests that IL-6 and IL-8 could be surrogate markers for response to GSI-RO49 in particular and opens new insights toward global screening and measuring the baseline levels of IL-6 and IL-8 in cancer patients to avoid any unwanted use of drug treatment that may add toxicity with minimal clinical benefit. Finally, investigation of these cytokines in evaluation the efficacy of other NOTCH inhibitors can be another point that may be considered.

In conclusion, our findings elucidate, for this first time, the ability of NOTCH3 to alter the aggressive behavior of glioma cells such as proliferation, invasion and GSC survival as well as its important roles in cell cycle progression and inhibition of apoptosis. In U87-MG and U251-MG cells, this modulatory effect of NOTCH3 can be predominantly attributed to NOTCH target genes as well as its cooperation with major aberrant signaling pathways in malignant glioma such as EGFR, c-Myc and cyclinD1, which are all often overexpressed in glioma. In addition, NOTCH3 knockdown renders the glioma cells more sensitive to conventional chemotherapy. Therefore, NOTCH3 could be a novel target of therapy in malignant glioma which may hold the promise via directing subset of glioma patients to GSI-based therapy.

Table 3.1: Sequence of shRNAs used for NOTCH3 knockdown.

ShRNA	Sequence
sh234	ATACAGATACAGGTGAACTGG
sh235	ATCTCCAGCATTACTACCGAG
sh236	ATCCTGCATGTCCTTATTGGC
sh237	TTCACCGGATTTGTGTCACAG
sh238	ATCCTCTTCAGTTGGCATTGG

Table 3.2: List of primers used in this study.

Gene	Forward primer (5…3)	Reverse primer (5…3)
NOTCH3	AGGTGATCGGCTCGGTAGTAA	TTACTACCGAGCCGATCACCT
NICD3	CGAAACCGCTCTACAGACTTG	AGCCCAGTGTAAGGCTGATTT
NOTCH1	CCTTTGTGCTTCTGTTCTTCG	CTCATTCTGGTTGTCGTCCAT
NOTCH2	ATGGTGGCAGAACTGATCAAC	TTGGCAAAATGGTCTAACAGG
NOTCH4	GATCCTCATGTGTGTGTGACG	GTGGGTCCTGTGTAGCCTGTA
Hey2	CGTCGGGATCGGATAAATAA	GCACTCTCGGAATCCTATGC
c-Myc	CCTACCCTCTCAACGACAGC	CTCTGACCTTTTGCCAGGAG
CyclinD1	GTTCATGGCCAGCGGGAAGAC	CTGCCGTCCATGCGGAAGATC
GAPDH	ACCACAGTCCATGCCATCAC	TCCACCACCCTGTTGCTGTA

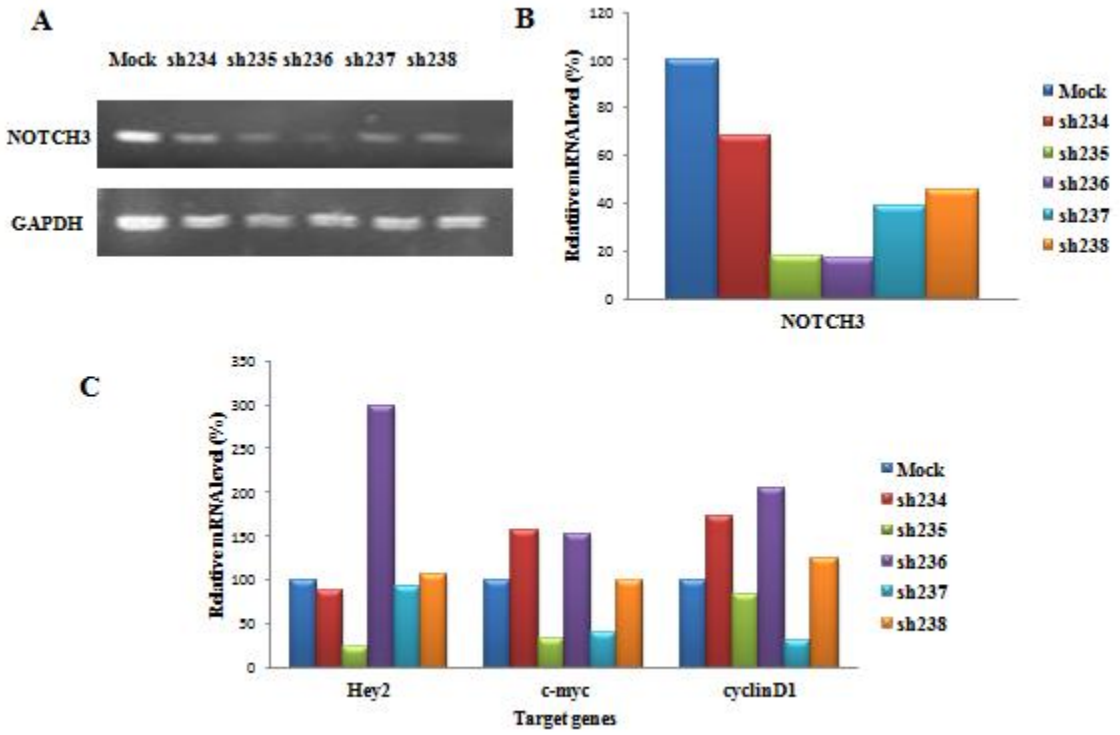

Figure 3.1: Initial screening of five different NOTCH3 shRNAs on U87-MG cells. (A) Semi-quantitative PCR in U87-MG cells showing reduction of NOTCH3 transcripts following shRNA treatment. GAPDH was used as loading control. (B) and (C) Quantitative-real time PCR showing downregulation of NOTCH3 transcripts and several of its known targets in U87-MG cells following shRNA treatment. Sh235 and sh237 are the best among all shRNAs in downregulating both NOTCH and target genes' transcripts.

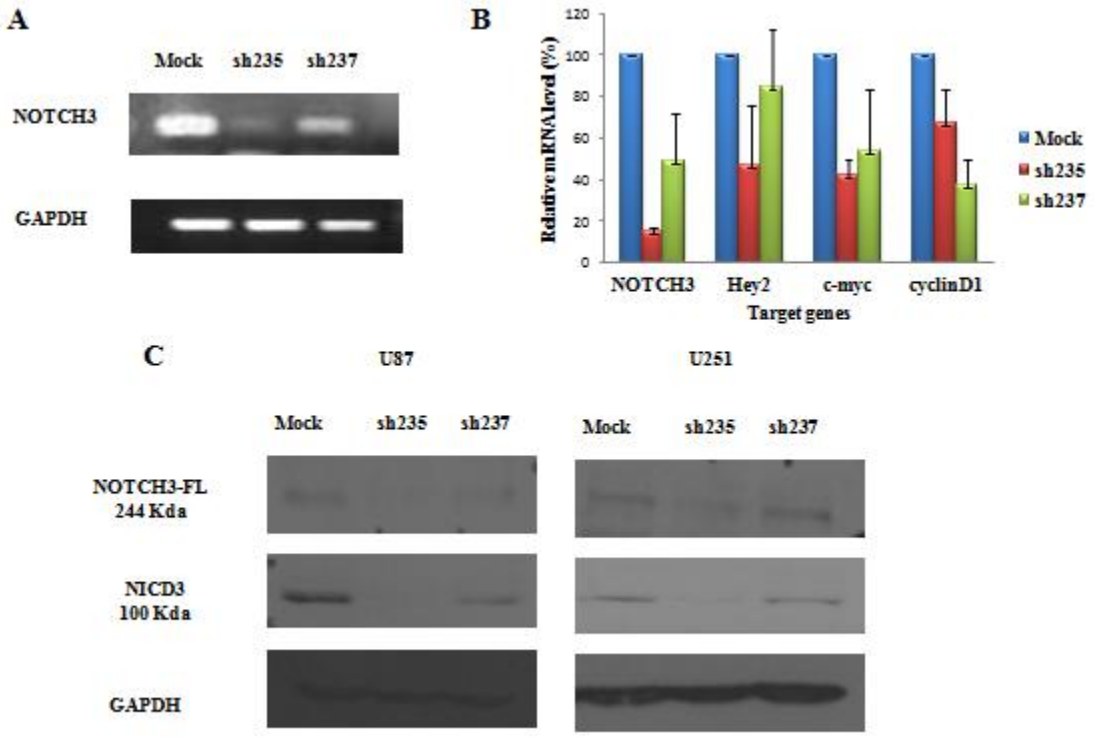

Figure 3.2: **NOTCH3 knockdown in U87-MG and U251-MG cells reduces expression of NOTCH3 and its target**. (A) and (B) Semi-quantitative and real time PCR showing downregulation of NOTCH3 transcripts and several of its known targets in U87-MG cells following shRNA treatment. (C) Western blot of U87-MG and U251-MG cells showing silencing of NOTCH3 protein expression at both full length and cleaved forms following shRNA treatment. GAPDH was used as loading control.

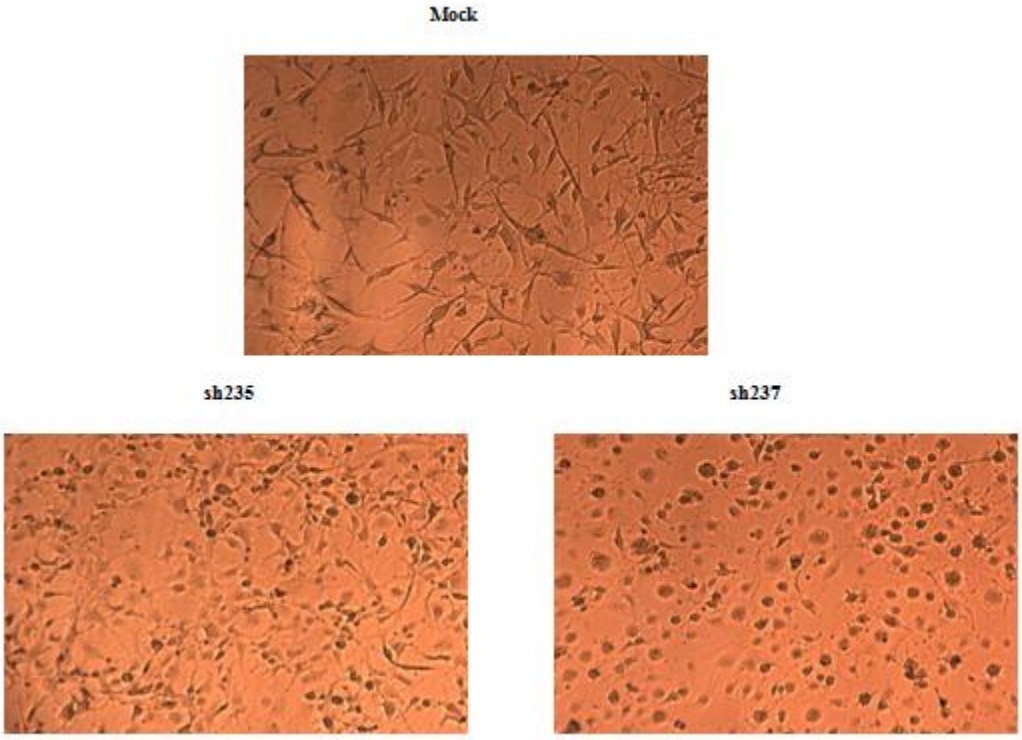

Figure 3.3: **NOTCH3 knockdown changes the morphology and growth characteristics of U87-MG cells**. Following shRNA treatments, the U87-MGcells turned into round slowly growing cells. Note the loss of end feet from the shRNA virus transduced cells compared to the mock. Following NOTCH3 knockdown, the cells died within 2-3 weeks and no stable clones have achieved.

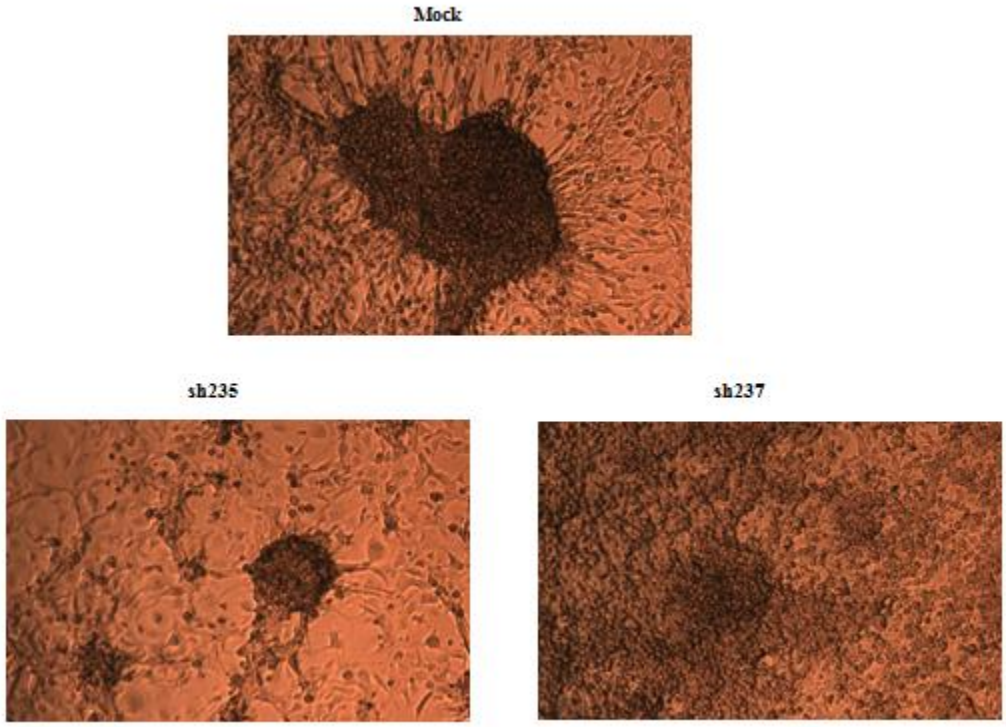

Figure 3.4: **NOTCH3 knockdown results in an ineffective neurosphere formation of U87-MG cells.** Representative images of U87-MG neurospheres with or without NOTCH3 knockdown. Following shRNA treatment, U87-MG cells (200,000 cells/well) were cultured in six-well plates for five days. Smaller size neurospheres with shRNA treatment are shown.

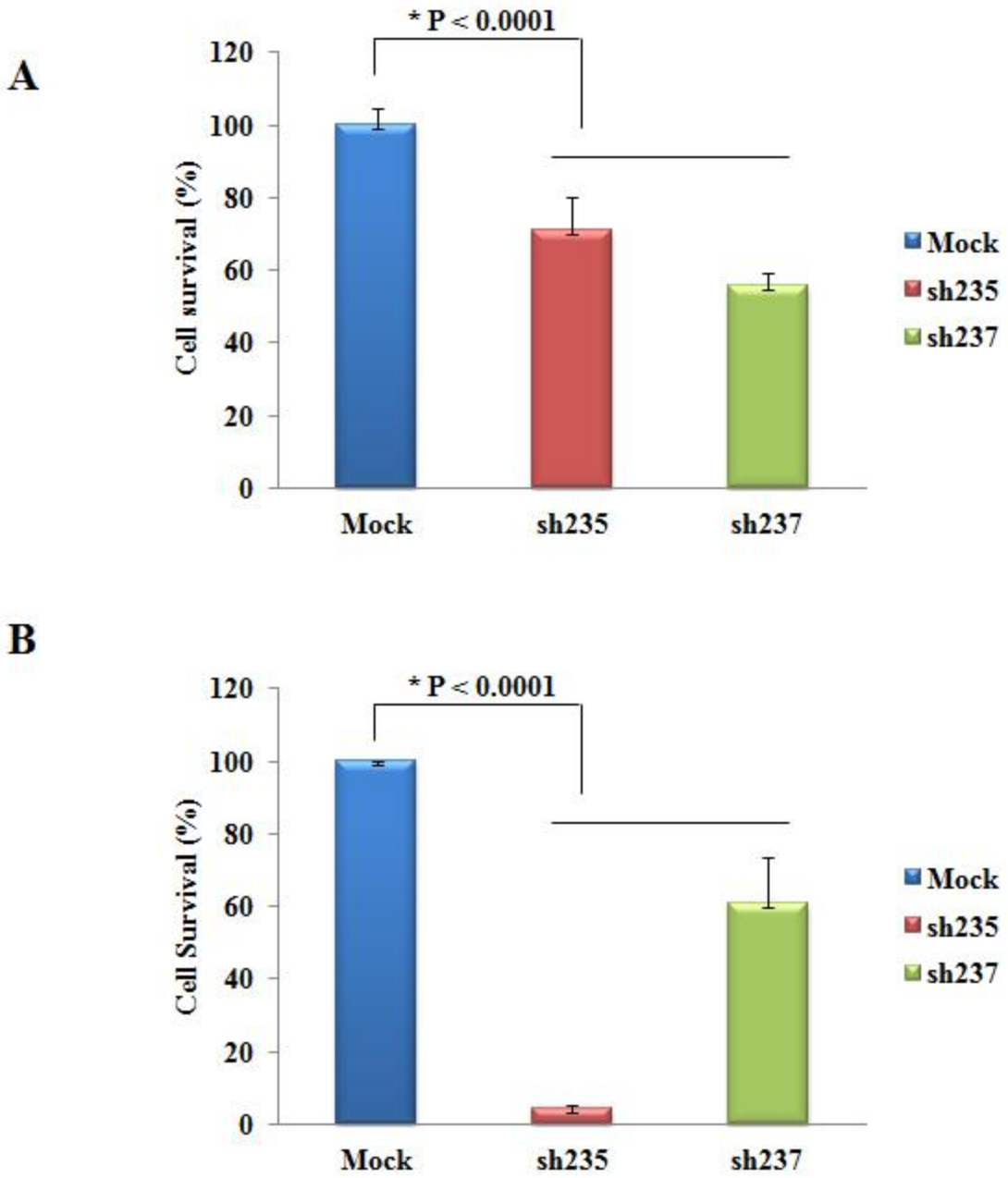

Figure 3.5: NOTCH3 knockdown reduces glioma cell viability. Cell viabilities of U87-MG and U251-MG cells following NOTCH3 knockdown were determined using MTT assay. The data represent mean ± SE of three independent experiments performed in triplicate.

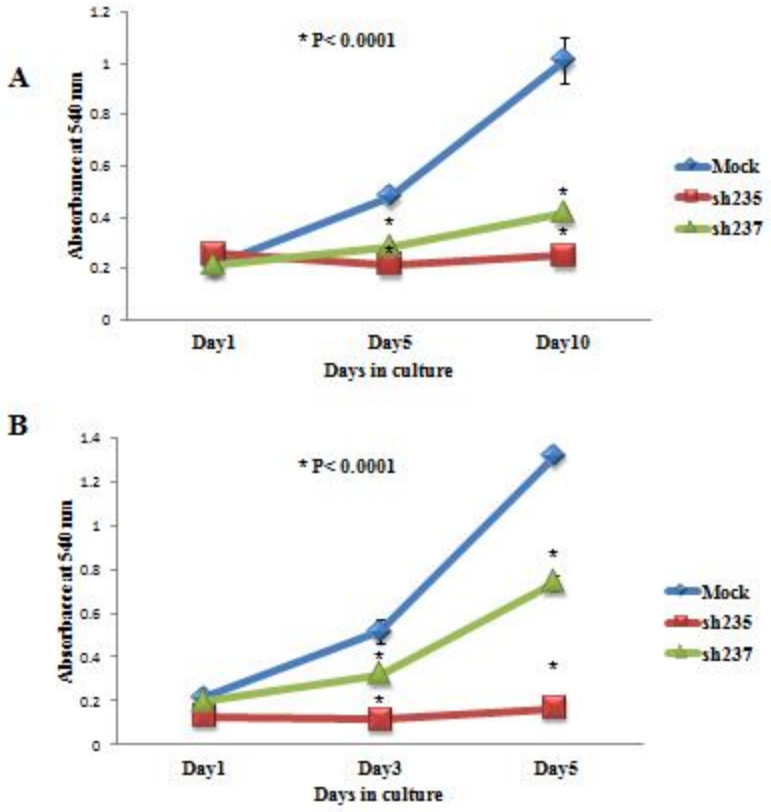

Figure 3. 6: **NOTCH3 knockdown reduces glioma cell growth.** Growth curves of (A) U87-MG and (B) U251-MG cells resulting from specific NOTCH3 knockdown were monitored with crystal violet staining at indicated time points. The results are plotted as the average growth ($A_{540\ nm}$) ± SE of three independent experiments.

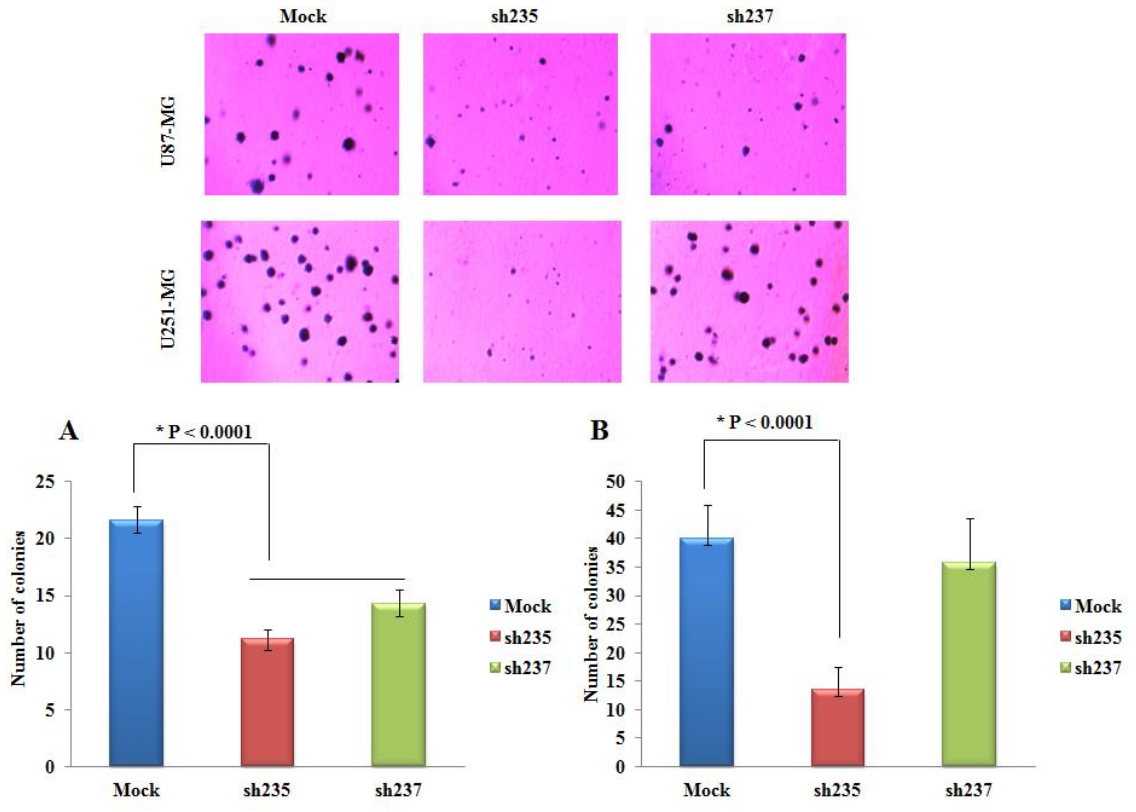

Figure 3.7: NOTCH3 knockdown reduces anchorage-independent glioma cell growth. Colony formation ability of (A) U87-MG and (B) U251-MG cells was determined with soft agar colony formation assay. Data represent mean ± SE of three independent experiments.

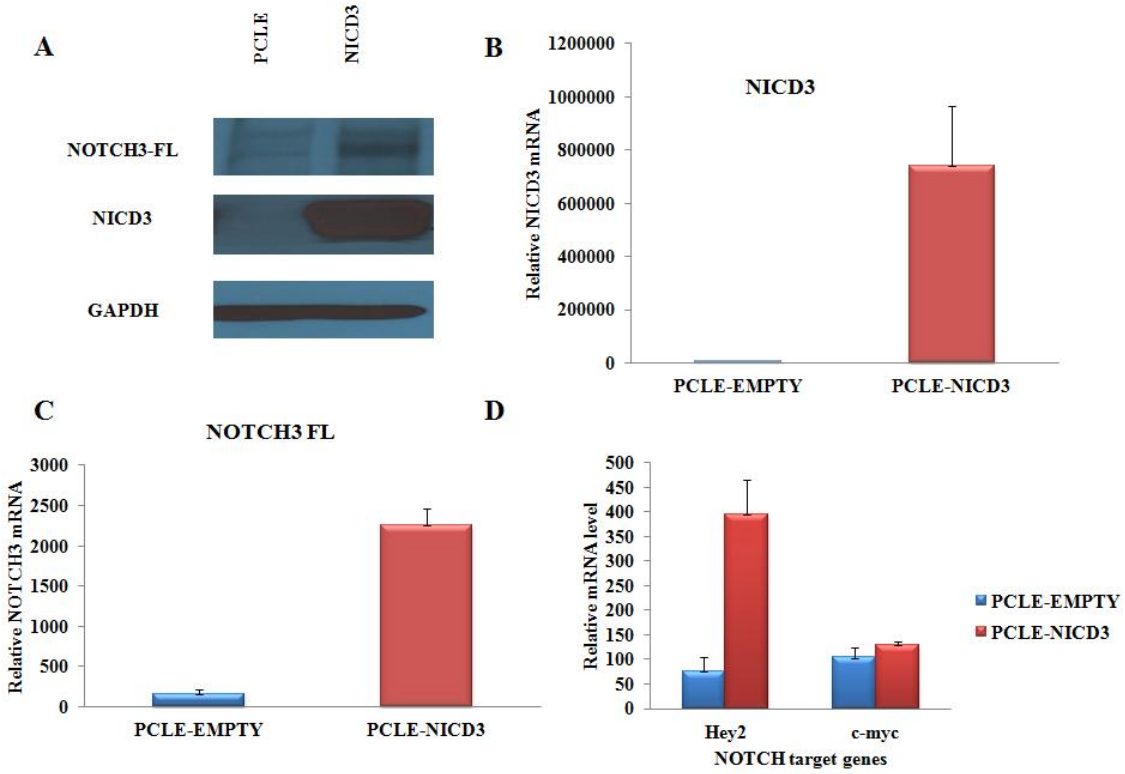

Figure 3.8: NICD3 overexpression U251-MG cells increases expression of NOTCH3 and its targets. (A) Western blot of U251-MG cells showing upregulation of NOTCH3 protein expression at both full length and cleaved forms following NICD3 transfection. GAPDH was used as loading control. (B), (C) and (D) Quantitative-real time PCR showing upregulation of NICD3, NOTCH3 and several of its known targets transcripts in U251-MG cells following NICD3 transfection, respectively.

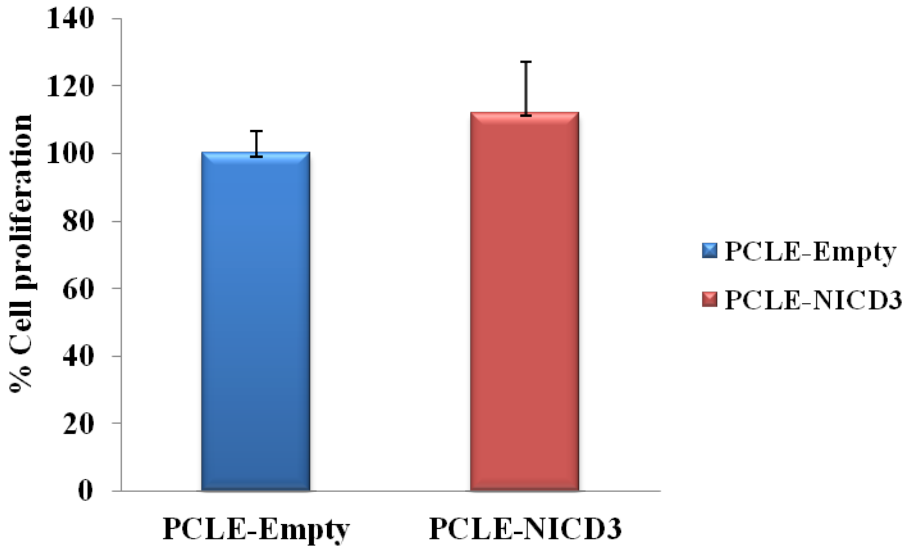

Figure 3.9: NOTCH3 overexpression did not increase glioma cell proliferation. Cell proliferation of U251-MG cells following NICD3 transfection was determined using MTT assay. The data represent mean ± SE of three independent experiments performed in triplicate.

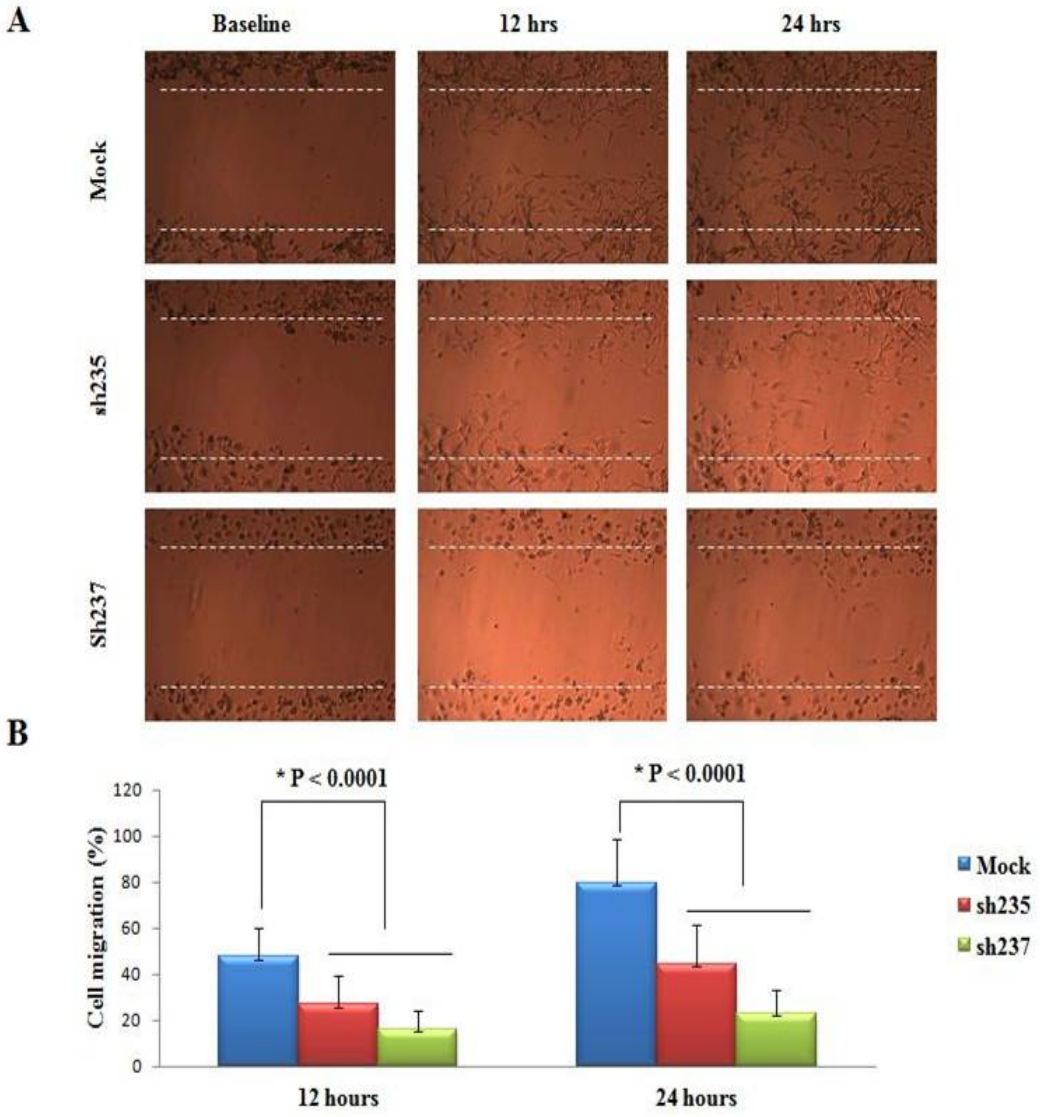

Figure 3.10: NOTCH3 knockdown in U87-MG cells suppresses cell migration. (A) Time course of U87-MG cell migration following NOTCH3 knockdown. Confluent monolayers of U87-MG cells were scratched using a pipette tip. Wound images were captured with a digital camera attached to the microscope at 0, 12 & 24 hours. The dashed lines indicate the width of the wound at indicated time points. (B) Wound healing assay for U87-MG cells. ImageJ software was used to measure changes in cell migration per time in U87-MG cells transduced with sh235 (N=20), sh237 (23) or control (N=23) lentivirus. Results are expressed as relative migration to the baseline.

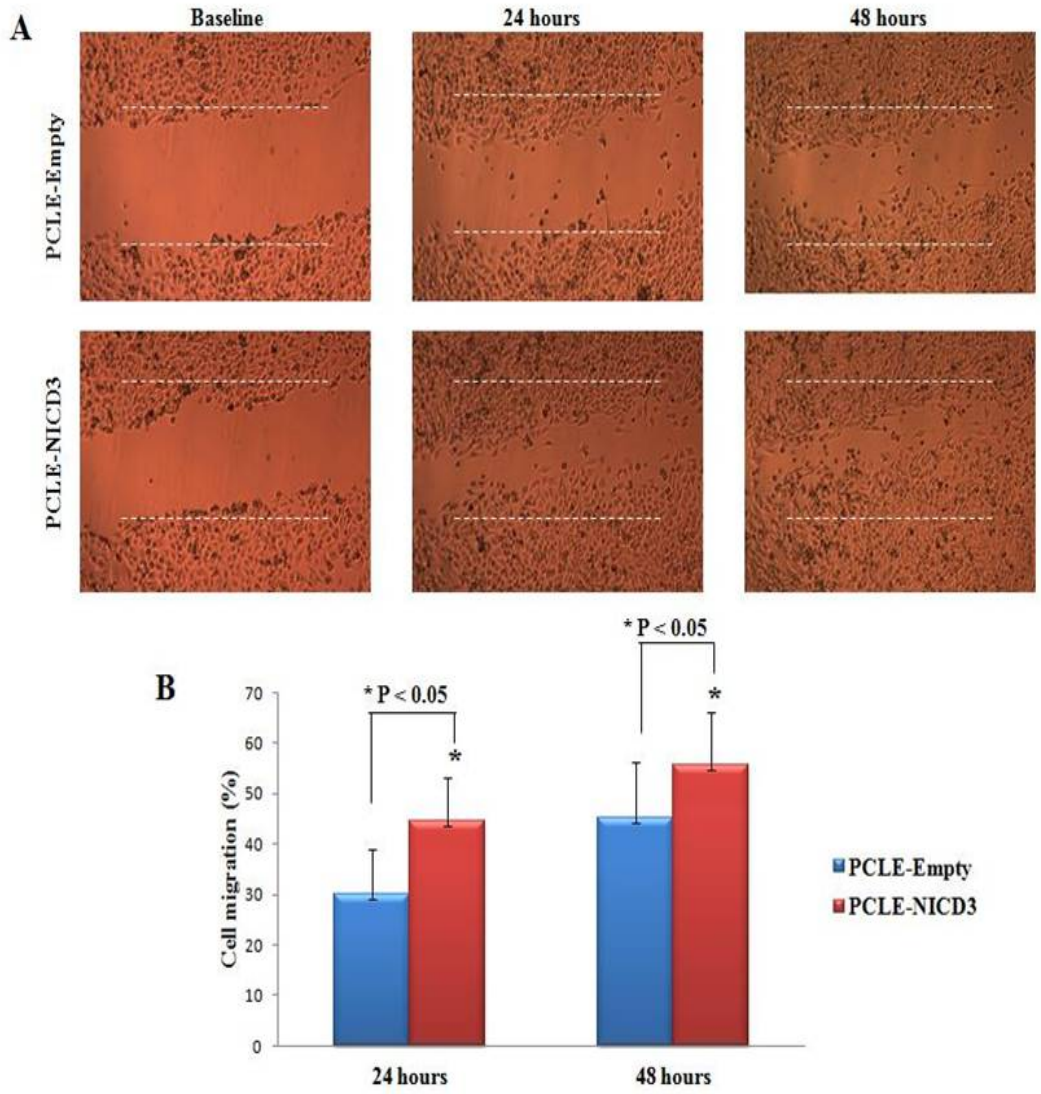

Figure 3.11: NICD3 overexpression in U251-MG cells induces cell migration. (A) Time course of U87-MG cell migration following NOTCH3 knockdown. Confluent monolayers of U251-MG cells were scratched using a pipette tip. Wound images were captured with a digital camera attached to the microscope at 0, 24 & 48 hours. The dashed lines indicate the width of the wound at indicated time points. (B) Wound healing assay for U251-MG cells. ImageJ software was used to measure changes in cell migration per time in U251-MG cells transfected with NICD3 (36) or control (35). Results are expressed as relative migration to the baseline.

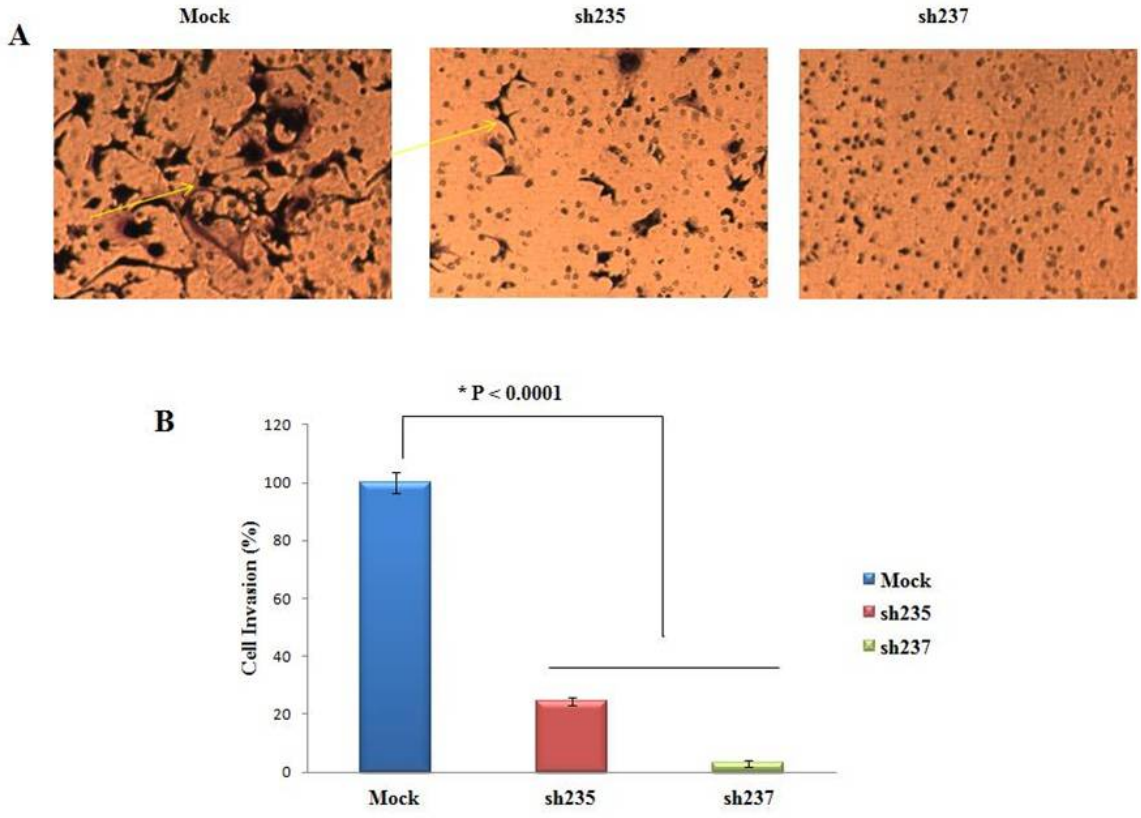

Figure 3.12: NOTCH3 knockdown in U87-MG cells hinders cell invasion. Invasion of the U87-MG cells was determined by measuring the cell ability to pass through the matrigel coated membrane. Arrows indicating the stained invasive cells are shown (A). Invasive cells were stained with crystal violet, photographed under an inverted light microscope and quantified using ImageJ software in four representative fields (B).

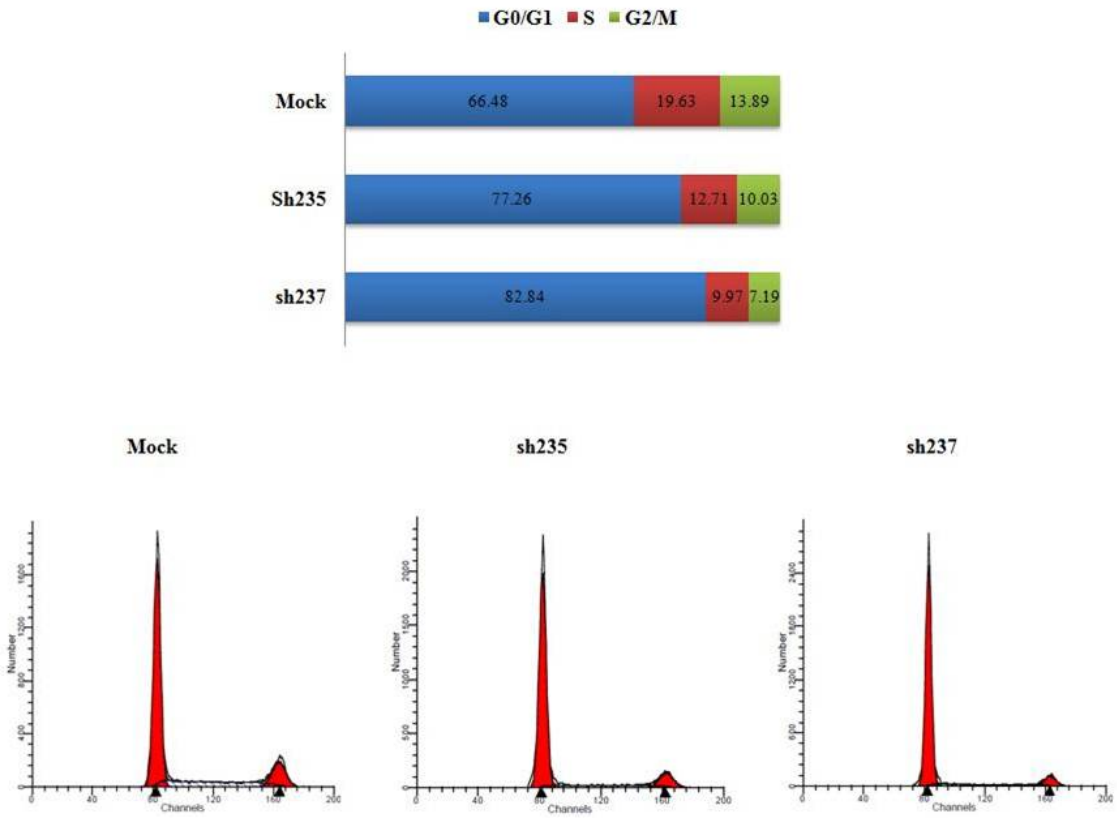

Figure 3.13: NOTCH3 knockdown alters cell cycle progression. Cell cycle profile of U87-MG cells on day 5 post-transduction with shRNA or control virus. Cells were synchronized to the G1/S boundary with serum free media before shRNA treatment. Cell cycle was assessed by propidium iodine staining followed by FACS analysis.

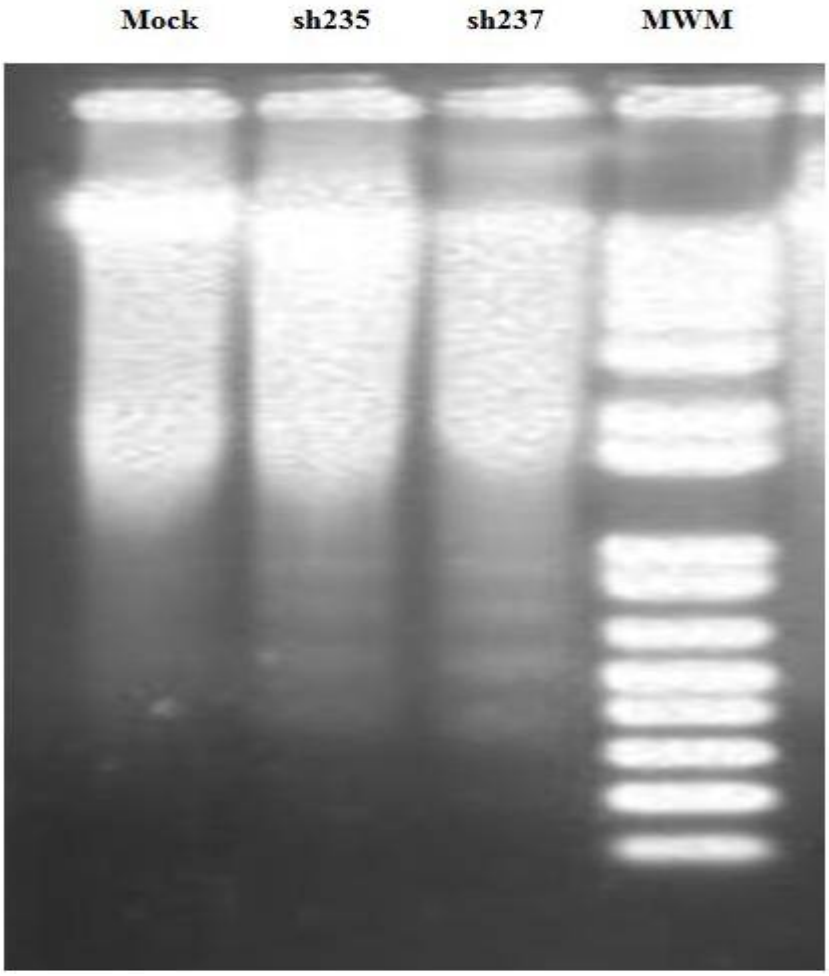

Figure 3.14: NOTCH3 knockdown induced apoptosis in U87-MG cells. Apoptosis assay was performed using DNA extraction followed by DNA integrity analysis on agarose gel. Visible DNA ladder in U87-MG cells following NOTCH3 knockdown is shown.

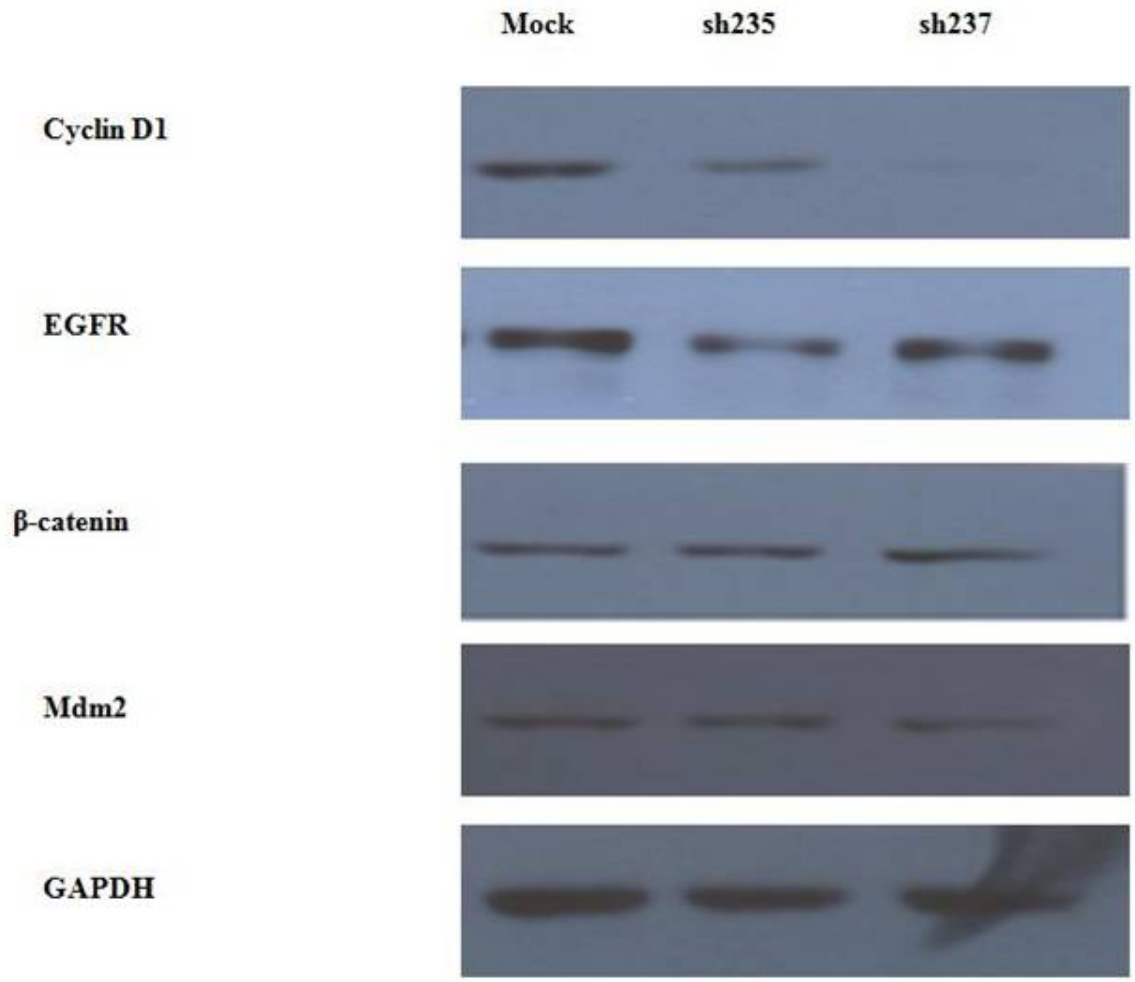

Figure 3.15: NOTCH3 knockdown in U87-MG cells results in downregulation of cyclin D1 and EGFR. Immunoblot analysis of protein content showing potential NOTCH3 targets downregulation explaining cell cycle arrest, apoptosis and inhibition of invasion following NOTCH3 knockdown. GAPDH was used as loading control.

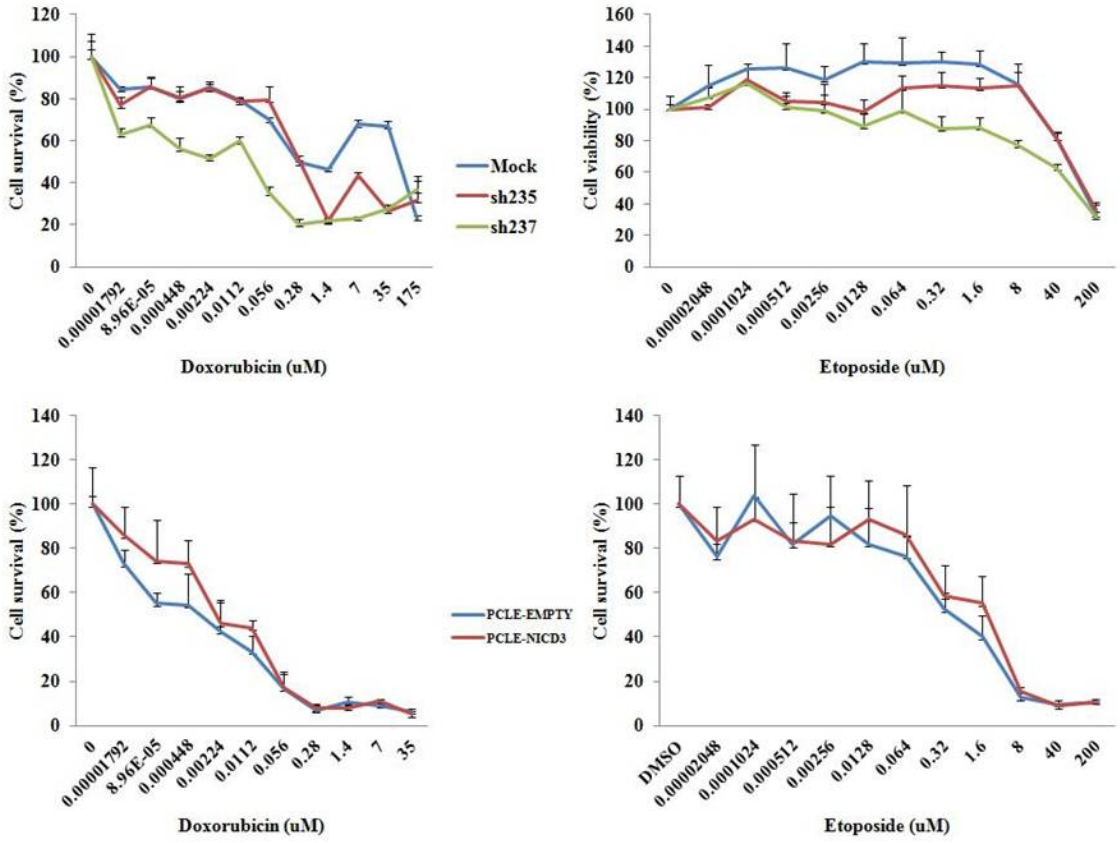

Figure 3.16: NOTCH3 modulations alter response to DXR and ETP. U87-MG (upper) transduced with shRNA and U251-MG cells (lower) expressing NICD3 were treated with various concentrations DXR and ETP. MTT assay was performed to assess cell survival. Data are represented as means ± standard error. NOTCH3 knockdown increased drug sensitivity. A trend of increase drug resistance with NICD3 is shown.

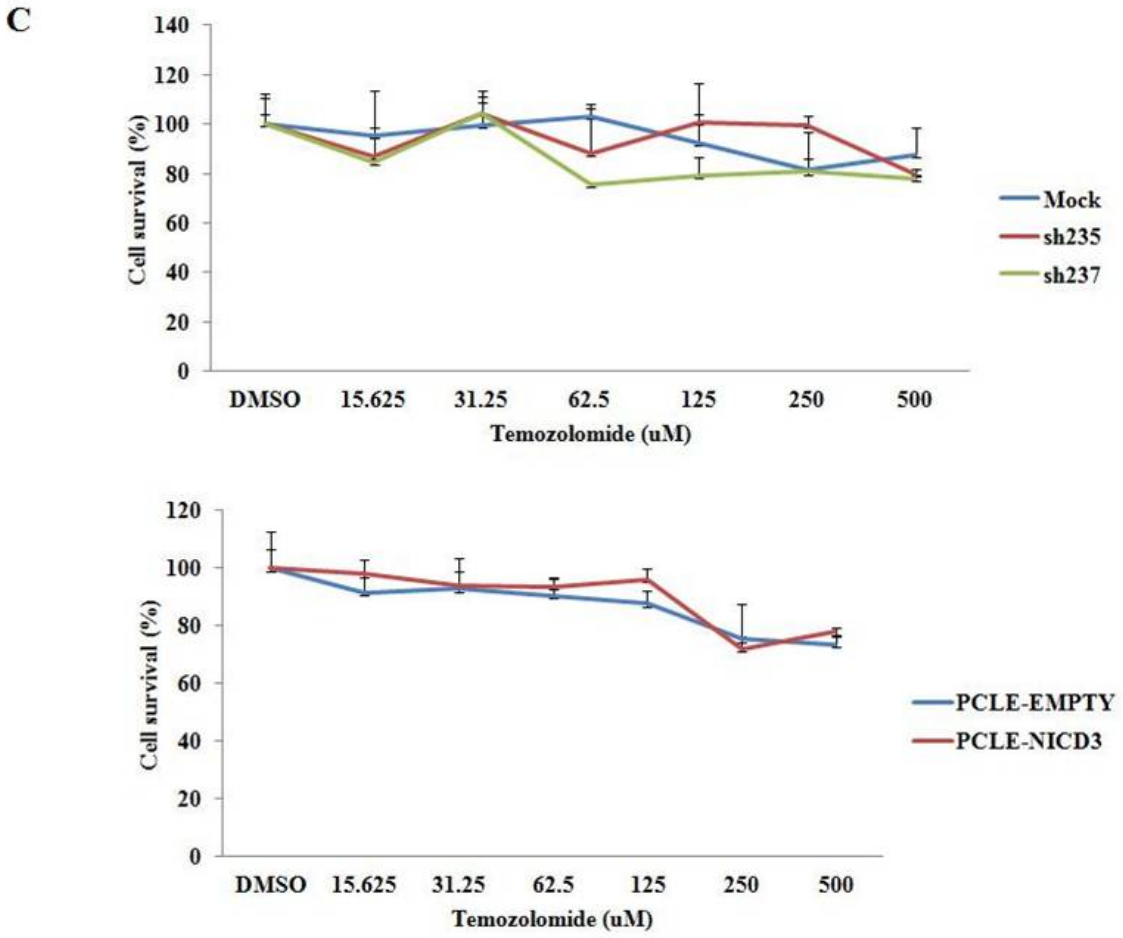

Figure 3.17: NOTCH3 modulations do not alter response to TMZ. U87-MG (upper) transduced with shRNA and U251-MG cells (lower) expressing NICD3 were treated with various concentrations TMZ. MTT assay was performed to assess cell survival.

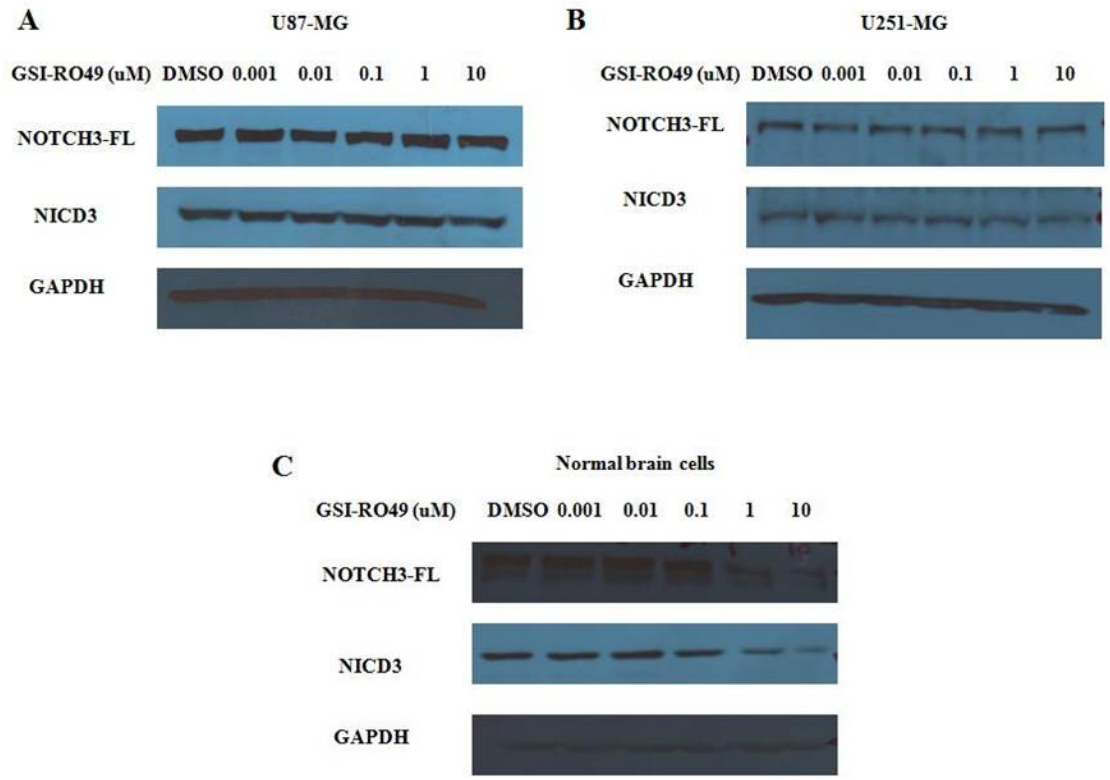

Figure 3.18: RO4929097 inhibits NOTCH cleavage in normal brain cells but not in glioma cells. Western blot analysis showing dose dependent reduction in NICD3 production and NOTCH-FL levels in normal brain cells while glioma cells were resistant to RO4929097.

CHAPTER IV

CONCLUSIONS, FUTURE WORK AND CHALLENGES

4.1 Conclusions

Chromosome 19 gain is one of the frequent CNAs in glioma patients, and it has been associated with poor outcome. Our study shows for the first time that this worsened outcome among glioma patients with this genetic alteration is mainly attributed to NOTCH3 gene amplification, which is highly expressed at both mRNA and protein level in this population. Additionally, our analysis shows that both the genomic and transcriptomic statuses of NOTCH3 can be considered as a prognostic marker for patient's survival.

In addition to its prognostic value, our findings provide unprecedented evidence that NOTCH3 offers a promising target for clinical development in glioma. Our study uncovers for the first time the oncogenic functional role of NOTCH3 in malignant glioma. Specifically, knocking down NOTCH3 inhibited neurosphere formation and abolished glioma cell growth and proliferation reflecting NOTCH3 glioma addiction phenomenon. Moreover, NOTCH3 silencing hindered glioma cell invasion and migration; and induced cell cycle arrest and apoptosis via cooperation with other major altered pathways in glioma.

Finally, knockdown of NOTCH3 sensitized glioma cells to conventional chemotherapeutic agents. Accordingly, our study provides strong evidence that targeting NOTCH3 in patients with chromosome 19 gain using currently available GSIs may improve therapeutic outcomes. This information can attribute to develop patient-specific approaches to individualize treatments via exploiting such prognostic and predictive

marker values of NOTCH3 and establishing the medical and scientific basis for personalized medicine in malignant glioma.

4.2 Future work

Because of the relatively small sample-size study, the prognostic value of NOTCH3 needs to be validated in a larger cohort of glioma samples. To avoid any possible false positive results from our genomic screening and to translate our findings into clinical practice, NOTCH3 alterations need to be confirmed using transcriptomic and proteomic profiling in larger glioma population using real time PCR analyses and immunohistochemistry, respectively. In addition, the oncogenic functional role of NOTCH3 will be confirmed in an *in vivo* mouse model in parallel to our *in vitro* studies. Moreover, given that cancer treatment is rarely monotherapy and loss of NOTCH3 was associated with lower glioma cell survival, NOTCH inhibitors will be used in combination with other standard chemotherapy drugs in an *in vitro/ in vivo* model to further confirm our data.

4.3 Challenges

After the recent implication of NOTCH signaling pathway in cancer pathogenesis, investigators aimed at identifying pharmacological strategies to block NOTCH pathway to eradicate CSCs, block the growth of tumor cells and inhibit angiogenesis. In fact, the only available and efficient therapy to block NOTCH pathway is the use of GSIs. These small molecules have been first investigated in the treatment of alzheimer's disease as they inhibit the cleavage of the amyloid precursor protein (APP), the most well-identified

substrate of γ-secretase (193). However, there are few issues that should be discussed before the use of GSIs in cancer treatment and in glioma in particular. First, most of the GSIs acts in a non-specific manner for γ-secretase cleavage of NOTCH and at the same time are able to block the processing of other substrates, such as cadherin family, CD44, HER4 and APP (194, 195). Most of these membrane-bound proteins are involved in cell adhesion, hematopoiesis and embryonic development (193) and thus inhibition of their processing may have an impact on the safety of these molecules. Identification of new compounds that target the substrate docking site instead of targeting the enzyme active site may help achieve specific blockade and avoid unwanted effects.

Second, NOTCH pathway plays an essential physiologic role in hematopoiesis, gastrointestinal tract function, and skin regeneration (196). Lack of target specificity and prolonged NOTCH blockade in normal tissues can be associated with toxicity in these organs. Identification of more specific strategies for targeting NOTCH will result in more specific target inhibition with minimal toxicity. Third, emergence of resistance to some GSIs through high expression and secretion levels of certain cytokines such as IL-6 and IL-8 necessitates initial screening for such patient selection marker prior the use of GSIs in cancer patients (190). Nevertheless, clinical trials testing the safety and efficacy of GSIs in glioma and in other cancers are ongoing as monotherapy and in combination with other treatment modalities to provide a rationale for the use of GSIs as one of the treatment modalities.

APPENDIX A

BUFFER COMPOSITIONS

Table A1: Compositions of the buffers used in this study.

Buffer	Stock recipe	Stock concentration	Working concentration
TBE (Tris/Boric acid/ EDTA)	10X: 108g Tris base, 55g Boric acid, 40 ml EDTA, q.s 1L ddH2D	10X: 890 mM Tris, 890 mM Boric acid, 20 mM EDTA, pH8.0	1X: 89 mM Tris, 89 mM Boric acid, 2 mM EDTA, pH8.0
Stringent Wash Buffer (Saline-Sodium Phosphate-EDTA (SSPE) /Tween-20)	20X SSPE: 175.3g NaCl, 27.6 g NaH2PO4xH2O, 7.4 g Na2EDTA	20X: 3 M NaCl, 200 mM NaH2PO4xH2O, 200 mM Na2EDTA	0.6 X: 90 mM NaCl, 6mM NaH2PO4xH2O, 6 mM Na2EDTA, 0.01 % Tween-20.
Running buffer for Tris-Glycine SDS-PAGE	10X: 30.2 g Tris base 144 g glycine 10 g SDS, q.s 1L ddH2O	10X: 250 mM Tris, 1.92 M glycine, 1% SDS	1X: 25 mM Tris, 192 mM glycine, 0.1% SDS
Transfer Buffer without methanol	10X: 30.2 g Trisbase, 144 g glycine, q.s 1L ddH2O	10X: 250 mM Tris, 1.92 M glycine.	1X: 25 mM Tris, 192 mM glycine, 10% methanol
Tris-Buffered Saline Tween-20 (TBST)	1X: 6.2 g Tris base, 8.76 g NaCl, 20ml HCL, 1ml Tween-20, 980 ml	Same as stock	1X: 20 mmol/L Tris-HCl, 0.5 M NaCl, and 0.1% Tween 20
1.5 M Tris buffer for separating gel	181.65 g Tris base, 800 ml ddH2O, 4 g SDS, pH 8.8, q.s 1L ddH2O	Same as stock	1.5 M Tris, 0.4% SDS
0.5 M Tris buffer for stacking gel	61 g Tris base, 4 g SDS 800 ml ddH2O, pH 6.8, q.s 1L ddH2O	Same as stock	0.5 M Tris, 0.4% SDS

APPENDIX B

PUBLICATIONS AND ABSTRACTS

Publications

Alqudah MAY, Al-Keilani MS, Agarwal S, Sibenaller Z, Ryken TC, and Assem M. NOTCH3 is a Prognostic Factor that Promotes Glioma Cell Proliferation, Migration and Invasion via Activation of CCND1 and EGFR. PLOS ONE, 2013; in press.

Agarwal S, Al-Keilani MS, **Alqudah MAY**, Sibenaller Z, Ryken TC, Assem M. Tumor derived mutations of Protein Tyrosine Phosphatase Receptor Type K affect its function and alter sensitivity to chemotherapeutics in glioma. PLOS ONE. 2013; 8(5):e62852.

Assem M, Sibenaller Z, Agarwal S, Al-Keilani MS, **Alqudah MAY**, Ryken TC. Enhancing diagnosis, prognosis and therapeutic outcome prediction of gliomas using genomics. OMICS, March 2012, 16(3): 113-122.

Abstracts

Mohammad A.Y. Alqudah, Zita Sibenaller, Timothy C. Ryken and Mahfoud Assem. NOTCH3 is a prognostic factor and critical element in gliomagenesis. Health Sciences Research Week–translational genomics, University of Iowa, IA, 2013.

Mohammad A.Y. Alqudah, Supreet Agarwal, Maha S. Al-Keilani, Zita Sibenaller, Timothy C. Ryken and Mahfoud Assem. NOTCH3: A Potential Predictive Biomarker in Malignant Glioma. Presented at the American College of Clinical Pharmacy annual meeting, 2012 October 21 24; Hollywood, Florida (FL): ACCP; 2012. Abstract # {203}.

Mohammad A.Y. Alqudah, Supreet Agarwal, Maha S. Al-Keilani, Zita Sibenaller, Timothy C. Ryken and Mahfoud Assem. NOTCH3: A Potential Predictive Biomarker in Malignant Glioma. Health Sciences Research Week–translational genomics, University of Iowa, IA, 2012.

REFERENCES

1. Hinsdale I. Central brain tumor registry of the united states; 2010. CBTRUS Statistical Report: Primary Brain and Central Nervous System Tumors Diagnosed in the United States in 2004–2008. 2012.

2. Jemal A, Siegel R, Xu J, Ward E. Cancer statistics, 2010. CA: a cancer journal for clinicians. 2010;60(5):277-300.

3. Lino M, Merlo A, Boulay J. Notch signaling in glioblastoma: A developmental drug target? BMC medicine. 2010;8(1):72.

4. Biernat W, Huang H, Yokoo H, Kleihues P, Ohgaki H. Predominant expression of mutant EGFR (EGFRvIII) is rare in primary glioblastomas. Brain pathology. 2004;14(2):131-6.

5. Ohgaki H, Kleihues P. Population-based studies on incidence, survival rates, and genetic alterations in astrocytic and oligodendroglial gliomas. Journal of Neuropathology & Experimental Neurology. 2005;64(6):479-8.

6. Louis DN, Ohgaki H, Wiestler OD, Cavenee WK, Burger PC, Jouvet A, et al. The 2007 WHO classification of tumours of the central nervous system. Acta Neuropathol. 2007;114(2):97-109.

7. Dunn GP, Rinne ML, Wykosky J, Genovese G, Quayle SN, Dunn IF, et al. Emerging insights into the molecular and cellular basis of glioblastoma. Genes Dev. 2012;26(8):756-84.

8. Walid MS. Prognostic factors for long-term survival after glioblastoma. The Permanente Journal. 2008;12(4):45.

9. Sanai N, Berger MS. Glioma extent of resection and its impact on patient outcome. Neurosurgery. 2008;62(4):753-66.

10. Bloch O, Han SJ, Cha S, Sun MZ, Aghi MK, McDermott MW, et al. Impact of extent of resection for recurrent glioblastoma on overall survival: Clinical article. J Neurosurg. 2012;117(6):1032-8.

11. Salazar OM, Rubin P, Mcdonald JV, Feldstein ML. High dose radiation therapy in the treatment of glioblastoma multiforme: A preliminary report. International Journal of Radiation Oncology* Biology* Physics. 1976;1(7):717-2.

12. McAleese J, Stenning S, Ashley S, Traish D, Hines F, Sardell S, et al. Hypofractionated radiotherapy for poor prognosis malignant glioma: Matched pair survival analysis with MRC controls. Radiotherapy and oncology. 2003;67(2):177-82.

13. Dresemann G. Temozolomide in malignant glioma. OncoTargets and therapy. 2010;3:139.

14. Buatti J, Ryken TC, Smith MC, Sneed P, Suh JH, Mehta M, et al. Radiation therapy of pathologically confirmed newly diagnosed glioblastoma in adults. J Neurooncol. 2008;89(3):313-37.

15. Ostermann S, Csajka C, Buclin T, Leyvraz S, Lejeune F, Decosterd LA, et al. Plasma and cerebrospinal fluid population pharmacokinetics of temozolomide in malignant glioma patients. Clinical cancer research. 2004;10(11):3728-36.

16. Zhang J, Stevens MF, Bradshaw TD. Temozolomide: Mechanisms of action, repair and resistance. Curr Mol Pharmacol. 2012 Jan;5(1):102-14.

17. Stupp R, Hegi ME, Mason WP, van den Bent, Martin J, Taphoorn MJ, Janzer RC, et al. Effects of radiotherapy with concomitant and adjuvant temozolomide versus radiotherapy alone on survival in glioblastoma in a randomised phase III study: 5-year analysis of the EORTC-NCIC trial. The lancet oncology. 2009;10(5):459-66.

18. Stupp R, Mason WP, Van Den Bent, Martin J, Weller M, Fisher B, Taphoorn MJ, et al. Radiotherapy plus concomitant and adjuvant temozolomide for glioblastoma. N Engl J Med. 2005;352(10):987-96.

19. Maher EA, Furnari FB, Bachoo RM, Rowitch DH, Louis DN, Cavenee WK, et al. Malignant glioma: Genetics and biology of a grave matter. Genes Dev. 2001;15(11):1311-33.

20. Chin L, Hahn WC, Getz G, Meyerson M. Making sense of cancer genomic data. Genes Dev. 2011;25(6):534-55.

21. Greenman C, Stephens P, Smith R, Dalgliesh GL, Hunter C, Bignell G, et al. Patterns of somatic mutation in human cancer genomes. Nature. 2007;446(7132):153-8.

22. Merlo A. Genes and pathways driving glioblastomas in humans and murine disease models. Neurosurg Rev. 2003;26(3):145-58.

23. Assem M, Sibenaller Z, Agarwal S, Al-Keilani MS, Alqudah MA, Ryken TC. Enhancing diagnosis, prognosis, and therapeutic outcome prediction of gliomas using genomics. OMICS: A Journal of Integrative Biology. 2012;16(3):113-22.

24. Zhu Y, Parada LF. The molecular and genetic basis of neurological tumours. Nature Reviews Cancer. 2002;2(8):616-2.

25. McLendon R, Friedman A, Bigner D, Van Meir EG, Brat DJ, Mastrogianakis GM, et al. Comprehensive genomic characterization defines human glioblastoma genes and core pathways. Nature. 2008;455(7216):1061-8.

26. Parsons DW, Jones S, Zhang X, Lin JC, Leary RJ, Angenendt P, et al. An integrated genomic analysis of human glioblastoma multiforme. Science. 2008;321(5897):1807-12.

27. Pelloski CE, Lin E, Zhang L, Yung WA, Colman H, Liu J, et al. Prognostic associations of activated mitogen-activated protein kinase and akt pathways in glioblastoma. Clinical cancer research. 2006;12(13):3935-41.

28. Sarkaria JN, Yang L, Grogan PT, Kitange GJ, Carlson BL, Schroeder MA, et al. Identification of molecular characteristics correlated with glioblastoma sensitivity to EGFR kinase inhibition through use of an intracranial xenograft test panel. Molecular cancer therapeutics. 2007;6(3):1167-74.

29. Watanabe T, Katayama Y, Yoshino A, Komine C, Yokoyama T. Deregulation of the TP53/p14ARF tumor suppressor pathway in low-grade diffuse astrocytomas and its influence on clinical course. Clinical cancer research. 2003;9(13):4884-90.

30. HALATSCH M, SCHMIDT U, UNTERBERG A, VOUGIOUKAS VI. Uniform MDM2 overexpression in a panel of glioblastoma multiforme cell lines with divergent EGFR and p53 expression status. Anticancer Res. 2006;26(6B):4191-4.

31. Lehrbach DM, Nita ME, Cecconello I. Molecular aspects of esophageal squamous cell carcinoma carcinogenesis. Arq Gastroenterol. 2003;40(4):256-61.

32. Sherr CJ, Roberts JM. CDK inhibitors: Positive and negative regulators of G1-phase progression. Genes Dev. 1999;13(12):1501-12.

33. Ekstrand AJ, Longo N, Hamid ML, Olson JJ, Liu L, Collins VP, et al. Functional characterization of an EGF receptor with a truncated extracellular domain expressed in glioblastomas with EGFR gene amplification. Oncogene. 1994 Aug;9(8):2313-20.

34. Bonavia R, Mukasa A, Narita Y, Sah DW, Vandenberg S, Brennan C, et al. Tumor heterogeneity is an active process maintained by a mutant EGFR-induced cytokine circuit in glioblastoma. Genes Dev. 2010;24(16):1731-45.

35. Phillips HS, Kharbanda S, Chen R, Forrest WF, Soriano RH, Wu TD, et al. Molecular subclasses of high-grade glioma predict prognosis, delineate a pattern of disease progression, and resemble stages in neurogenesis. Cancer cell. 2006;9(3):157-73.

36. Verhaak R, Hoadley KA, Purdom E, Wang V, Qi Y, Wilkerson MD, et al. Cancer genome atlas research network. integrated genomic analysis identifies clinically relevant subtypes of glioblastoma characterized by abnormalities in PDGFRA, IDH1, EGFR, and NF1. Cancer Cell. 2010;17(1):98-110.

37. Clarke I, Dirks P. A human brain tumor-derived PDGFR-α deletion mutant is transforming. Oncogene. 2003;22(5):722-33.

38. Ozawa T, Brennan CW, Wang L, Squatrito M, Sasayama T, Nakada M, et al. PDGFRA gene rearrangements are frequent genetic events in PDGFRA-amplified glioblastomas. Genes Dev. 2010;24(19):2205-18.

39. Sandsmark DK, Zhang H, Hegedus B, Pelletier CL, Weber JD, Gutmann DH. Nucleophosmin mediates mammalian target of Rapamycin–Dependent actin cytoskeleton dynamics and proliferation in neurofibromin-deficient astrocytes. Cancer Res. 2007;67(10):4790-9.

40. Banerjee S, Byrd JN, Gianino SM, Harpstrite SE, Rodriguez FJ, Tuskan RG, et al. The neurofibromatosis type 1 tumor suppressor controls cell growth by regulating signal transducer and activator of transcription-3 activity in vitro and in vivo. Cancer Res. 2010;70(4):1356-6.

41. Wei Y, Jiang Y, Zou F, Liu Y, Wang S, Xu N, et al. Activation of PI3K/akt pathway by CD133-p85 interaction promotes tumorigenic capacity of glioma stem cells. Proceedings of the National Academy of Sciences. 2013.

42. Maccario H, Perera NM, Davidson L, Downes CP, Leslie NR. PTEN is destabilized by phosphorylation on Thr366. Biochem J. 2007;405(Pt 3):439.

43. Wang X, Trotman LC, Koppie T, Alimonti A, Chen Z, Gao Z, et al. NEDD4-1 is a proto-oncogenic ubiquitin ligase for PTEN. Cell. 2007;128(1):129-3.

44. Molina JR, Agarwal NK, Morales FC, Hayashi Y, Aldape KD, Cote G, et al. PTEN, NHERF1 and PHLPP form a tumor suppressor network that is disabled in glioblastoma. Oncogene. 2011;31(10):1264-7.

45. Nishio T, Kawaguchi S, Yamamoto M, Iseda T, Kawasaki T, Hase T. Tenascin-C regulates proliferation and migration of cultured astrocytes in a scratch wound assay. Neuroscience. 2005;132(1):87-102.

46. Garcion E, Faissner A. Knockout mice reveal a contribution of the extracellular matrix molecule tenascin-C to neural precursor proliferation and migration. Development. 2001;128(13):2485-96.

47. Tanaka M, Yamazaki T, Araki N, Yoshikawa H, Yoshida T, Sakakura T, et al. Clinical significance of tenascin-C expression in osteosarcoma: Tenascin-C promotes distant metastases of osteosarcoma. Int J Mol Med. 2000 May;5(5):505-10.

48. Puget S, Grill J, Valent A, Bieche I, Dantas-Barbosa C, Kauffmann A, et al. Candidate genes on chromosome 9q33-34 involved in the progression of childhood ependymomas. Journal of Clinical Oncology. 2009;27(11):1884-92.

49. Rajasekhar VK, Holland EC. Postgenomic global analysis of translational control induced by oncogenic signaling. Oncogene. 2004;23(18):3248-64.

50. Brennan C, Momota H, Hambardzumyan D, Ozawa T, Tandon A, Pedraza A, et al. Glioblastoma subclasses can be defined by activity among signal transduction pathways and associated genomic alterations. PLoS One. 2009;4(11):e7752.

51. Huntly BJ, Gilliland DG. Leukaemia stem cells and the evolution of cancer-stem-cell research. Nature Reviews Cancer. 2005;5(4):311-2.

52. Lapidot T, Sirard C, Vormoor J, Murdoch B, Hoang T, Caceres-Cortes J, et al. A cell initiating human acute myeloid leukaemia after transplantation into SCID mice. . 1994.

53. Meszoely IM, Means AL, Scoggins CR, Leach SD. Developmental aspects of early pancreatic cancer. Cancer J. 2000;7(4):242-50.

54. Al-Hajj M, Wicha MS, Benito-Hernandez A, Morrison SJ, Clarke MF. Prospective identification of tumorigenic breast cancer cells. Proceedings of the National Academy of Sciences. 2003;100(7):3983-8.

55. Hudson D. Epithelial stem cells in human prostate growth and disease. Prostate cancer and prostatic diseases. 2004;7(3):188-94.

56. Ignatova TN, Kukekov VG, Laywell ED, Suslov ON, Vrionis FD, Steindler DA. Human cortical glial tumors contain neural stem-like cells expressing astroglial and neuronal markers in vitro. Glia. 2002;39(3):193-206.

57. Singh SK, Clarke ID, Terasaki M, Bonn VE, Hawkins C, Squire J, et al. Identification of a cancer stem cell in human brain tumors. Cancer Res. 2003;63(18):5821-8.

58. Singh SK, Hawkins C, Clarke ID, Squire JA, Bayani J, Hide T, et al. Identification of human brain tumour initiating cells. Nature. 2004;432(7015):396-401.

59. Dean M, Fojo T, Bates S. Tumour stem cells and drug resistance. Nature Reviews Cancer. 2005;5(4):275-84.

60. Bao S, Wu Q, Sathornsumetee S, Hao Y, Li Z, Hjelmeland AB, et al. Stem cell–like glioma cells promote tumor angiogenesis through vascular endothelial growth factor. Cancer Res. 2006;66(16):7843-8.

61. Fan X, Matsui W, Khaki L, Stearns D, Chun J, Li Y, et al. Notch pathway inhibition depletes stem-like cells and blocks engraftment in embryonal brain tumors. Cancer Res. 2006;66(15):7445-52.

62. Bleau A, Hambardzumyan D, Ozawa T, Fomchenko EI, Huse JT, Brennan CW, et al. PTEN/PI3K/akt pathway regulates the side population phenotype and ABCG2 activity in glioma tumor stem-like cells. Cell stem cell. 2009;4(3):226.

63. Sherry MM, Reeves A, Wu JK, Cochran BH. STAT3 is required for proliferation and maintenance of multipotency in glioblastoma stem cells. Stem Cells. 2009;27(10):2383-92.

64. Radisky DC. Epithelial-mesenchymal transition. J Cell Sci. 2005;118(19):4325-6.

65. Thiery JP, Acloque H, Huang RY, Nieto MA. Epithelial-mesenchymal transitions in development and disease. Cell. 2009;139(5):871-90.

66. Kalluri R, Weinberg RA. The basics of epithelial-mesenchymal transition. J Clin Invest. 2009;119(6):1420.

67. Ouyang G. Epithelial-mesenchymal transition and cancer stem cells. Cancer Stem Cells-The Cutting Edge. 2011:167-88.

68. Zhang X, Chen T, Zhang J, Mao Q, Li S, Xiong W, et al. Notch1 promotes glioma cell migration and invasion by stimulating β-catenin and NF-κB signaling via AKT activation. Cancer science. 2012;103(2):181-90.

69. Carro MS, Lim WK, Alvarez MJ, Bollo RJ, Zhao X, Snyder EY, et al. The transcriptional network for mesenchymal transformation of brain tumours. Nature. 2009;463(7279):318-25.

70. Lipinski CA, Tran NL, Menashi E, Rohl C, Kloss J, Bay RC, et al. The tyrosine kinase pyk2 promotes migration and invasion of glioma cells. Neoplasia (New York, NY). 2005;7(5):435.

71. Brabletz T, Jung A, Spaderna S, Hlubek F, Kirchner T. Migrating cancer stem cells—an integrated concept of malignant tumour progression. Nature Reviews Cancer. 2005;5(9):744-9.

72. Mani SA, Guo W, Liao M, Eaton EN, Ayyanan A, Zhou AY, et al. The epithelial-mesenchymal transition generates cells with properties of stem cells. Cell. 2008;133(4):704-15.

73. Gunia S, Hussein S, Radu DL, Pütz K, Breyer R, Hecker H, et al. CD44s-targeted treatment with monoclonal antibody blocks intracerebral invasion and growth of 9L gliosarcoma. Clin Exp Metastasis. 1999;17(3):221-30.

74. Merzak A, Koocheckpour S, Pilkington GJ. CD44 mediates human glioma cell adhesion and invasion in vitro. Cancer Res. 1994;54(15):3988-92.

75. Cheng W, Kandel JJ, Yamashiro DJ, Canoll P, Anastassiou D. A multi-cancer mesenchymal transition gene expression signature is associated with prolonged time to recurrence in glioblastoma. PLoS One. 2012;7(4):e34705.

76. Bouck N. P53 and angiogenesis. Biochimica et biophysica acta, CR.Reviews on cancer. 1996;1287(1):63-6.

77. Patenaude A, Parker J, Karsan A. Involvement of endothelial progenitor cells in tumor vascularization. Microvasc Res. 2010;79(3):217-23.

78. Ricci-Vitiani L, Pallini R, Biffoni M, Todaro M, Invernici G, Cenci T, et al. Tumour vascularization via endothelial differentiation of glioblastoma stem-like cells. Nature. 2010;468(7325):824-8.

79. Long DM. Capillary ultrastructure and the blood-brain barrier in human malignant brain tumors. J Neurosurg. 1970;32(2):127.

80. Brat DJ, Van Meir EG. Vaso-occlusive and prothrombotic mechanisms associated with tumor hypoxia, necrosis, and accelerated growth in glioblastoma. Laboratory investigation. 2004;84(4):397-405.

81. Semenza GL. Targeting HIF-1 for cancer therapy. Nature Reviews Cancer. 2003;3(10):721-32.

82. Bergers G, Benjamin LE. Tumorigenesis and the angiogenic switch. Nature Reviews Cancer. 2003;3(6):401-10.

83. Carmeliet P, Jain RK. Molecular mechanisms and clinical applications of angiogenesis. Nature. 2011;473(7347):298-307.

84. Weis SM, Cheresh DA. Tumor angiogenesis: Molecular pathways and therapeutic targets. Nat Med. 2011;17(11):1359-70.

85. Norden AD, Drappatz J, Wen PY. Novel anti-angiogenic therapies for malignant gliomas. The Lancet Neurology. 2008;7(12):1152-60.

86. Vredenburgh JJ, Desjardins A, Herndon JE, Dowell JM, Reardon DA, Quinn JA, et al. Phase II trial of bevacizumab and irinotecan in recurrent malignant glioma. Clinical Cancer Research. 2007;13(4):1253-9.

87. Batchelor TT, Duda DG, di Tomaso E, Ancukiewicz M, Plotkin SR, Gerstner E, et al. Phase II study of cediranib, an oral pan–vascular endothelial growth factor receptor tyrosine kinase inhibitor, in patients with recurrent glioblastoma. Journal of Clinical Oncology. 2010;28(17):2817-23.

88. Cohen MH, Shen YL, Keegan P, Pazdur R. FDA drug approval summary: Bevacizumab (avastin®) as treatment of recurrent glioblastoma multiforme. Oncologist. 2009;14(11):1131-8.

89. Vredenburgh JJ, Desjardins A, Herndon JE, Marcello J, Reardon DA, Quinn JA, et al. Bevacizumab plus irinotecan in recurrent glioblastoma multiforme. Journal of Clinical Oncology. 2007;25(30):4722-9.

90. Ellis LM, Hicklin DJ. Pathways mediating resistance to vascular endothelial growth factor–targeted therapy. Clinical Cancer Research. 2008;14(20):6371-5.

91. Quant EC, Norden AD, Drappatz J, Muzikansky A, Doherty L, LaFrankie D, et al. Role of a second chemotherapy in recurrent malignant glioma patients who progress on bevacizumab. Neuro-oncology. 2009;11(5):550-5.

92. Weinstein IB, Begemann M, Zhou P, Han E, Sgambato A, Doki Y, et al. Disorders in cell circuitry associated with multistage carcinogenesis: Exploitable targets for cancer prevention and therapy. Clinical Cancer Research. 1997;3(12):2696-702.

93. Weinstein IB. Addiction to oncogenes--the achilles heal of cancer. Science. 2002;297(5578):63-4.

94. Weinstein IB, Joe AK. Mechanisms of disease: Oncogene addiction—a rationale for molecular targeting in cancer therapy. Nature Clinical Practice Oncology. 2006;3(8):448-57.

95. Slamon DJ, Leyland-Jones B, Shak S, Fuchs H, Paton V, Bajamonde A, et al. Use of chemotherapy plus a monoclonal antibody against HER2 for metastatic breast cancer that overexpresses HER2. N Engl J Med. 2001;344(11):783-92.

96. Jackman DM, Miller VA, Cioffredi L, Yeap BY, Jänne PA, Riely GJ, et al. Impact of epidermal growth factor receptor and KRAS mutations on clinical outcomes in previously untreated non–small cell lung cancer patients: Results of an online tumor registry of clinical trials. Clinical Cancer Research. 2009;15(16):5267-73.

97. Mellinghoff IK, Wang MY, Vivanco I, Haas-Kogan DA, Zhu S, Dia EQ, et al. Molecular determinants of the response of glioblastomas to EGFR kinase inhibitors. N Engl J Med. 2005;353(19):2012-24.

98. Raizer JJ, Abrey LE, Lassman AB, Chang SM, Lamborn KR, Kuhn JG, et al. A phase II trial of erlotinib in patients with recurrent malignant gliomas and nonprogressive glioblastoma multiforme postradiation therapy. Neuro-oncology. 2010;12(1):95-103.

99. Stommel JM, Kimmelman AC, Ying H, Nabioullin R, Ponugoti AH, Wiedemeyer R, et al. Coactivation of receptor tyrosine kinases affects the response of tumor cells to targeted therapies. Science. 2007;318(5848):287-90.

100. Alonso MM, Cascallo M, Gomez-Manzano C, Jiang H, Bekele BN, Perez-Gimenez A, et al. ICOVIR-5 shows E2F1 addiction and potent antiglioma effect in vivo. Cancer Res. 2007;67(17):8255-63.

101. Fueyo J, Gomez-Manzano C, Yung W, Liu T, Alemany R, Bruner J, et al. Suppression of human glioma growth by adenovirus-mediated rb gene transfer. Neurology. 1998;50(5):1307-15.

102. Wollmann G, Ozduman K, van den Pol, Anthony N. Oncolytic virus therapy for glioblastoma multiforme: Concepts and candidates. The Cancer Journal. 2012;18(1):69-81.

103. Poulson D. Chromosomal deficiencies and the embryonic development of drosophila melanogaster. Proc Natl Acad Sci U S A. 1937;23(3):133.

104. Artavanis-Tsakonas S, Muskavitch M, Yedvobnick B. Molecular cloning of notch, a locus affecting neurogenesis in drosophila melanogaster. Proceedings of the National Academy of Sciences. 1983;80(7):1977-81.

105. Allenspach EJ, Maillard I, Aster JC, Pear WS. Notch signaling in cancer. Cancer biology & therapy. 2002;1(5):460-.

106. Stockhausen M, Kristoffersen K, Poulsen HS. The functional role of notch signaling in human gliomas. Neuro-oncology. 2010;12(2):199-211.

107. Ranganathan P, Weaver KL, Capobianco AJ. Notch signalling in solid tumours: A little bit of everything but not all the time. Nature Reviews Cancer. 2011;11(5):338-51.

108. Kageyama R, Ohtsuka T, Hatakeyama J, Ohsawa R. Roles of bHLH genes in neural stem cell differentiation. Exp Cell Res. 2005;306(2):343-8.

109. Ellisen LW, Bird J, West DC, Soreng AL, Reynolds TC, Smith SD, et al. < I> TAN-1, the human homolog of the drosophila< i> notch gene, is broken by chromosomal translocations in T lymphoblastic neoplasms. Cell. 1991;66(4):649-61.

110. Radtke F, Raj K. The role of notch in tumorigenesis: Oncogene or tumour suppressor? Nature Reviews Cancer. 2003;3(10):756-67.

111. Rangarajan A, Talora C, Okuyama R, Nicolas M, Mammucari C, Oh H, et al. Notch signaling is a direct determinant of keratinocyte growth arrest and entry into differentiation. EMBO J. 2001;20(13):3427-36.

112. Park JT, Shih I, Wang T. Identification of Pbx1, a potential oncogene, as a Notch3 target gene in ovarian cancer. Cancer Res. 2008;68(21):8852-60.

113. Konishi J, Yi F, Chen X, Vo H, Carbone DP, Dang TP. Notch3 cooperates with the EGFR pathway to modulate apoptosis through the induction of bim. Oncogene. 2009;29(4):589-96.

114. Yamaguchi N, Oyama T, Ito E, Satoh H, Azuma S, Hayashi M, et al. NOTCH3 signaling pathway plays crucial roles in the proliferation of ErbB2-negative human breast cancer cells. Cancer Res. 2008;68(6):1881-8.

115. Palomero T, Dominguez M, Ferrando AA. The role of the PTEN/AKT pathway in NOTCH1-induced leukemia. Cell Cycle. 2008;7(8):965-70.

116. Tanigaki K, Nogaki F, Takahashi J, Tashiro K, Kurooka H, Honjo T. Notch1 and Notch3 instructively restrict bFGF-responsive multipotent neural progenitor cells to an astroglial fate. Neuron. 2001;29(1):45-5.

117. Grandbarbe L, Bouissac J, Rand M, de Angelis MH, Artavanis-Tsakonas S, Mohier E. Delta-notch signaling controls the generation of neurons/glia from neural stem cells in a stepwise process. Development. 2003;130(7):1391-402.

118. Taylor MK, Yeager K, Morrison SJ. Physiological notch signaling promotes gliogenesis in the developing peripheral and central nervous systems. Development. 2007;134(13):2435-47.

119. Hu Y, Zheng M, Cheng G, Li L, Liang L, Gao F, et al. Notch signaling contributes to the maintenance of both normal neural stem cells and patient-derived glioma stem cells. BMC Cancer. 2011;11(1):82.

120. Tchorz J, Tome M, Cloëtta D, Sivasankaran B, Grzmil M, Huber R, et al. Constitutive Notch2 signaling in neural stem cells promotes tumorigenic features and astroglial lineage entry. Cell Death & Disease. 2012;3(6):e325.

121. Sivasankaran B, Degen M, Ghaffari A, Hegi ME, Hamou M, Ionescu MS, et al. Tenascin-C is a novel RBPJκ-induced target gene for notch signaling in gliomas. Cancer Res. 2009;69(2):458-65.

122. Purow BW, Haque RM, Noel MW, Su Q, Burdick MJ, Lee J, et al. Expression of notch-1 and its ligands, delta-like-1 and jagged-1, is critical for glioma cell survival and proliferation. Cancer Res. 2005;65(6):2353-6.

123. Ohgaki H, Dessen P, Jourde B, Horstmann S, Nishikawa T, Di Patre P, et al. Genetic pathways to glioblastoma A population-based study. Cancer Res. 2004;64(19):6892-9.

124. Purow BW, Sundaresan TK, Burdick MJ, Kefas BA, Comeau LD, Hawkinson MP, et al. Notch-1 regulates transcription of the epidermal growth factor receptor through p53. Carcinogenesis. 2008;29(5):918-25.

125. Boulay J, Miserez AR, Zweifel C, Sivasankaran B, Kana V, Ghaffari A, et al. Loss of NOTCH2 positively predicts survival in subgroups of human glial brain tumors. PLoS One. 2007;2(6):e576.

126. Xu P, Qiu M, Zhang Z, Kang C, Jiang R, Jia Z, et al. The oncogenic roles of Notch1 in astrocytic gliomas in vitro and in vivo. J Neurooncol. 2010;97(1):41-5.

127. Jin R, Nakada M, Teng L, Furuta T, Sabit H, Hayashi Y, et al. Combination therapy using notch and akt inhibitors is effective for suppressing invasion but not proliferation in glioma cells. Neurosci Lett. 2012.

128. Gimbrone MA, Leapman SB, Cotran RS, Folkman J. Tumor dormancy in vivo by prevention of neovascularization. J Exp Med. 1972;136(2):261-76.

129. Hashizume H, Baluk P, Morikawa S, McLean JW, Thurston G, Roberge S, et al. Openings between defective endothelial cells explain tumor vessel leakiness. The American journal of pathology. 2000;156(4):1363-80.

130. Li J, Sainson RC, Oon CE, Turley H, Leek R, Sheldon H, et al. DLL4-notch signaling mediates tumor resistance to anti-VEGF therapy in vivo. Cancer Res. 2011;71(18):6073-8.

131. Tamura K, Aoyagi M, Wakimoto H, Ando N, Nariai T, Yamamoto M, et al. Accumulation of CD133-positive glioma cells after high-dose irradiation by gamma knife surgery plus external beam radiation: Clinical article. J Neurosurg. 2010;113(2):310-8.

132. Lee Y, Scheck AC, Cloughesy TF, Lai A, Dong J, Farooqi HK, et al. Gene expression analysis of glioblastomas identifies the major molecular basis for the prognostic benefit of younger age. BMC medical genomics. 2008;1(1):52.

133. Rich JN, Hans C, Jones B, Iversen ES, McLendon RE, Rasheed BA, et al. Gene expression profiling and genetic markers in glioblastoma survival. Cancer Res. 2005;65(10):4051-8.

134. Smith JS, Alderete B, Minn Y, Borell TJ, Perry A, Mohapatra G, et al. Localization of common deletion regions on 1p and 19q in human gliomas and their association with histological subtype. Oncogene. 1999;18(28):4144.

135. Ino Y, Zlatescu MC, Sasaki H, Macdonald DR, Stemmer-Rachamimov AO, Jhung S, et al. Long survival and therapeutic responses in patient histologically disparate high-grade gliomas demonstrating chromosome 1p loss. J Neurosurg. 2000;92(6):983-90.

136. Wick W, Hartmann C, Engel C, Stoffels M, Felsberg J, Stockhammer F, et al. NOA-04 randomized phase III trial of sequential radiochemotherapy of anaplastic glioma with procarbazine, lomustine, and vincristine or temozolomide. Journal of Clinical Oncology. 2009;27(35):5874-80.

137. Burton EC, Lamborn KR, Feuerstein BG, Prados M, Scott J, Forsyth P, et al. Genetic aberrations defined by comparative genomic hybridization distinguish long-term from typical survivors of glioblastoma. Cancer Res. 2002;62(21):6205-10.

138. Huhn SL, Mohapatra G, Bollen A, Lamborn K, Prados MD, Feuerstein BG. Chromosomal abnormalities in glioblastoma multiforme by comparative genomic hybridization: Correlation with radiation treatment outcome. Clinical cancer research. 1999;5(6):1435-43.

139. Park JT, Li M, Nakayama K, Mao T, Davidson B, Zhang Z, et al. Notch3 gene amplification in ovarian cancer. Cancer Res. 2006;66(12):6312-8.

140. Rey JA, Bello MJ, de Campos J, Kusak ME, Ramos C, Benitez J. Chromosomal patterns in human malignant astrocytomas. Cancer Genet Cytogenet. 1987;29(2):201-2.

141. Mohapatra G, Bollen AW, Kim DH, Lamborn K, Moore DH, Prados MD, et al. Genetic analysis of glioblastoma multiforme provides evidence for subgroups within the grade. Genes, Chromosomes and Cancer. 1998;21(3):195-206.

142. Bellacosa A, De Feo D, Godwin AK, Bell DW, Cheng JQ, Altomare DA, et al. Molecular alterations of the AKT2 oncogene in ovarian and breast carcinomas. International journal of cancer. 1995;64(4):280-5.

143. Rao PH, Arias-Pulido H, Lu X, Harris CP, Vargas H, Zhang FF, et al. Chromosomal amplifications, 3q gain and deletions of 2q33-q37 are the frequent genetic changes in cervical carcinoma. BMC Cancer. 2004;4(1):5.

144. Staal SP. Molecular cloning of the akt oncogene and its human homologues AKT1 and AKT2: Amplification of AKT1 in a primary human gastric adenocarcinoma. Proceedings of the National Academy of Sciences. 1987;84(14):5034-7.

145. Kim T, Yim S, Lee J, Kwon M, Ryu J, Kang H, et al. Genome-wide screening of genomic alterations and their clinicopathologic implications in non–small cell lung cancers. Clinical cancer research. 2005;11(23):8235-42.

146. Romeike BF, Jung V, Feiden W, Moringlane JR, Zang KD, Urbschat SM. Distribution of epidermal growth factor receptor protein correlates with gain in chromosome 7 revealed by comparative genomic hybridization after microdissection in glioblastoma multiforme. Pathology-Research and Practice. 2001;197(6):427-31.

147. Hui AB, Lo K, Yin X, Poon W, Ng H. Detection of multiple gene amplifications in glioblastoma multiforme using array-based comparative genomic hybridization. Laboratory investigation. 2001;81(5):717-23.

148. Lindsell CE, Boulter J, diSibio G, Gossler A, Weinmaster G. Expression patterns of< i> jagged, Delta1, Notch1, Notch2, and< i> Notch3 genes identify Ligand–Receptor pairs that may function in neural development. Molecular and Cellular Neuroscience. 1996;8(1):14-27.

149. Park JT, Chen X, Tropè CG, Davidson B, Shih I, Wang T. Notch3 overexpression is related to the recurrence of ovarian cancer and confers resistance to carboplatin. The American journal of pathology. 2010;177(3):1087-94.

150. Büschges R, Weber RG, Actor B, Lichter P, Collins VP, Reifenberger G. Amplification and expression of cyclin D genes (CCND1 CCND2 and CCND3) in human malignant gliomas. Brain pathology. 1999;9(3):435-42.

151. Fults D, Brockmeyer D, Tullous MW, Pedone CA, Cawthon RM. p53 mutation and loss of heterozygosity on chromosomes 17 and 10 during human astrocytoma progression. Cancer Res. 1992;52(3):674-9.

152. Shih I, Nakayama K, Wu G, Nakayama N, Zhang J, Wang T. Amplification of the ch19p13. 2 NACC1 locus in ovarian high-grade serous carcinoma. Modern Pathology. 2011;24(5):638-45.

153. Wu A, Aldape K, Lang FF. High rate of deletion of chromosomes 1p and 19q in insular oligodendroglial tumors. J Neurooncol. 2010;99(1):57-64.

154. Reddy KS. Assessment of 1p/19q deletions by fluorescence in situ hybridization in gliomas. Cancer Genet Cytogenet. 2008;184(2):77-86.

155. Barbashina V, Salazar P, Holland EC, Rosenblum MK, Ladanyi M. Allelic losses at 1p36 and 19q13 in gliomas: Correlation with histologic classification, definition of a 150-kb minimal deleted region on 1p36, and evaluation of CAMTA1 as a candidate tumor suppressor gene. Clinical cancer research. 2005;11(3):1119-28.

156. Tews B, Felsberg J, Hartmann C, Kunitz A, Hahn M, Toedt G, et al. Identification of novel oligodendroglioma-associated candidate tumor suppressor genes in 1p36 and 19q13 using microarray-based expression profiling. International journal of cancer. 2006;119(4):792-800.

157. Ngo TB, Peng T, Liang X, Akeju O, Pastorino S, Zhang W, et al. The 1p-encoded protein stathmin and resistance of malignant gliomas to nitrosoureas. J Natl Cancer Inst. 2007;99(8):639-52.

158. Sasaki H, Zlatescu MC, Betensky RA, Ino Y, Cairncross JG, Louis DN. < I> PTEN is a target of chromosome 10q loss in anaplastic oligodendrogliomas and< i> PTEN alterations are associated with poor prognosis. The American journal of pathology. 2001;159(1):359-67.

159. Doucas H, Mann CD, Sutton CD, Garcea G, Neal CP, Berry DP, et al. Expression of nuclear Notch3 in pancreatic adenocarcinomas is associated with adverse clinical features, and correlates with the expression of STAT3 and phosphorylated akt. J Surg Oncol. 2008;97(1):63-8.

160. Gramantieri L, Giovannini C, Lanzi A, Chieco P, Ravaioli M, Venturi A, et al. Aberrant Notch3 and Notch4 expression in human hepatocellular carcinoma. Liver International. 2007;27(7):997-1007.

161. Konishi J, Kawaguchi KS, Vo H, Haruki N, Gonzalez A, Carbone DP, et al. Γ-secretase inhibitor prevents Notch3 activation and reduces proliferation in human lung cancers. Cancer Res. 2007;67(17):8051-7.

162. Nakayama K, Nakayama N, Jinawath N, Salani R, Kurman RJ, Shih I, et al. Amplicon profiles in ovarian serous carcinomas. International journal of cancer. 2007;120(12):2613-7.

163. Fan X, Mikolaenko I, Elhassan I, Ni X, Wang Y, Ball D, et al. Notch1 and notch2 have opposite effects on embryonal brain tumor growth. Cancer Res. 2004;64(21):7787-93.

164. Karlström H, Beatus P, Dannaeus K, Chapman G, Lendahl U, Lundkvist J. A CADASIL-mutated notch 3 receptor exhibits impaired intracellular trafficking and maturation but normal ligand-induced signaling. Proceedings of the National Academy of Sciences. 2002;99(26):17119-24.

165. Ohka F, Natsume A, Wakabayashi T. Current trends in targeted therapies for glioblastoma multiforme. Neurology research international. 2012;2012.

166. Xiang J, Ouyang Y, Cui Y, Lin F, Ren J, Long M, et al. Silencing of Notch3 using shRNA driven by survivin promoter inhibits growth and promotes apoptosis of human T-cell acute lymphoblastic leukemia cells. Clinical Lymphoma Myeloma and Leukemia. 2012;12(1):59-65.

167. Dang TP. Notch, apoptosis and cancer. In: Notch Signaling in Embryology and Cancer. Springer; 2012. p. 199-20.

168. Lin J, Zhang X, Yang J, Ye Y, Luo S. Γ-secretase inhibitor-I enhances radiosensitivity of glioblastoma cell lines by depleting CD133< sup> </sup> tumor cells. Arch Med Res. 2010;41(7):519-2.

169. Overmeyer JH, Young AM, Bhanot H, Maltese WA. A chalcone-related small molecule that induces methuosis, a novel form of non-apoptotic cell death, in glioblastoma cells. Mol Cancer. 2011;10:69.

170. Agarwal S, Al-Keilani MS, Alqudah MA, Sibenaller ZA, Ryken TC, Assem M. Tumor derived mutations of protein tyrosine phosphatase receptor type K affect its function and alter sensitivity to chemotherapeutics in glioma. PLOS ONE. 2013;8(5):e62852.

171. Baldin V, Lukas J, Marcote M, Pagano M, Draetta G. Cyclin D1 is a nuclear protein required for cell cycle progression in G1. Genes Dev. 1993;7(5):812-21.

172. Meltzer PS, Kallioniemi A, Trent J. Chromosome alterations in human solid tumors. The genetic basis of human cancer.New York: McGraw-Hill. 2002:93-113.

173. Dang L, Fan X, Chaudhry A, Wang M, Gaiano N, Eberhart C. Notch3 signaling initiates choroid plexus tumor formation. Oncogene. 2005;25(3):487-91.

174. Dang L, Yoon K, Wang M, Gaiano N. Notch3 signaling promotes radial glial/progenitor character in the mammalian telencephalon. Dev Neurosci. 2006;28(1-2):58-69.

175. Yao J, Qian C. Inhibition of Notch3 enhances sensitivity to gemcitabine in pancreatic cancer through an inactivation of PI3K/akt-dependent pathway. Medical Oncology. 2010;27(3):1017-22.

176. Man C, Wei-Man Lun S, Wai-Ying Hui J, To K, Choy K, Wing-Hung Chan A, et al. Inhibition of NOTCH3 signalling significantly enhances sensitivity to cisplatin in EBV-associated nasopharyngeal carcinoma. J Pathol. 2012;226(3):471-8.

177. Chen J, Kesari S, Rooney C, Strack PR, Chen J, Shen H, et al. Inhibition of notch signaling blocks growth of glioblastoma cell lines and tumor neurospheres. Genes & cancer. 2010;1(8):822-35.

178. Hodkinson PS, Elliott PA, Lad Y, McHugh BJ, MacKinnon AC, Haslett C, et al. Mammalian NOTCH-1 activates β1 integrins via the small GTPase R-ras. J Biol Chem. 2007;282(39):28991-900.

179. Mason HA, Rakowiecki SM, Raftopoulou M, Nery S, Huang Y, Gridley T, et al. Notch signaling coordinates the patterning of striatal compartments. Development. 2005;132(19):4247-58.

180. Haruki N, Kawaguchi KS, Eichenberger S, Massion PP, Olson S, Gonzalez A, et al. Dominant-negative Notch3 receptor inhibits mitogen-activated protein kinase pathway and the growth of human lung cancers. Cancer Res. 2005;65(9):3555-61.

181. Ciznadija D, Liu Y, Pyonteck SM, Holland EC, Koff A. Cyclin D1 and cdk4 mediate development of neurologically destructive oligodendroglioma. Cancer Res. 2011;71(19):6174-83.

182. Wang J, Wang H, Li Z, Wu Q, Lathia JD, McLendon RE, et al. C-myc is required for maintenance of glioma cancer stem cells. PLoS One. 2008;3(11):e3769.

183. Saito K, Yoshida K, Toda M. Brain tumor stem cells and anti-angiogenic therapy.

184. Zhou L, Wang D, Li Q, Sun W, Zhang Y, Dou K. Downregulation of the Notch signaling pathway inhibits hepatocellular carcinoma cell invasion by inactivation of matrix metalloproteinase-2 and -9 and vascular endothelial growth factor. Oncol Rep. 2012;28(3):874-82.

185. Lowe SW, Lin AW. Apoptosis in cancer. Carcinogenesis. 2000;21(3):485-9.

186. Fassl A, Tagscherer K, Richter J, Diaz MB, Llaguno SA, Campos B, et al. Notch1 signaling promotes survival of glioblastoma cells via EGFR-mediated induction of anti-apoptotic mcl-1. Oncogene. 2012;31(44):4698-70.

187. Opferman J. Unraveling MCL-1 degradation. Cell Death & Differentiation. 2006;13(8):1260-2.

188. Bhattacharya S, Das A, Mallya K, Ahmad I. Maintenance of retinal stem cells by Abcg2 is regulated by notch signaling. J Cell Sci. 2007;120(15):2652-6.

189. Luistro L, He W, Smith M, Packman K, Vilenchik M, Carvajal D, et al. Preclinical profile of a potent γ-secretase inhibitor targeting notch signaling with in vivo efficacy and pharmacodynamic properties. Cancer Res. 2009;69(19):7672-80.

190. He W, Luistro L, Carvajal D, Smith M, Nevins T, Yin X, et al. High tumor levels of IL6 and IL8 abrogate preclinical efficacy of the γ-secretase inhibitor, RO4929097. Molecular oncology. 2011;5(3):292-301.

191. Sullivan N, Sasser A, Axel A, Vesuna F, Raman V, Ramirez N, et al. Interleukin-6 induces an epithelial–mesenchymal transition phenotype in human breast cancer cells. Oncogene. 2009;28(33):2940-7.

192. Wang H, Lathia JD, Wu Q, Wang J, Li Z, Heddleston JM, et al. Targeting interleukin 6 signaling suppresses glioma stem cell survival and tumor growth. Stem Cells. 2009;27(10):2393-404.

193. Evin G, Sernee MF, Masters CL. Inhibition of γ-secretase as a therapeutic intervention for alzheimer's disease. CNS drugs. 2006;20(5):351-72.

194. Tolia A, De Strooper B. Structure and function of γ-secretase. Seminars in cell & developmental biology; Elsevier; 2009.

195. Kopan R, Ilagan MXG. Γ-secretase: Proteasome of the membrane? Nature Reviews Molecular Cell Biology. 2004;5(6):499-504.

196. Purow B. Notch inhibitors as a new tool in the war on cancer: A pathway to watch. Curr Pharm Biotechnol. 2009;10(2):154.